A FEASIBILITY STUDY OF
A PERSISTENT MONITORING SYSTEM
FOR THE FLIGHT DECK OF
U.S. NAVY AIRCRAFT CARRIERS

THESIS

Jeffrey S. Johnston, Lieutenant, USN

AFIT/GAE/ENY/09-M12

DEPARTMENT OF THE AIR FORCE
AIR UNIVERSITY

AIR FORCE INSTITUTE OF TECHNOLOGY

Wright-Patterson Air Force Base, Ohio

A Feasibility Study of a Persistent Monitoring System for the Flight Deck of U.S. Navy Aircraft Carriers

THESIS

Presented to the Faculty

Department of Aeronautics and Astronautics

Graduate School of Engineering and Management

Air Force Institute of Technology

Air University

Air Education and Training Command

In Partial Fulfillment of the Requirements for the

Degree of Master of Science in Aeronautical Engineering

Jeffrey S. Johnston, B.S.

Lieutenant, USN

March 2009

AFIT/GAE/ENY/09-M12

A Feasibility Study of a Persistent Monitoring System for the Flight Deck of U.S. Navy Aircraft Carriers

Jeffrey S. Johnston, B.S.

Lieutenant, USN

Approved:

/signed/		4 Mar 2009
Lt.Col. E.D. Swenson, PhD (Chairman)		date
/signed/		4 Mar 2009
Lt.Col. F.G. Harmon, PhD (Member)		date
/signed/		4 Mar 2009
J. F. Raquet, PhD (Member)		date

AFIT/GAE/ENY/09-M12

Abstract

This research analyzes the use of modern Real Time Locating Systems (RTLS), such as the Global Positioning System (GPS), to improve the safety of aircraft, equipment, and personnel onboard a United States Navy (USN) aircraft carrier. The results of a detailed analysis of USN safety records since 1980 show that mishaps which could potentially be prevented by a persistent monitoring system result in the death of a sailor nearly every other year and account for at least \$92,486,469, or 5.55% of the total cost of all flight deck and hangar bay related mishaps. A system to continually monitor flight deck operations is proposed with four successive levels of increasing capability. A study of past and present work in the area of aircraft carrier flight deck operations is performed.

This research conducted a study of the movements of USN personnel and an FA-18C aircraft being towed at NAS Oceana, VA. Using two precision GPS recorders mounted on the aircraft wingtips, the position and orientation of the aircraft, in two-dimensions, are calculated and the errors in this solution are explored. The distance between personnel and the aircraft is calculated in the nearest neighbor sense. Pseudospectral motion planning techniques are presented to provide route prediction for aircraft, support equipment, and personnel.

Concepts for system components, such as aircraft and personnel receivers, are described. Methods to recognize and communicate the presence of hazardous situations are discussed. The end result of this research is the identification of performance requirements, limitations, and definition of areas of further research for the development of a flight deck persistent monitoring system with the capability to warn of hazardous situations, ease the incorporation of UAVs, and reduce the risk of death or injury faced by sailors on the flight deck.

Acknowledgements

Table of Contents

List of Figures

xi

List of Tables

List of Symbols

List of Abbreviations

A Feasibility Study of

a Persistent Monitoring System

for the Flight Deck of

U.S. Navy Aircraft Carriers

I. Introduction

The flight deck of a U.S. Navy Aircraft Carrier (CV/CVN), depicted in Figure 1.1, is an inherently dangerous place to work. An embarked Carrier Air Wing (CVW), usually composed of around 64 aircraft, must perform all of its flight deck operations using only 4.5 acres of flight deck space. These close quarters combined with the rapid pace of flight deck operations and the dangers faced by any ocean-going vessel create conditions that are among the most dangerous in the world. The official U.S. Navy records of flight deck mishaps [8] include many serious injuries and fatalities, as well as numerous instances of damage to or loss of aircraft.

After examining 29 years of recorded flight deck related mishap records provided by the Naval Safety Center, a new mishap classification system was developed. Rather than classifying mishaps by cost, a new system is proposed to group mishaps by cause. New methods and systems to mitigate the risks which contribute to these mishaps are proposed. This research will focus exclusively on the CV/CVN class of aircraft carrier although many aspects may be applicable to the smaller amphibious assault vessels.

The safety of sailors and aviation assets is of the utmost importance to all levels of leadership. There is continual effort to improve safety in carrier operations. Despite a focus on safety, it is very common for a sailor involved in Naval Aviation to have been personally involved in a mishap where someone was injured or significant damage was incurred by an aircraft.
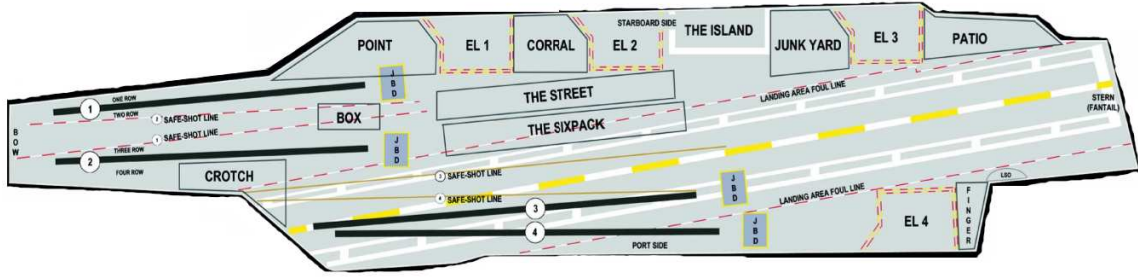
Figure 1.1:   Diagram of Modern Aircraft Carrier (CV/CVN) Flight Deck [35]: JBD denotes the location of a jet blast deflector, EL denotes the location of one of four elevators, and a circled number (①) over a long black line provides the location and identification of each catapult.

Through constant training and vigilant supervision, the safety record of Naval Aviation has been kept at acceptably high levels. With new technologies, especially Unmanned Aerial Vehicles (UAV), being examined for introduction to the fleet, the procedures presently used to keep equipment and personnel safe will be insufficient. The use of modern Real Time Locating Systems (RTLS) will be explored to determine their ability to improve the level of safety.

1.1   Hazards

This section will describe many of the hazards faced by aircraft, equipment, and personnel involved in Naval Aviation. Figure 1.1 depicts the layout of a modern aircraft carrier showing the locations of the catapults, elevators, jet blast deflectors, and island. A full description of the operations onboard an aircraft carrier is beyond the scope of this document. A brief introduction to flight deck operations is provided in the Naval Safety Center's *Flight Deck Awareness Guide* [35]. A complete layout of the flight deck and hangar bay, both with and without an embarked CVW, is provided (See Figure 1.15, page 31 and Figure 1.16, page 32).

While this section treats the flight deck and hangar bay hazards separately, the term flight deck will be used throughout this research to refer to both.

Figure 1.2:   View of Flight Deck From the Island: Depicts numerous hazards common to flight deck operations. Taken in 2004 by the author onboard USS John F. Kennedy (CV-67).

1.1.1   Flight Deck.   Figure 1.2 is a photographic view of the landing area as well as catapults three and four on a modern aircraft carrier. The picture is taken facing to port from the island. In this picture, an FA-18C aircraft (top left) is taxiing to catapult four and the port engine of a propeller-driven E-2C aircraft (bottom right) is being started in preparation for launch. It is important to note that in a typical launch cycle there may be 10-12 other aircraft elsewhere on the flight deck preparing for launch. This image is presented as an example of many of the hazards of flight deck operations. The nose of the FA-18C is over the edge of the deck, and the pilot cannot see the location of the nose wheel. The pilot is being directed by a sailor wearing a yellow shirt to the right. With improper direction, the pilot can easily taxi the aircraft over the edge of the ship. There are several instances of this type of mishap in the data provided by the Naval Safety Center (Mishap Event 19749 - Fiscal Year 1987, Appendix A).

3

Propeller driven aircraft, such as the E-2C Hawkeye and C-2 Greyhound, present a significant hazard to personnel on the flight deck. When turning, the propeller blades are virtually invisible. Also, with the extra hearing protection that sailors must wear because of the high noise levels, the sound generated by the propeller blades can be below a sailor's hearing threshold. Within the E-2C community, there is significant emphasis on preventing contact between a sailor and rotating propeller blades.

It is also important to understand the challenges faced by the flight deck crews (ship's company) as they typically work the entire duration of a long flight schedule. If the first launch is at 0600 and the final recovery is at 2300, the flight deck crew will be on the flight deck for virtually all of that time. Fatigue, due to these long schedules, can lead to numerous mistakes being made, not necessarily after just one day, but after days or weeks with such a long schedule. With Figure 1.2 representing a typical day of operations on the flight deck, the pilot of the FA-18C must be aware that the taxi director who is telling them when to turn may be impaired by a significant lack of sleep. The human factors present in flight deck operations can have a greater impact on safety and performance than equipment failures.

1.1.2 Hangar Bay. Any aircraft not airborne or on the flight deck will be located in the hangar bay which is located approximately 40 feet below the surface of the flight deck. Typically, aircraft in a maintenance cycle will be parked in the hangar bay since they are unable to participate in the flight schedule. The hangar bay is divided into three sections by two sliding doors running the width of the bay. Aircraft are transferred between the flight deck and hangar bay by one of four aircraft elevators. There are also doors in the hangar bay's deck which open to reveal ordnance elevators.

Much of the hangar bay is used for purposes besides storing aircraft. The Aviation Intermediate Maintenance Department (AIMD) is located forward of the hangar bay. AIMD is responsible for aviation support equipment (SE) such as tow tractors, fire trucks, and hydraulic generator carts, which take up much of the forward

Figure 1.3:   View of Hangar Bay, Facing Forward: Taken onboard USS Nimitz (CVN-68). The close proximity of the aircraft often leads to collisions. Photo credit: U.S. Navy.

section for the storage of these components. The Supply Department is responsible for a large stack of supplies in the aft section of the hangar bay, often called 'the mountain.' The cramped conditions combine with only four entry/exit locations to make for a dangerous environment. Figure 1.3 shows a typical view of the hangar bay of a deployed aircraft carrier.

In Figure 1.3, the track for the dividing door can be seen as a horizontal line extending from the port wing of aircraft 212. It appears that aircraft 212 is parked across this track, meaning that a closure of the door would significantly damage it. Two tow tractors can be seen above the same wing. There are 12 aircraft in this view illustrating the close quarters present in the hangar bay. Aircraft 212 is also parked with another aircraft directly off its starboard wing. If the wings of aircraft 212 were to unfold they could be damaged, as well as the neighboring aircraft.

Table 1.1:   Data Elements Provided by Naval Safety Center

Data	Explanation
Event Serial	Unique number assigned to mishap
Aircraft Serial	Unique number assigned to each asset involved
Fiscal Year	Fiscal year in which mishap occurred
Event Class	Letter designation based upon severity of injuries and/or damage
Type/Model/Series	Description of asset involved (ex: FA-18C)
Total Event Cost	Cost including all damage and injuries
Days Lost	Total days of work lost by all personnel injured
Total Event Injury Cost	Cost of all injuries
Narrative	Short description of mishap

1.2   Examining the Naval Safety Center Mishap Data

This section discusses the Navy's policies and procedures for mishap reporting and data collection and introduces new methods for classifying mishaps. It then examines the data provided by the Naval Safety Center, available under the Freedom of Information Act, on all reported mishaps involving an aircraft carrier from 1980 through 2008.

This data includes 3,228 mishaps, both airborne and onboard the ship. Only 1,506 of the mishaps provided have a narrative, or description of the mishap. The narratives are required to determine the appropriate grouping for the event. The mishaps without narratives require privileged access, which could not be provided for this study. Therefore, only the 1,506 mishaps with narratives were evaluated in this study. Table 1.1 describes the data elements provided by the Naval Safety Center.

1.2.1   Data Collection Methods.   Before examining the data further, it is important to discuss how it is collected. For any aviation related mishap resulting in injury to personnel or damage to equipment, the squadron or activity responsible must submit either a Hazard Report (HAZREP) or Mishap Data Report (MDR). Some of the information these reports contain is described in Table 1.1, but they generally contain many more elements including a full length description of the event.

These reports are all collected by the Naval Safety Center and stored in a computer database, AVIATION DATABASE NSIRS.

The purpose of the HAZREP or MDR is to record objective data for analysis by the Naval Safety Center, but there are numerous reasons why the data contained in the report may not reflect the totality of reality. Due to the natural desire to downplay the significance of a mishap and the amount of damage as well as the inherent difficulty in capturing the true total cost of a mishap, the estimated cost is typically much lower than one would expect.

The Naval Aviation Safety Program [9] classifies mishaps based upon the number of workdays lost due to injury or the financial severity of damage to equipment. Mishaps are also categorized as Flight, Flight-Related, or Aviation Ground Mishaps, but for the purposes of this research these distinctions are not sufficient. According to the instructions for this program, a mishap is categorized as Flight or Flight-Related if the intent for flight existed, not simply if it occurs in the air. A collision between a sailor or parked aircraft and an aircraft launching from a catapult is reported as a Flight mishap, but it is still of interest to this research because it is potentially preventable. On the other hand, a mishap caused by system failure on the aircraft during launch, also reported as a Flight mishap, is outside the scope of this research.

The severity of the mishap is classified by assigning a letter designator, based upon cost, as outlined in Table 1.2 [9]. The process of determining the cost of a mishap is detailed in Section 314 of the Naval Aviation Safety Program [9]. The reporting activity is directed to *"Compute the cost of damage to DoD property using the best known cost of repair or replacement. Base these cost estimates on the price of materials and man-hours necessary to repair the damage."* This does little to account for the cost of lost sorties or lost productivity due to mishap investigation. It is unclear how to estimate the cost of an extreme case like a sailor being lost overboard. In the 2008 PBS Documentary *Carrier*, there was a sailor lost overboard and the Carrier Strike Group spent three days searching with multiple surface ships as well

Table 1.2:   Classification Criteria for Aviation Mishaps

Class	Damage Requirements	Injury Requirements
A	> $1,000,000$ or Aircraft Destroyed	Fatal Injury and/or Permanent Total Disability
B	> $200,000$	Permanent Partial Disability and/or Three or More Personnel Hospitalized
C	> $20,000$	Five Lost Workdays
HAZREP	< $20,000$	Beyond First Aid But Less Than Five Lost Workdays

as U.S. and allied aircraft. The cost of the search effort and loss of life must have been staggering, considering the cost of operating a CVN is typically thought of as over $1M per day. It is unclear how the full cost of such an event would be accurately determined. One must not only account for the fuel consumed by the searching surface vessels and aircraft but also the cost of tasking those assets with duties other than the mission of the Strike Group.

It is a common perception in the fleet that there will be negative repercussions when reporting a mishap, so efforts are often made to minimize the reported value of damage that occurred. This is usually characterized by extra effort on the part of the maintainers to repair a component instead of ordering a costly replacement. The dollar amounts reported for these mishaps may not always represent the actual cost to the Navy. Even listing the pre-determined cost of a replacement part doesn't necessarily capture the full logistics costs associated with its procurement and shipment. These statements are not intended as a criticism of the Naval Aviation Safety Program but to make the reader aware that the costs presented in Section 1.2.4 do not completely capture the total cost.

Even more important than the cost associated with a mishap is the impact it has on the CVW's mission. The collision of two aircraft on the flight deck can lead

to the loss of scheduled sorties, delays in the scheduled maintenance of other aircraft, and increased strain on the logistics train. The effect of one mishap is typically felt for days or weeks as schedules are adjusted with the result being a reduction in the ability to provide striking power from the sea.

The goal of this research is to evaluate technological improvements which could be implemented to prevent injury, save lives, and reduce expenses. However, the incalculable or unrecorded factors in the total cost of a mishap make it difficult to estimate the true cost benefit of a system designed to prevent mishaps.

1.2.2 Classifying Mishaps.   Because the focus of this research is to evaluate methods to reduce or prevent mishaps, it is necessary to group mishaps into categories based upon causes, not costs, so that the causes can be targeted for mitigation. The next step is to evaluate the causes of the mishaps in each category and research technological improvements that could be leveraged in an attempt to reduce their occurrence. A set of categories was created which describes all of the flight deck related mishaps which could potentially be prevented by applying modern RTLS technologies. If a narrative described a mishap which the author thought was potentially preventable, it was marked an *Interest Mishap*.

In the first step of this research, the narratives of 1,506 mishaps were reviewed to determine these new classifications. After reading through all available mishap narratives, the mishaps were either classified into the primary and secondary categories described below or excluded from further evaluation. These mishap categories are not exclusive, as some mishaps may fall into multiple categories (primarily when there is both injury and equipment damage). There were 261 mishaps that fell into one or more of these categories, which is 8.1% of the total and 14.3% of those with narratives. It is reasonable to assume that a similar percentage of those mishaps without narratives would also fall into these categories, since no significant changes have been made over the period of the recorded data which would have decreased the rate of occurrence of such mishaps. The primary categories are listed in descending

order of total cost of all mishaps falling into that category as reported in the data provided by Naval Safety Center. The occurrence and mean cost [1] of these categories is presented in Table 1.3.

Primary *Interest Mishap* Categories:

1. Spotting: Aircraft is stationary when another object in its normal operation impacts it or aircraft begins uncontrolled movement due to ship's motion. (Note: If an aircraft is towed into another aircraft, it is considered a towing mishap regardless of the position of the stationary aircraft.)

2. Towing: While under tow, aircraft or tow tractor collides with (non-human) object. This classification also covers aircraft being pushed into a parking position.

3. Taxiing: With pilot in command, aircraft collides with (non-human) object.

4. Exhaust: Aircraft is damaged or sailor is injured by engine exhaust.

5. Contact: A sailor is injured or killed by contact with a moving aircraft (excludes engine/exhaust contact).

6. Engine: Aircraft is damaged or sailor is injured by contact with turning engine (usually propeller).

7. Wingfold: The spreading (or folding) of an aircraft's wings impacts another object (usually another aircraft).

8. Non-aviation: Aircraft damaged during non-aviation related event, such as an underway replenishment.

Secondary Categories:

1. Miscellaneous: Any flight deck or hangar bay mishap that does not fall into the above categories but may still be potentially preventable.

---

[1]Cost data used in this research is unchanged from the data provided. As an example, adjustments for inflation are not made.

Table 1.3:   Occurrence and Average Cost of Mishap Categories: Occurrence given as percent of total mishaps with narratives (excluding HAZREPS).

Category	Occurrence (%)	Mean Reported Cost ($)
Spotting	5.19	1,251,800
Towing	10.71	335,800
Taxiing	8.93	319,100
Exhaust	5.03	181,000
Contact	4.06	83,800
Engine	1.46	60,600
Wingfold	0.32	10,900
Non-aviation	0.16	1,200
Miscellaneous	2.44	39,800
Unknown	1.79	906,100

2. Unknown: Some mishap that could potentially be prevented occurred on the flight deck or hangar bay but the exact circumstances cannot be determined from the available information.

Mishaps that have narratives and were identified as belonging to one of these categories are termed *Interest Mishaps* for the purposes of this research. To further illustrate the method by which mishaps were classified based upon their narrative, an example for each of the primary categories is provided in Table 1.4. The *Interest Mishaps* will be examined further to evaluate methods of mishap detection or prevention. The complete list of *Interest Mishaps* is provided in Appendix A on page 135.

1.2.3   Preliminary Analysis.   Figure 1.4 illustrates the trends in mishap occurrence during the period of time covered by the available data. Total mishaps include every mishap within the available data[2], including airborne mishaps and Hazard Reports. It is interesting to observe that in more recent years the *Interest Mishaps* make up a larger percentage of the total. The primary reason for this is that the more recent data has a larger percentage with narratives. If narrative data were available

---

[2]Few mishaps are listed for fiscal year 2008 as the data was provided early in the fall of 2007. They are included in this analysis for the sake of thoroughness.

Table 1.4:   Examples of Mishap Narratives and their Classifications: Narratives are presented exactly as recorded by Naval Safety Center.

Event Serial	Fiscal Year	Narrative	Classification
22273	1986	PARKED ACFT SUSTAINED DAMAGE WHEN BARRICADE STANCHION STRCK HORIZ STAB	Spotting
40688	1994	ACFT UNDER TOW IN HANGAR DECK BAY COLLIDED WITH PARKED ACFT.	Towing
47673	1998	ACFT RADOME IMPACTED BY AILERON OF SECOND ACFT WHICH WAS TAXIING ON DK	Taxiing
53357	2001	FLIGHT SURGEON BLOWN OVERBOARD DURING CQ OPERATIONS.	Exhaust
35370	1992	BLUE SHIRT RUN OVER BY ACFT MAIN MOUNT.	Contact
47642	1998	PLANE CAPTAIN STRUCK BY TURNING PROPELLER.	Engine
50548	2000	UNCOMMANDED WING SPREAD CAUSED WINGS TO STRIKE ACFT IN CLOSE PROXIMITY	Wingfold
69377	2006	ACFT PARKED ON FLT DECK STRUCK BY FORK LIFT TRACTOR DUR REPLENISHMENT.	Non-aviation
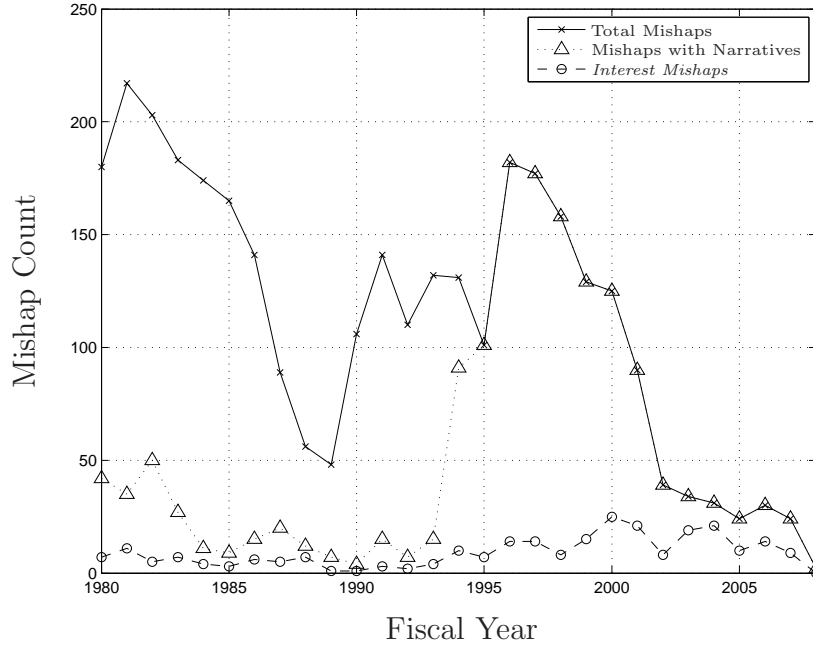
Figure 1.4:   Number of all Mishaps and Hazard Reports by Year

for a larger percentage of earlier mishaps, it is likely that *Interest Mishaps* would constitute a much larger percentage of the overall total.

The data in Figure 1.4 includes HAZREPS which, as noted earlier, have associated costs less than $20,000. There are 1,373 HAZREPS in the data provided by Naval Safety Center with a total reported cost of $750.00, while the vast majority have a reported cost of zero dollars. Removing these from the evaluation shows, as illustrated in Figure 1.5, that *Interest Mishaps* make up a larger portion of each year's totals than is depicted in Figure 1.4.

From Figure 1.6, it can be seen that the missing narratives from the first 15 years of data should hold a significant number of *Interest Mishaps*. The noticeable drop in mishaps in the late 1980s seen in Figure 1.5 shows an improvement in flight and carrier landing safety achieved primarily through new policies and procedures since there were few physical changes to aircraft or the deck during this time. This leads to *Interest Mishaps*, those that are potentially preventable, becoming a larger percentage of the total number of mishaps each year. *Interest Mishaps* make up an average of 35.2% of all mishaps with narratives each year, with a standard deviation
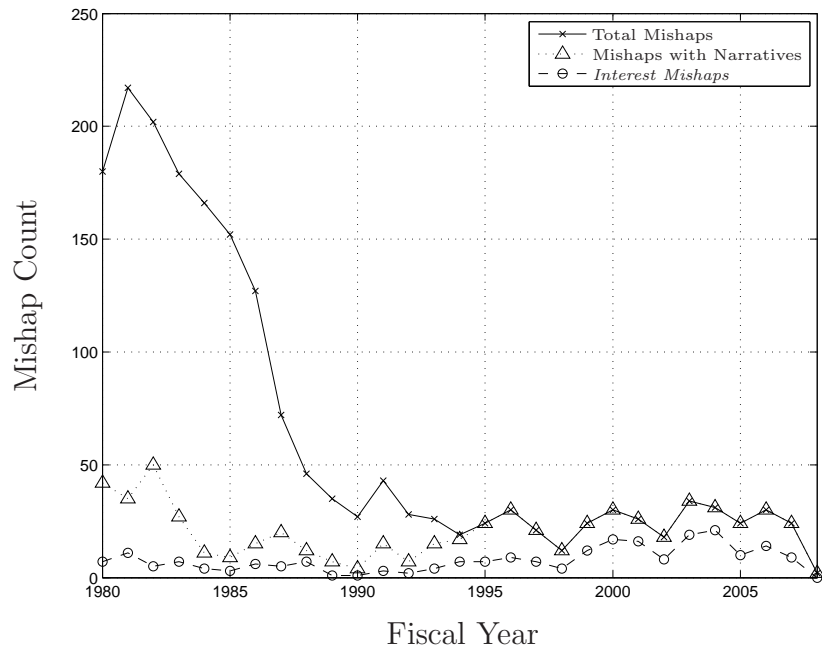
Figure 1.5:   Number of all Mishaps by Year (Excludes Hazard Reports)
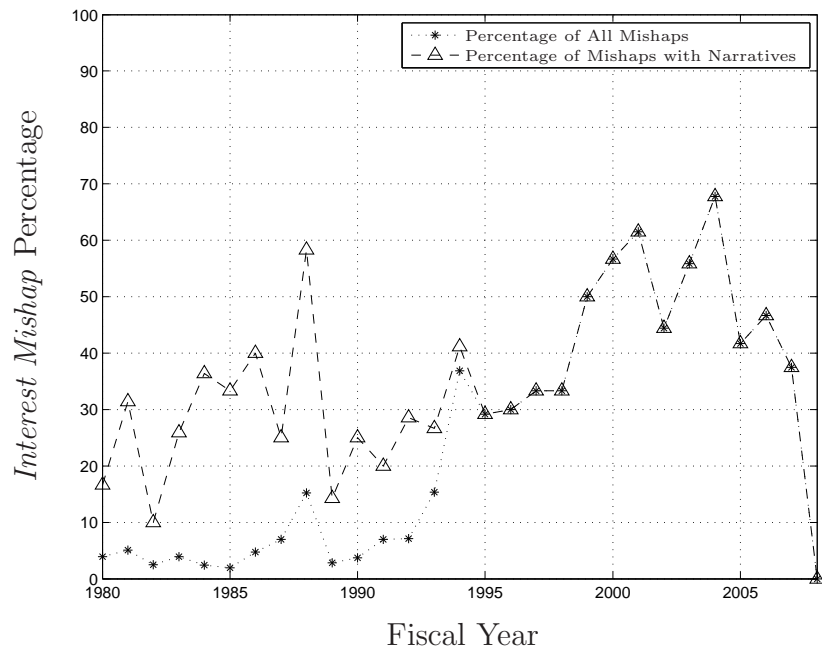
Figure 1.6:   Occurrence of *Interest Mishaps* as Percentage of Total Mishaps

14
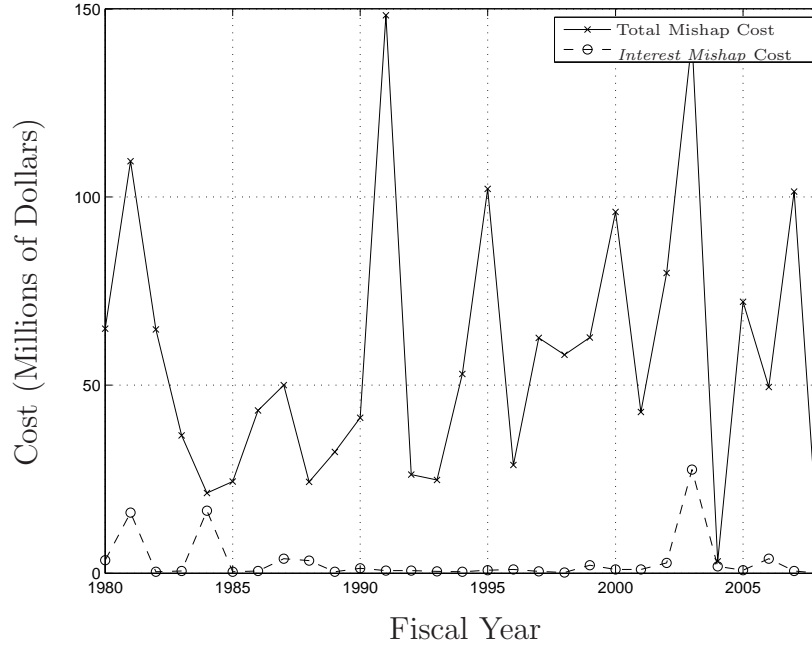
Figure 1.7:   Cost of Mishaps with Narratives

of 15.93%. Since improved policies and procedures have been unable to significantly reduce the number of *Interest Mishaps* over the period of recorded data, improvements to flight deck safety must be achieved by other means.

1.2.4 Cost of Mishaps.   With an understanding of the limitations on the collection of mishap cost data as described in Section 1.2.1, the cost of mishaps over the time period available can be evaluated as illustrated in Figure 1.7. Due to the great difference between Total and *Interest Mishap* costs, the *Interest Mishap* costs are reproduced in Figure 1.8.

A single flight mishap resulting in the loss of an aircraft (or multiple aircraft), can incur a cost higher than all of the *Interest Mishaps* over an entire year. With the aircraft purchase costs in Table 1.5, it is easy to see why. But, the total cost of *Interest Mishaps* since 1980 is $92,486,469, 5.55% of the cost of all recorded mishaps in this data (including those lacking narratives). This should provide significant motivation to explore means of reducing the occurrence of *Interest Mishaps*.

15
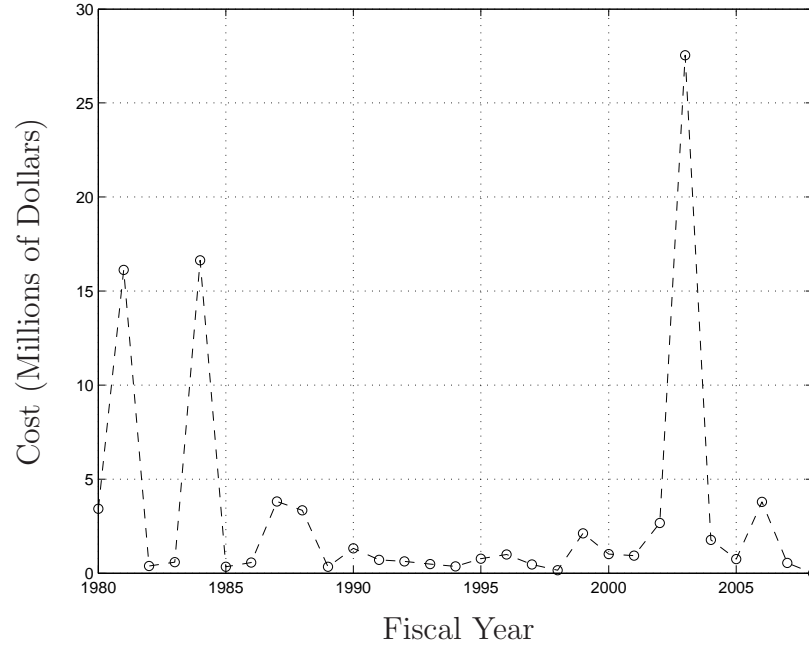
Figure 1.8:   Cost of *Interest Mishaps*

Table 1.5:   Aircraft Purchase Costs [23]

Aircraft	Cost (Millions of $)
FA-18(A-D)	25
FA-18(E-F)	43.6
EA-6B	55.7
E-2C	70

Table 1.6:   *Interest Mishaps* With No Reported Cost

Event Serial	Fiscal Year	Narrative	Classification
27475	1982	FLT DECK PERS SUSTAINED LEG INJ WHEN LEG WAS TRAPPED UNDER TAXIING A/C	Contact
42144	1995	DURING NIGHT FRS CQ AIRCRAFT TAXIED OVER AIRMAN'S FOOT.	Contact
51762	2000	CV FLT DECK CAT OFFICER KNOCKED DOWN BY JET BLAST;SUSTAINED BKN FIBULA.	Exhaust
65193	2003	AIRCRAFT ON DECK PUSHED BACKWARDS INTO OTHER AIRCRAFT.	Towing
68161	2004	DURING FLT DECK VERTREP, FORCKLIFT STRUCK PORT HORIZ STAB OF PARKED AC.	Non-aviation
47643	1998	PLANE CAPTAIN STRUCK BY TURNING PROPELLER.	Engine

1.2.5   Errors in Data.   The actual cost of the mishaps is greater than shown here due to errors, omissions, or inability to capture the true cost in the mishap reports. Of the 3,228 mishaps in the report provided by Naval Safety Center, there are 46 mishaps (excluding HAZREPS) which have a total event cost of less than $20,000. They may have initially been reported as Class A, B, or C mishaps and after further investigation were downgraded, or their total cost was incorrectly reported and never updated in the database. Of these 46 mishaps, 11 had no associated cost, and 5 of those were classified as *Interest Mishaps*. Information on these 5 mishaps is presented in Table 1.6. It should be clear from reading the provided narratives that the cost of these mishaps must have been greater than $0.

Table 1.7:   Mandated Injury and Fatality Costs [8]

Personnel	Partial Disability ($)	Total Disability ($)	Fatality ($)
Flying Officer	210,000	1,300,000	1,100,000
Other Officers	145,000	845,000	395,000
Enlisted	115,000	500,000	125,000

Also shown in Table 1.6 is Event 47643 which was listed as a Hazard Report. When a person is struck by a turning propeller there is little chance of survival, much less avoiding significant injury. In fact, this is the only mishap of this type in the data without an associated fatality or major injury. Without further information, such as a complete description of the scenario, a detailed analysis of this mishap cannot be performed. It is presented to illustrate why the true cost of mishaps cannot be easily determined. One can only hope that since it was reported as a Hazard Report the sailor survived. There are other mishaps in the data which, based upon the available data, appear to have discrepancies, but they will be left out of further evaluation.

1.2.6   The Human Cost.   The injury-related mishaps in Table 1.6 are significant and should be compared to the mandated cost values for similar injuries in Table 1.7. Interestingly, the mandated costs presented here were last updated in 1988 "so that analysts can make generalized comparisons against historical data" [8].

From the 261 *Interest Mishaps*, there are 13 fatalities and 34 major injuries. The major injuries counted here involved sailors being run over by an aircraft, ingested into a turning engine, or being blown overboard. These numbers were generated from reading the brief narratives which do not always expressly state the severity of the injury. A fatality was only recorded if the narrative expressly said the sailor was killed. Figures 1.9 and 1.10 show the number and recorded costs of fatalities and major injuries.

Interestingly, the mean cost of both the fatalities and major injuries is below what would be expected from the mandated costs from Table 1.7 [8]. The mean
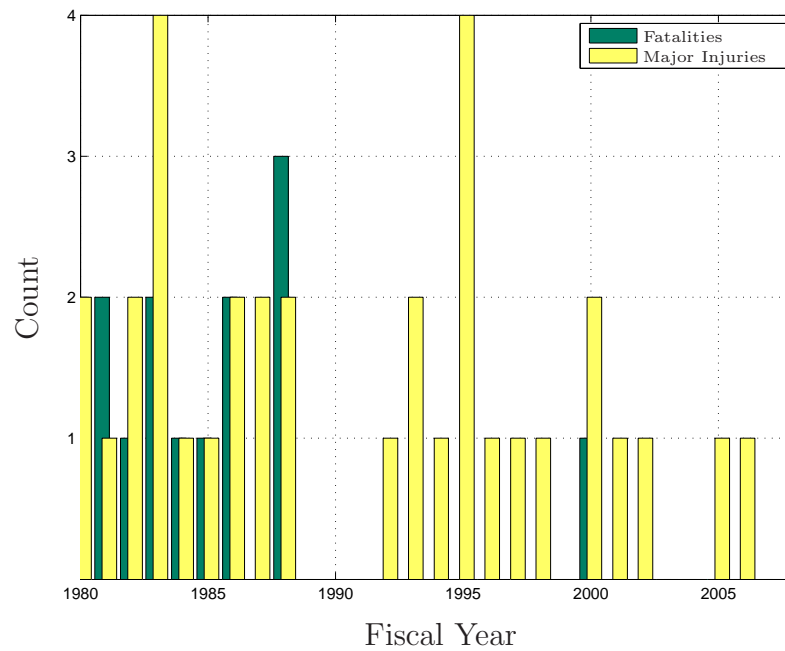
Figure 1.9: Number of Fatalities/Major Injuries from *Interest Mishaps*
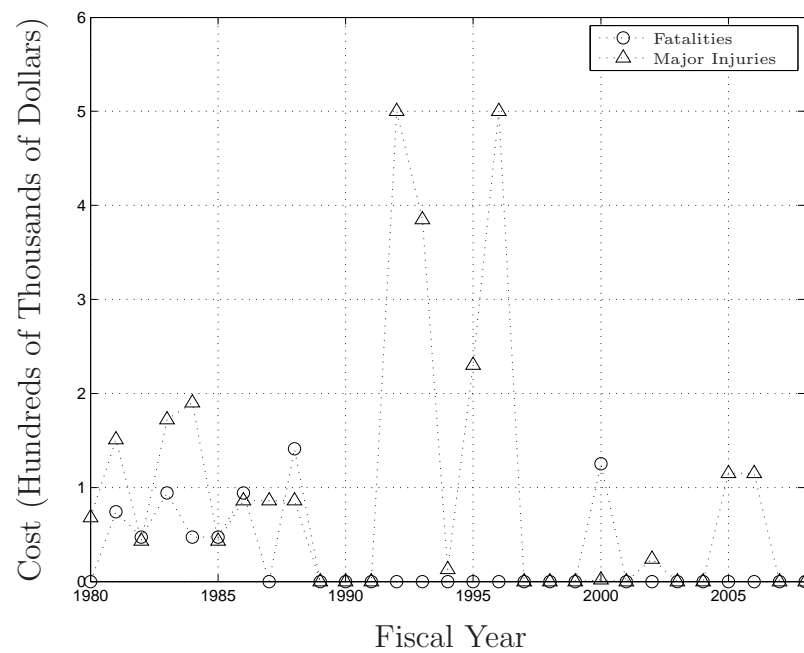
Figure 1.10: Cost of Fatalities/Major Injuries from *Interest Mishaps*

fatality cost is $51,462, less than half the mandated amount. This is due to the fact that through the 1980s the cost associated with the death of an enlisted servicemember was only $37,000. The mean major injury cost is $82,611. It is not possible to determine the severity of every injury based upon the available data, but this is still less than the mandated cost of a partial disability for an enlisted sailor. There are seven mishaps with associated major injuries that have a cost of zero for injuries. The narrative for the first of these is "FLT DECK PERS SUSTAINED LEG INJ WHEN LEG WAS TRAPPED UNDER TAXIING A/C", which certainly had unreported associated medical costs.

Beyond the direct medical, life insurance, or disability costs the government must pay for a mishap involving a fatality or major injury there are other losses that cannot be calculated with any certainty. A killed or injured sailor affects the performance, morale, and retention of those they serve with. Leadership and experience are lost with a senior member, and their potential with a junior. The effects of these factors may be difficult or impossible to calculate, but it should be clear that they are not taken into account when determining the cost of a mishap.

1.2.7 Conclusions From Data Analysis. With the improvements in flight safety over the last decade, mishaps occurring on the flight deck of an aircraft carrier are taking an increasing share of each year's total mishap cost. The annual cost of *Interest Mishaps* is consistently in the $2-4 million range, as seen in Figure 1.8, except for three years where an aircraft was destroyed and the cost was much higher. With an average of 0.448 sailors killed every year by an *Interest Mishap*, it is important to make every effort to prevent them.

By closely examining the data reported to the Naval Safety Center, and an analysis of its limitations, it has been shown that potentially preventable mishaps, and their cost, make up a significant percentage of the total each year. This mishap cost analysis was performed to show that there is still a significant cost every year to the U.S. Navy for mishaps which have been identified as potentially preventable.

This cost analysis is presented as a baseline for the cost benefit of a system that could predict and potentially prevent mishaps.

1.3 Persistent Monitoring

To prevent mishaps from occurring, it is necessary to provide key personnel with more accurate and timely data describing the state of all aircraft, equipment, and personnel on the flight deck and in the hangar bay. To do this, a system must first be developed to more accurately estimate the aircraft position, orientation, and velocity than is currently done by the Taxi Director or Handling Officer. Such a system would be persistent, in that it would continually monitor activities on the flight deck and hangar bay. This section will explore how modern RTLS technology can be leveraged to provide a more accurate depiction of state and reduce the occurrence of mishaps both on the flight deck and in the hangar bay.

1.3.1 Determining Flight Deck State. Since the creation of carrier-based aviation, the management of the carrier flight deck has been an extremely challenging task requiring hundreds of personnel each having years of experience. The current system has changed very little since the 1950s. Personnel on the flight deck use hand signals to communicate with each other and direct the pilot to make aircraft control system inputs. The position and orientation of each aircraft are loosely monitored in Flight Deck Control with objects representing aircraft on a table commonly referred to as the "Ouija Board" depicted in Figure 1.11. When towing an aircraft personnel are assigned as Wing and Tail Safeties to ensure the towed aircraft does not impact another, while the Tow Tractor Driver ensures the route is clear of obstructions. Currently, the state of each aircraft (position, orientation, and translational/rotational velocities) is estimated only by a human observer's judgement.

It is this human-based estimation of state approach which creates a capacity for mishaps. With a very large quantity of aircraft, SE, and personnel as well as flight deck surfaces such as jet blast deflectors, elevators, and catapults, the flight

Figure 1.11: Flight Deck Represented by a "Ouija Board": Photo credit: U.S. Navy.

deck naturally lends itself to a computer-based tracking system. Table 1.8 illustrates many of the elements required for a useful depiction of flight deck state. To reduce the occurrence of mishaps, it is possible to improve the accuracy of the flight deck state through the use of modern RTLS. For the purposes of this research, the fidelity with which such a system can determine the state will be divided into four levels based upon the capabilities the system would provide, increased expected difficulty, and cost of implementation. Each successive level would include the capabilities of all previous levels. Further research beyond this effort would be required to determine the optimal means of achieving these levels as well as their performance requirements.

1.3.1.1 Level One: Aircraft. The purpose of a Level One observation system is to reduce or eliminate Spotting and Taxiing mishaps as listed in Section 1.2.2. As previously stated, the position, orientation, and translational/rotational velocities of aircraft on the flight deck are currently determined only by a visual estimation. To improve this, a new computer-based system can be developed which provides measurements of aircraft state in near real-time to Flight Deck Control or other systems and personnel concerned. Level One would also need to determine the

Table 1.8:   Elements to Describe Flight Deck State

Element	Variable	Measurement
Elevator Status	$[el_1, el_2, el_3, el_4]$	Up/Down/In Transit
JBD Status	$[j_1, j_2, j_3, j_4]$	Up/Down/In Transit
Catapult Location	$[c_1, c_2, c_3, c_4]_{pos}$	Distance of catapult from launch position
Catapult Status	$[c_1, c_2, c_3, c_4]_T$	Applied Tension
Barricade Stanchion Status	$[b_1, b_2]$	Up/Down/In Transit
Hangar Bay Door Status	$[hbd_1, hbd_2]$	Open/Closed/In Transit
Wind Speed	$\bar{v}_{wind}$	Free-stream wind velocity
Deck Roll/Pitch	$[\Theta, \phi]_{deck}$	Roll/pitch angle
Aircraft Position	$[x, y, z, \Theta, \phi, \psi]_{AC_i}$	Location and orientation relative to ship
Aircraft Velocity	$\left[\dot{x}, \dot{y}, \dot{z}, \dot{\Theta}, \dot{\phi}, \dot{\psi}\right]_{AC_i}$	Translational and rotational velocities relative to ship
SE Position	$[x, y, z, \psi]_{SE_j}$	Location and yaw relative to ship
SE Velocity	$\left[\dot{x}, \dot{y}, \dot{z}, \dot{\psi}\right]_{SE_j}$	Translational and yaw velocities relative to ship
Personnel Position	$[x, y, z]_{pers_k}$	Location relative to ship
Personnel Velocity	$[\dot{x}, \dot{y}, \dot{z}]_{pers_k}$	Velocity relative to ship
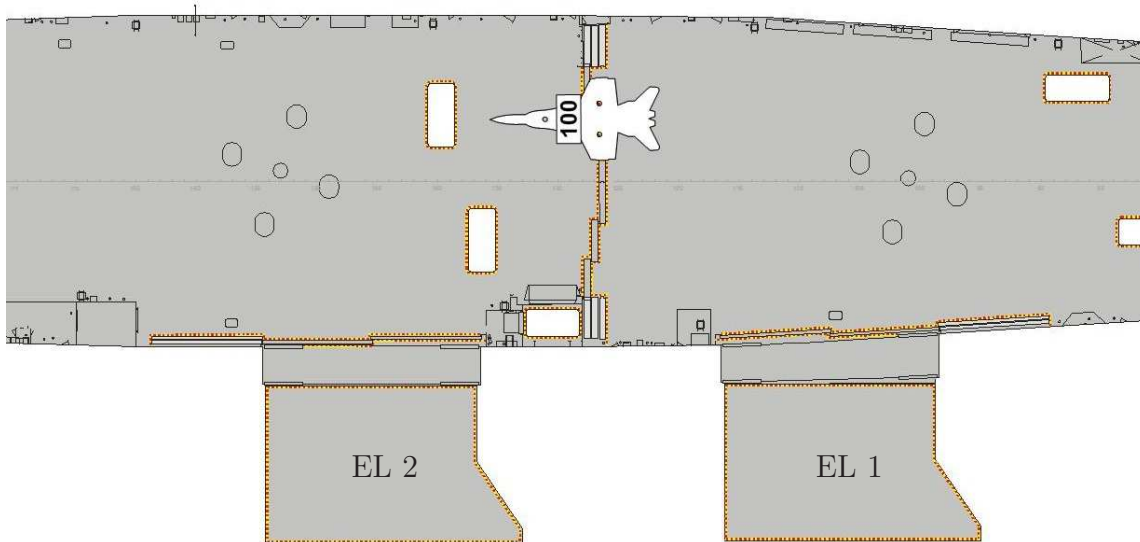
Figure 1.12:   Aircraft Parked Over the Track of Hangar Bay Door One [37]

status of flight deck surfaces, such as the elevation angle of a jet blast deflector or the location of an elevator. Many different types of RTLS could be leveraged to acquire this data including radio locating systems and optical scanning.

A computer system provided with the state measurements in the top two sections of Table 1.8 could be programmed to recognize many potential hazards and either prevent them or warn of their pending occurrence. For example, given an aircraft parked in the Hangar Bay across the tracks of Hangar Bay Door One as in Figure 1.12, the system could prevent the closing of Door One but allow the closing of Door Two if requested (assuming it is unobstructed). This principle can similarly be applied to Jet Blast Deflectors, Elevators, and Barricade Stanchions.

Such a system would also be able to track taxiing aircraft and warn of impending mishaps. Recalling the example of an aircraft turning near the edge of the Flight Deck in Section 1.1.1, the pilot would have two sources of information to ensure the nose tire does not go over the edge. If the system uses wingtip location measurements to calculate aircraft state, it may even be possible to determine the wingfold status of the aircraft by measuring the distance between wingtips. This could allow a Level One system to warn of impending Wingfold mishaps.

24

1.3.1.2 Level Two: Support Equipment. A Level Two system adds the ability to reduce or eliminate Towing mishaps and to further reduce Spotting mishaps. Many mishaps with collision damage to aircraft involve SE, whether it is a tow tractor, fire truck, power generator, or forklift. With a system that can determine the instantaneous position, orientation, and translational/rotational velocities of SE it would be possible to reduce the occurrence of many Spotting, Towing, and Non-aviation mishaps. For much of the larger SE, this could be achieved with a system similar to that used for Level One, but many smaller items of support equipment, such as weapon carts, may require different treatment.

By adding the state of SE to the system described in Section 1.3.1.1, warnings could be provided for pending mishaps involving the collision between SE and aircraft. Reports of unsafe operation of self-propelled SE, such as excessive speed or unnecessary proximity to aircraft, could be provided to personnel concerned. The location of smaller SE, such as ordnance carts, could be tracked to warn taxiing pilots of unsafe areas.

1.3.1.3 Level Three: Personnel. To improve the safety of flight deck operations for individual sailors, it would be beneficial to determine their instantaneous position and velocity relative to hazards caused by aircraft, SE, elevators, jet blast deflectors, and exhaust plumes. With the rapid, relatively erratic motion of personnel on deck as well as the requirement for close proximity to aircraft to perform many critical tasks, the detection of a potential mishap involving personnel could be the most difficult to determine. Such a system could serve to mitigate Contact mishaps and reduce the number of flight deck casualties.

If the system described in Section 1.3.1.2 is further enhanced to measure the point velocity and position of each sailor on the flight deck and hangar bay, many of the worst mishaps could potentially be prevented. Warnings to the sailor and leadership could be provided if any sailor gets within a specified perimeter of an aircraft with engines turning, especially for unauthorized personnel. If a sailor were

Figure 1.13: F-14 Tomcat Preparing for Launch: Of interest are two maintenance personnel immediately beneath the hot engine exhaust nozzles. Taken in 2004 by the author onboard USS John F. Kennedy (CV-67).

to fall or be forced overboard, the system could recognize that and inform the Bridge immediately. This capability is significantly more complicated than the prior two, as the intended motion of personnel is much more difficult to predict than that of aircraft or SE. Figure 1.13 illustrates the inherent difficulties in detecting potential personnel mishaps with sailors crawling under the aft end of the aircraft with engines turning prior to launch.

It is also critical that the identification of personnel be reported as well as their position. By combining the identification of each sailor with their position it will also be possible to ensure that they are only performing actions or in areas which their level of experience warrants. While an experienced squadron troubleshooter may need to crawl under a powered aircraft, the system should warn of a trainee performing a similar dangerous action.

1.3.1.4 Level Four: Aircraft System Status. Many Engine, Exhaust, and Wingfold mishaps could be prevented by remotely monitoring an aircraft's throt-

Table 1.9:   Mishap Cost by Category and Minimum Observation Level

Category	Total Reported Cost ($)	Mean Annual Cost ($)	Mitigating Level
Spotting	36,301,190	1,251,800	1
Towing	9,739,576	335,800	2
Taxiing	9,225,025	318,100	1
Exhaust	5,248,076	181,000	4
Contact	2,430,815	83,800	3
Engine	1,756,015	60,600	4
Wingfold	316,596	10,900	4
Non-aviation	35,883	1,200	2

tle or wingfold status. Utilizing a datalink to report necessary aircraft status information to Flight Deck Control could provide this capability. There are current systems to provide this information when an aircraft is powered, but it could prove beneficial to transmit this information when unpowered.

1.3.2   Benefits.   Using the mishap data from Naval Safety Center, this research aims to estimate the cost benefit of implementing such a system. Table 1.9 provides the cost of the different mishap categories and the lowest observation level which could reduce their occurrence. From the mean annual cost of each category and the observation level needed to reduce that category, the potential savings of employing a particular level can be determined as depicted in Figure 1.14. Recalling the issues with mishap cost data discussed in Section 1.2.4, the dollar amounts described represent the absolute lowest estimate of potential cost benefits.

Beyond the potential reduction in mishaps there are many additional, significant benefits to a persistent monitoring system. Such a system could ease the integration of UAVs into the Carrier Air Wing. The persistent monitoring system would track all vehicles, manned and unmanned, and could provide a flight deck "map" to unmanned systems. This could allow UAVs to plan a path to their designated position around obstacles such as other aircraft and personnel.
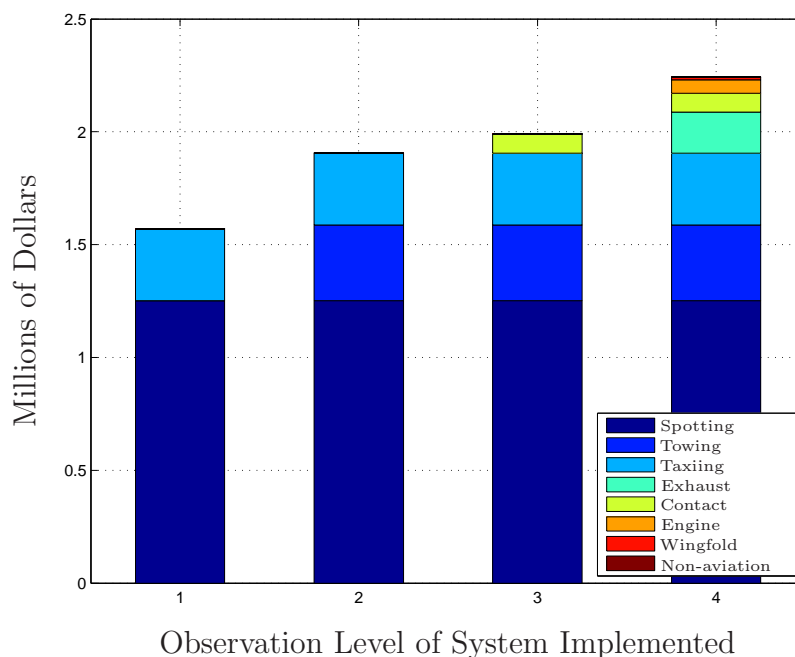
Figure 1.14:   Potential Annual Savings of Implementing Observation System

A persistent monitoring system could provide all levels of Naval leadership with accurate recordings of all flight deck activity. The current reporting system for mishaps does not document "near mishaps", or those which were narrowly averted. Recording and reporting "near mishaps" could become the primary mechanism in reducing potential mishaps. "Close calls" occur frequently, and if recorded and reported, they could contribute to preventing mishaps through changes in policy, training, and modifications to the hazard identification algorithms. A complete recording of flight deck activity would provide the Naval Safety Center with significantly improved documentation on the hazards of flight deck operations, especially for forensic analysis. It would also provide commanders with detailed records of personnel actions which can be used to document training and experience, as well as justify manpower requirements.

1.4 Research Discussion

This section discusses the objectives and assumptions of this research as well as the methodology used. An overview of this document is presented.

1.4.1 Research Objectives. This research intends to be a feasibility study in which the minimum requirements of a persistent monitoring system for parameters such as position and orientation measurement precision, translational and rotational velocity measurement precision, update rate, and computational power are examined to provide the capability of predicting and warning of potentially hazardous situations. These requirements are described in more detail in Chapters II and IV.

1.4.2 Assumptions. While this research is concerned with preventing mishaps aboard aircraft carriers, the tests to gather data were all performed ashore. It is assumed that the differences in aircraft tow procedures afloat and ashore are minimal. It is also assumed that the tow procedures performed at NAS Oceana, discussed in Chapter III, are representative of those used across the fleet.

1.4.3 Hypothesis. Mishaps onboard an aircraft carrier present a significant cost to the Navy and pose a significant risk to personnel. The implementation of a persistent monitoring system, able to measure the state of the flight deck, has the potential to recognize and prevent mishaps.

1.4.4 Methodology. Beyond evaluating and establishing the performance requirements, this research investigates methods by which the different Levels can be achieved using modern positioning, sensing, and communication technologies, but is primarily focused on the Global Positioning System (GPS). As an example, an analysis of the capabilities, limitations, and requirements to achieve a Level One system using one or more types of modern RTLS such as GPS and pseudo-GPS is performed. These systems could be combined with video or LIDAR data using sensor fusion to provide visual confirmation of reported positions. Chapter II describes the capabilities and limitations of such systems.

To demonstrate the ability of modern RTLS to measure the state of aircraft and personnel, a series of tests were devised for data collection at both the Air Force Institute of Technology (AFIT) and Naval Air Station (NAS) Oceana. Described

in detail in Chapter III, these tests used highly accurate civilian survey-grade GPS receivers to measure the position and orientation of an FA-18C Hornet being towed on the flight line by personnel with flight deck experience. The data collected provides an accurate depiction of USN aircraft movement procedures as well as the ability to develop software algorithms which can monitor for and warn of impending hazardous situations. The analysis of this data, described in Chapter IV, allows a determination of whether the positioning accuracy and noise levels of the receivers used are sufficient to predict paths for aircraft and personnel.

GPS was selected as the measurement source for this research as the survey-grade receivers used are considered to provide "truth data" for the purposes of surveying property. The persistent monitoring system envisioned by this research should be measurement source agnostic, such that any sufficiently accurate measurement source can be utilized.

1.4.5 Document Overview. This chapter presented an analysis of safety records showing the high risk associated with flight deck operations. A persistent monitoring system was proposed to potentially reduce the occurrence of mishaps. Chapter II provides a detailed overview of past and present research in fields related to the development of a persistent monitoring system. The tests conducted and equipment used are described in detail in Chapter III. The results of these tests are presented in Chapter IV with conclusions discussed in Chapter V.

(a) Flight Deck
(b) Hangar Bay

Figure 1.15:   CVN Flight Deck and Hangar Bay Without CVW [37]

(a) Flight Deck (b) Hangar Bay

Figure 1.16:   CVN Flight Deck and Hangar Bay With CVW (notional) [37]

II. Literature Review

This chapter presents a study of topics relevant to this research. Proposed computer-based systems to improve flight deck operations are discussed. Background information on RTLS such as the Global Positioning System (GPS) and similar pseudolite systems, as well as methods to determine the position and orientation of an aircraft based on known GPS receiver location are presented. Algorithms to provide warnings of hazardous situations are also discussed.

2.1 Flight Deck Systems

Little information is available in open literature on historical and current efforts to improve flight deck operations with computer-based systems. One possibility for this is the fact that the U.S. Navy is deeply rooted in tradition. The "Ouija Board" system of flight deck management described in Section 1.3.1 performs adequately and is well understood by the personnel involved. Another is that only recently, with significant advances in RTLS and computers, has a computer-based system to improve flight deck operations become practicable. This section discusses previous research into computer-based flight deck management systems, as well as current efforts to modernize flight deck operations.

2.1.1 Early Research. With a sensing system in place that is able to measure the flight deck state to one of the four levels discussed in Section 1.3, a means must be developed to use the state measurement to its greatest potential. Studies of methods to improve the communication of flight deck state to Flight Deck Control and other personnel concerned for 'man-in-the-loop' control were performed at the Naval Postgraduate School from 1974-1975 [13, 24], the only open literature found on the subject. These studies did not incorporate RTLS as precise positioning technology was just being developed.

In 1966, a report was published entitled *An Exploratory Study of an Automated Carrier Aircraft Deck Operation Control System* (CADOCS) [43]. This is the first de-
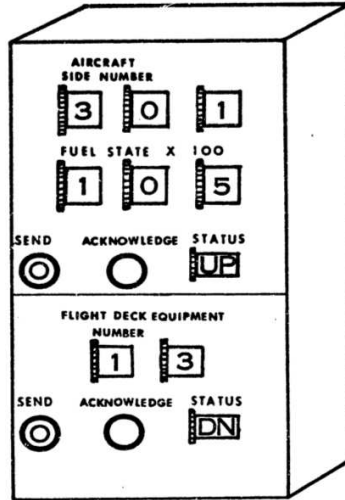
Figure 2.1: Proposed Handheld "Flight Deck Data Entry Device", Circa 1974: by Giardina [13, pg. 54] (from microfiche).

scription of an attempt at using computer systems to improve flight deck operations. It argued that since many flight deck management operations are repetitive in nature, they can be performed by a computer. It recognized that the quality of a solution provided by the computer is dependent upon the quality of the data it is provided. A variety of stationary and handheld devices used by flight deck personnel were recommended for data entry. An example of a proposed handheld device is depicted in Figure 2.1 [13, pgs. 9-10].

The CADOCS concept was further refined in 1967 by the report: *Systems Definition Study of Carrier Aircraft Deck Operations Control System* [25]. A system actually capable of generating the aircraft spotting plan for the entire flight deck based upon maintenance status and flight schedule requirements was proposed. Two of the unfavorable aspects of CADOCS described by Giardina in 1974 are: inaccuracy of position data and performance of existing computers [13, pgs. 10-13]. The CADOCS system was further refined in two additional reports [42, 44][1].

---

[1]The reports on CADOCS ([25, 42–44]) remain authorized for distribution only to government agencies. No information present in this research comes from them directly.

34
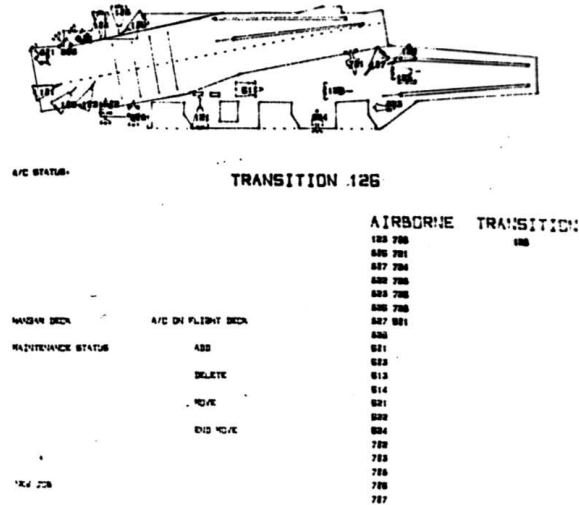
Figure 2.2:   Mock 'Flight Deck Status' Display, Circa 1975: Used in simulation created by Johnson and Woolley [24] (from microfiche).

Johnson and Woolley developed a computer simulation to allow the input and display of flight deck state [24]. Their 'Flight Deck Status' display is shown in Figure 2.2. Their software was capable of storing and displaying state information as entered by a user. With the limited computing technology available in 1975, this modest task required the maximum computing power available and was enormously costly.

Even with the limited computing power available when this research was performed, the conclusion was that an interactive computer interface provides the best means of distributing integrated information to all decision makers. Modern computers possess far greater flexibility and capability, such that the computations for the system proposed by Johnson and Woolley are trivial. A major concern of their research was the equipment used to input and display information. Modern computers, as depicted in Figure 2.3, support touch sensitive, high-resolution displays capable of accepting inputs from multiple users simultaneously. Such a system was recently used to coordinate security at a major sporting event [32]. Advances in RTLS allow modern computer systems to not only provide near real-time information of the flight

35

Figure 2.3:   Modern Multi-touch, Tabletop Display

Figure 2.4:   ADMACS Electronic "Ouija Board" [31]

deck state but also predict and warn personnel of potential hazards based upon the measured trajectories of aircraft, equipment, and personnel.

2.1.2   *Current Developments.*   A system currently installed on CVNs, Aviation Data Management and Control System (ADMACS), currently provides systems to track the flight schedule as well as visual records of launch and recovery operations. The Block 3 upgrade, scheduled for installation on USS Abraham Lincoln (CVN-72) in fiscal year 2010, will provide an automated, digital "Ouija Board". Measurements of aircraft position and orientation will be made by video analysis software. Expected accuracies of aircraft position measurements are approximately 0.3 m [31].

2.1.3   *Carrier-based Unmanned Aerial Vehicles.*   The problem of UAV incorporation on the flight deck is currently being actively pursued by many programs.

The Unmanned Combat Aircraft System - Carrier Demonstration (UCAS-D) is a UAV prototype to demonstrate aircraft carrier launch and recovery capabilities. The contract was awarded in August, 2007 with a carrier landing attempt planned for 2012 [7, pg. 74]. The method of providing positive control during flight deck operations is left to the vendor [34, pg. 36].

Venetsky, *et al.* performed an extensive study on the use of gesture recognition to enable UAVs to follow the directions of Taxi Directors, as pilots are trained to do. Each UAV would have a visual sensor mounted on it to watch its assigned director. There are significant obstacles such as low light, light source blooming, sun glare, steam, occlusion, and clutter. The results of the study are that such a system is feasible if visibility of taxi directors is augmented, sensors are placed high on the aircraft, and Taxi Director practices are more standardized [54].

2.2 *The Global Positioning System*

This section will provide a brief overview of GPS. It will focus on the basic system architecture, signals transmitted, methods of determining position, and errors in the solution. The risks inherent in a system that relies on GPS will be explored as well as the modernization efforts to mitigate these risks. Comparable foreign systems, such as the Russian GLONASS and Europe's Galileo, will not be discussed.

It is assumed that the reader is familiar with the terminology used to describe the orbit of a satellite. A comprehensive discussion of satellite orbits is provided by Vallado [53], while a more thorough description of GPS is provided by Misra and Enge [33].

2.2.1 Architecture. GPS is a passive radio navigation system based upon measuring the receiver's position from known radio transmitters, a method called trilateration, as depicted in Figure 2.5. Provided by the U.S. DoD, GPS allows users to accurately calculate position, velocity, and time. GPS was originally intended for U.S. military forces, but as of this writing, civilians are the primary user and it has
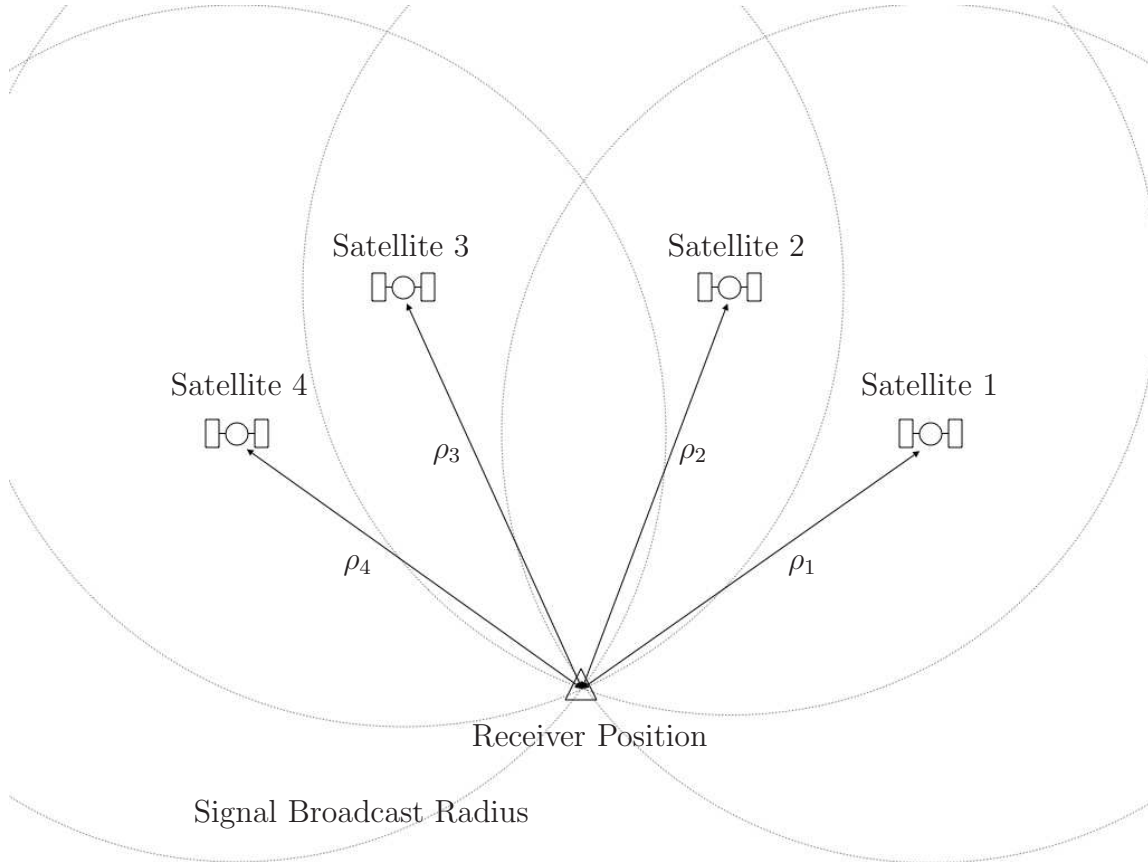
Figure 2.5:   Illustration of GPS Passive Radio Navigation: Tracing an arc of equal length from each satellite, the position of the receiver is the only point where every arc intersects.

become an integral component of the global economy [33, p. 32]. The system is divided into three segments: space, control, and user.

2.2.1.1 Space Segment.   A constellation of 24 satellites (nominal) transmit pre-defined code sequences, termed Pseudorandom Noise (PRN) code, which can be acquired and tracked by a GPS receiver. The satellites are in a near-circular orbit with a radius of 26,560 km. There are six orbital planes, each with at least four satellites. The orbital planes have an inclination of 55° from the equator. [33, p. 33]

The GPS satellite constellation was designed so that at least four satellites would be visible from any point on Earth at any time. It is more common that a user sees

six to eight satellites at any given time. Built with a design life of 7.5 years, most GPS satellites have doubled their expected functional lifespan. [33, pp. 33-34]

2.2.1.2 Control Segment. The GPS control segment serves to accurately monitor and predict the orbits of the satellites. Multiple tracking stations are deployed around the world to measure the satellite orbits. Without the services of the control segment, the accuracy of a GPS solution would be severely degraded [33, pp. 34-35].

Headquartered at Schriever Air Force Base, the Master Control Station is responsible for maintaining the currency and accuracy of information transmitted by the GPS constellation. Updates are normally transmitted to the satellites once daily [33, pg. 35].

2.2.1.3 User Segment. Anyone with a GPS receiver is part of the user segment. While originally designed to primarily support military users, the vast majority of users now are civilians. Aside from automobile and aircraft navigation, GPS is used in a wide variety of fields such as farming [16], geology [47], and atmospheric study [18].

The construction of receivers is the domain of corporations and businesses. Major manufacturers design and build their own hardware from the specifications provided by the GPS Interface Control Document (ICD-GPS-200C) [15].

2.2.2 Signals. Each GPS satellite transmits a pre-defined code on one of two radio frequencies termed L1 (1575.42 MHz) and L2 (1227.60 MHz) [33, p. 37]. The L2 frequency transmission, termed P(Y) code, is currently encrypted and intended for military use only. Some civilian receivers, such as those used in this research, are able to utilize L2 measurements via proprietary methods. The coarse/acquisition (C/A) code transmitted on L1 is used for the vast majority of GPS position solutions.

Table 2.1:   Orbital Parameters in GPS Ephemeris Message

Parameter	Explanation
M_0	Mean anomaly at reference time
Δn	Mean motion difference from computed value
e	Eccentricity
$A^{\frac{1}{2}}$	Square root of semi-major axis
Ω_0	Longitude of ascending node at weekly epoch
i_0	Inclination angle at reference time
ω	Argument of perigee
$\dot{\Omega}$	Rate of right ascension
$\dot{i}$	Rate of inclination angle
t_{0e}	Reference time ephemeris

The power of the signals transmitted by GPS satellites is extremely low, only 10^{-16} W of received power on the surface of the earth [33, pg. 42]. Receiving this signal is roughly equivalent to attempting to see a flashlight shined by an astronaut in orbit. The only way a receiver can pick the GPS signal out of the background noise levels is by knowing what signals to look for. Therefore, the Pseudorandom Noise (PRN) codes transmitted by the satellites are specified in the GPS Interface Control Document [15].

Each satellite also transmits an ephemeris message containing its orbital parameters and an almanac message containing the approximate orbital parameters of other satellites as well as the status of the GPS constellation [33, p. 126]. A section of the contents of the ephemeris message are contained in Table 2.1 [15, pg. 94]. This information is transmitted in a 50 bps stream, and the ephemeris for a single satellite can be transmitted in 30 seconds. The complete navigation message contains both almanac and ephemeris information. Split into 25 frames, each frame containing 1,500 bits, the complete navigation message takes 12.5 minutes to transmit [33, pp. 127-128].

2.2.3 Solutions.   There are three primary methods to utilize the signals transmitted by GPS.

2.2.3.1 Code Phase. The primary measurement intended for GPS is the transit time of a signal from the satellite to a receiver. This is the measurement used by the vast majority of commercial GPS receivers and requires the use of only one frequency.

Each satellite transmits a different, pre-defined sequence of 1023 bits, referred to as chips, and repeats it indefinitely for the C/A-code. A receiver generates the same sequence of chips and uses it to correlate with the broadcast signal. This allows the receiver to calculate the transit time of the signal [33, pp. 38-39].

Using the position of each satellite calculated from the ephemeris data $[x_k, y_k, z_k]$, the transit time of the signal t_k, and the speed of light c, it is possible to calculate the range to the satellite. Due to clock bias in the receiver, each calculated range is too long or short by an equal amount. Therefore the calculated ranges are called pseudoranges [33, p. 23]. The pseudorange ρ to the kth satellite can be calculated by

$$\rho_k = c \cdot \left(t_k + \Delta t_{corrections} \right). \tag{2.1}$$

The Newton-Raphson method can be used to solve the resulting system of equations for the receiver's position $[x_{rcvr}, y_{rcvr}, z_{rcvr}]$ by solving

$$\rho_k = \sqrt{\left(x_k - x_{rcvr}\right)^2 + \left(y_k - y_{rcvr}\right)^2 + \left(z_k - z_{rcvr}\right)^2} + b + \epsilon_k \tag{2.2}$$

where b is the receiver clock bias and ϵ_k represents unknown errors [33, p. 48].

Experiments have shown that the pseudorange solution is capable of three-dimensional position accuracy on the order of 4 m [33, p. 216]. While very effective, higher levels of accuracy are required for this research.

2.2.3.2 Doppler Shift. While it is possible to differentiate a time history of GPS position estimates to calculate a velocity profile, it is often desired to

determine an instantaneous velocity. This is possible using the principle of Doppler shift.

Satellites in the GPS constellation travel in their orbits at approximately 4 km/s. This motion provides a consistent doppler shift in the transmission frequency when a receiver is stationary. A receiver in motion can measure a difference from this nominal frequency. The receiver velocity $\bar{v}_{rcvr}$ can be calculated by

$$\dot{\bar{\rho}} = \underline{G} \begin{bmatrix} \bar{v}_{rcvr} \\ \dot{b} \end{bmatrix} + \tilde{\epsilon}_{\dot{\phi}} \tag{2.3}$$

where $\dot{\bar{\rho}}$ is a vector containing the rate of change of each pseudorange calculated, $\dot{b}$ is the rate of change in the receiver clock (m/s), and $\tilde{\epsilon}_{\dot{\phi}}$ represents errors in the pseudorange rate calculation. $\underline{G}$ is a matrix containing estimated line-of-sight unit vectors from the receiver to each satellite, given by

$$\underline{G} = \begin{bmatrix} -\hat{\mathbf{1}}_1 & 1 \\ -\hat{\mathbf{1}}_2 & 1 \\ \vdots \\ -\hat{\mathbf{1}}_k & 1 \end{bmatrix} \tag{2.4}$$

and

$$\hat{\mathbf{1}}_k = \frac{[x_k - x_{rcvr}, y_k - y_{rcvr}, z_k - z_{rcvr}]}{|\bar{x}_k - \bar{x}_{rcvr}|}. \tag{2.5}$$

The rate of change of each pseudorange can then be used to calculate local frame velocities just as pseudoranges are used to calculate local frame coordinates in Equation (2.2) [33, pgs. 203, 204, 218-219].

2.2.3.3 Carrier Phase. While code phase measurements use the chips contained in the unique signal of each satellite, carrier phase measurements use the difference in phase between the receiver generated signal and the signal received from

the satellite. Each chip of the C/A code is 293 m along the length of the broadcast signal, but a single cycle of the L1 frequency is only 19 cm [4, pg. 21]. This allows for a much more accurate measurement of the signal's transit time, leading to a more accurate position solution.

For a carrier phase measurement, the receiver must measure the initial fractional phase difference between the signals and track all changes to this measurement. This way the phase of a received signal can be related to the phase at time of transmission. The phase offset as a function of time $\phi(t)$ is computed from

$$\phi(t) = f \cdot \tau + N \tag{2.6}$$

where f if the carrier frequency and τ is the transit time of the signal, and N is the integer cycle ambiguity [33, pg. 153].

Carrier phase measurements are ambiguous, leading to the integer ambiguity term N in Equation 2.6. The integer ambiguity represents the number of whole cycles of the carrier signal, and based upon the calculated transit time τ it could be a large number of cycles. Resolving this integer ambiguity usually requires a stationary receiver in a known location which collects accurate data on the motion of available satellites [4, pg. 6]. The details behind carrier phase ambiguity resolution are beyond the scope of this document, but are given by Misra and Enge [33]. When using carrier phase a receiver is able to provide a position solution with centimeter level accuracy [33, pg. 234].

2.2.4 Errors. This section discusses the major errors in the GPS solution and methods to mitigate them. These errors must factor significantly into any persistent monitoring system implemented for the flight deck if it used GPS or another radio navigation system. Errors in the GPS solution generally fall into one of three groups [33, pg. 155]:

1. Broadcast message errors,

2. Signal propagation uncertainty, and

3. Measurement errors.

Broadcast message errors typically are associated with incorrect parameters in the ephemeris message [33, pg. 156]. The prediction of satellite orbits is very accurate for the two-body problem, where only the Earth and a satellite are considered. However, each satellite is affected by the gravity of every celestial body. Corrections for many of these factors are contained within the broadcast ephemeris message, such as the effect of lunar and solar gravity which can account for 25 m of orbital perturbation after only one hour [33, pg. 124-125]. Currently, the broadcast ephemeris can provide 2 m accuracy in pseudorange measurements [33, pg. 127].

Signal propagation uncertainty errors are caused by the Earth's atmosphere's ability to change the velocity of radio signals, and the pseudorange method described in Section 2.2.3 requires a constant signal velocity. The upper layer of the atmosphere, from 40-100 km, is known as the ionosphere and contains free electrons which can slow the speed of a radio wave. The lower region of the atmosphere, or troposphere, is much denser and contains relatively large amounts of water which can refract a radio signal. The effects of both the ionosphere and troposphere vary with time and location on the Earth [33, pg. 157-158].

There are two primary measurement errors which affect a receiver: noise and multipath. Receiver noise is the reception of unrelated signals in the frequency band of interest. The receiver can only see the sum of the signal of interest and the noise received with it. If the noise is strong enough, the receiver could lose lock on the signal, or if their signal strength is of the same order, the signal could be misinterpreted. Signals from satellites low on the horizon are received with less power than those with higher elevation angles and are more prone to noise [33, pg. 175].

Multipath is the greatest error source in GPS, after applying correction factors, as of this writing. It is caused by the reflection of a GPS signal so that it reaches a receiver on multiple paths. Receiving the same signal at multiple times, such as

receiving the line of sight signal and one reflected from the ground, adds the additional reflected distance to the pseudorange measurement. In highly reflective environments, such as the flight deck of an aircraft carrier, the error in pseudorange measurements can be as great as 5 m while carrier phase measurement errors can be as high as 5 cm [33, pg. 175-177].

2.2.5 *Error Mitigation.* Each of the error sources listed in Section 2.2.4 can be corrected for or mitigated through a variety of techniques. This section will provide a background on GPS error mitigation techniques.

The correction of broadcast message errors is the domain of the Control Segment, and improvements in satellite tracking will provide improved measurements to all users, without the need for a receiver upgrade. As an example, when six monitoring stations operated by the National Geospatial-Intelligence Agency (NGA) were added in 2005 the quality of predicted orbits was improved [33, pg. 126]. Another method to improve the estimate of satellite locations is to use precise ephemerides, produced by the NGA and the Naval Surface Warfare Center. These are post-processed satellite position measurements, which after only three hours for calculation and dissemination, can provide satellite position errors of less than 5 cm [33, pg 127].

The errors caused by the troposphere and ionosphere can be mitigated, with varying success, by applying modeled error corrections. The *Klobuchar model* can be used to model ionospheric errors using parameters contained in the broadcast navigation message. This model is able to reduce the pseudorange measurement error by nearly 50%, but this can be 10 m on a normal day [33, pgs. 168-169]. Tropospheric errors can also be mitigated by a model or mapping function, yielding a residual error of 5-10 cm.

If a receiver is capable of acquiring both GPS frequencies, then the ionospheric error can be effectively eliminated. Each frequency is affected differently by the ionosphere, so the signal delay can be calculated [33, pg. 166]. This actually allows for

Table 2.2:   Effect of Differential GPS on Measurement Errors

Source	Potential Size (m)	Residual Error (m)
Ephemeris	2	0.1
Ionosphere	2-10	0.2
Troposphere	2.5	0.2

precise, continual tracking of ionospheric activity, as well as improving the position solution [18].

2.2.6   *Differential GPS.*   Given a GPS receiver in a known position, referred to as a base station, it is possible to estimate the errors discussed in Section 2.2.4 that are present in the solution [33]. For a near real-time differential GPS correction, it is necessary to have a datalink between the base station and the mobile receivers to which the corrections are to be applied. Many commercial survey-grade receivers, including those used in the tests described in Chapter III are capable of applying differential corrections in near real-time. It is also possible to apply the corrections to recorded data in post-processing. This can be done by software such as NovAtel Waypoint GrafNav™ [40] or GPStk [51].

The use of differential GPS corrections significantly decreases the amount of error in the position solution, as shown in Table 2.2. The errors estimated by the base station are only valid for measurements made near the base station, but in the case of an aircraft carrier flight deck all measurements would be made near the base station. The use of differential GPS also provides measurements needed for carrier phase integer ambiguity resolution, as discussed in Section 2.2.3.3. When they are combined the solution is often referred to as Carrier-Phase Differential GPS (CDGPS) [4, pg. 6].

2.2.7   *Solution Quality.*   The geometry of the GPS satellites used by a receiver for its solution has a significant impact on its precision. GPS satellite geometry refers to the configuration of the visible constellation, such as satellite elevation rel-

ative to the horizon, angular separation, and total number of visible satellites. A "good" satellite geometry would have $6 - 8$ satellites all above $15 - 18°$ elevation, and with at least $5 - 10°$ of angular separation between satellites. As discussed in Section 2.2.4, measurements made using signals from satellites low on the horizon are more susceptible to tropospheric error. The satellite geometry can be quantified by the matrix $\underline{H}$ [33, pg. 207], calculated by

$$\underline{H} = \left(\underline{G}^T \underline{G}\right)^{-1} \tag{2.7}$$

where $\underline{G}$ is given by Equation 2.4. The geometry quality measurement, or Dilution of Precision[2] (DOP) can be calculated from the elements of $\underline{H}$ by

$$D = \sqrt{H_{11} + H_{22} + H_{33}}. \tag{2.8}$$

DOP is useful as a simple, scalar measure of the satellite geometry used in the solution. A lower DOP implies a better satellite geometry. The GPS Control Segment provides maps showing nationwide and worldwide maximum DOP. An example is given in Figure 2.6.

2.2.8 Limitations. There are many limitations to the use of GPS. Due to the weak signal strength a receiver generally requires a clear, unobstructed view of the sky. This generally prevents GPS from being used for indoor positioning. Another limitation is the requirement for continual updating of GPS ephemeris data by the Control Segment. The Control Segment has continuously updated ephemeris data for over twenty years, but it is presented as a limitation because it is a single point of failure.

A limitation which is the subject of much discussion by military users is the jamming of GPS signals, especially intentional jamming by enemy forces. Simply

---

[2]For this research, the term DOP is synonymous with Position DOP, or PDOP.

Figure 2.6:   World DOP Assessment [52]

broadcasting a high power signal on the L1 frequency can prevent the acquisiton of GPS signals by all users in range.

2.2.9 Modernization. Efforts to modernize GPS, first announced in 1998, have the potential to significantly improve its performance for all users, military and civilian. For civilian users, an unencrypted signal will be broadcast on the L2 frequency, called L2C. The first satellite capable of broadcasting L2C was launched in 2005. This will allow for civilian receivers to eliminate ionospheric error in a manner similar to military receivers. In addition, a new signal, L5 will be broadcast on 1176.45 MHz. It it a wider bandwidth signal, allowing for better carrier phase positioning, and will be broadcast with more power than L1 or L2 signals [33, pgs. 73-77].

These improvements, when completed, will enable the mass production of receivers that have the capability of advanced military or civilian surveying systems. Given the worldwide demand for precise positioning, it is likely that receivers with dramatically increased position accuracy will be available in extremely small form factors.

2.3   Pseudolite Positioning

As discussed in Section 2.2, precise positioning with GPS ($\bar{e} \leq 1$ cm) requires a carrier-phase solution and a differential correction. Pseudolites provide a method of achieving precise positioning that does not depend exclusively on the GPS constellation. This section will provide a brief description of the theory behind pseudolites, their benefits, and limitations. A more thorough overview of pseudolites is provided by Cobb [4].

2.3.1 Theory. Pseudolite is a term used to describe a radio broadcasting system, not in orbit, which transmits signals capable of being used by a RTLS (generally GPS) receiver. Pseudolites operate on the same principle as GPS: trilateration. When GPS was being developed pseudolites were used in place of unlaunched satel-

49

lites [4, pg. 13]. Given sufficient pseudolites in known locations a code or carrier phase solution can be computed using the same algorithms described in Sections 2.2.3.1 and 2.2.3.3, and differential corrections can be provided. A pseudolite can generate its own PRN code, or simply rebroadcast a replica of a received signal [4, pg. 28]. Using a pseudolite system with rebroadcasting, navigation is possible with three pseudolites and only one GPS satellite [4, pg. 34].

2.3.2 Benefits. The primary advantage of pseudolites is that they don't need to be launched into orbit. Satellite launches cost millions of dollars, but a pseudolite can be made operational for roughly $1,000 [4, pg. 9]. Furthermore, pseudolites are not governed by orbital dynamics and can be placed in any configuration desirable, as long as there is sufficient structure to support them. Pseudolites are able to provide positioning indoors where GPS satellite signals cannot be received, and are even used in subterranean mining operations [4, pg. 125].

Pseudolites do not have to transmit GPS compatible signals. Position solution accuracy could be improved by increasing the chipping rate for code phase measurements or the carrier frequency for carrier phase solutions. Increasing the frequency by a factor of ten would allow for carrier phase accuracy at the sub-millimeter level [4, pg. 130].

2.3.3 Limitations. Recalling from Section 2.2.2 that GPS signals are received with extremely low power levels, having a pseudolite nearby can overwhelm a receiver with broadcast power. Cobb's Near/Far Problem describes a scenario where a receiver far away from the pseudolite cannot track its signals, but a receiver near the pseudolite cannot receive signals broadcast by GPS satellites [4, pg. 50]. Between these near and far boundaries both GPS satellite and pseudolite signals can be received. Most consumer GPS receivers, designed for the low power of GPS satellites, do not possess the dynamic range needed to receive GPS and pseudolite signals simultaneously [4, pg. 53].

There are numerous methods to mitigate the Near/Far Problem. Pseudolite signals can be transmitted outside of the L1 or L2 frequency bands, or simply offset [4, pg. 58]. The pseudolite transmission frequency can also *hop* between different regions of the L1 or L2 bands. The mitigation technique which can virtually eliminate the constraints of the Near/Far Problem is to use pulsed pseudolite signals [4, pg. 6]. For this method, the pseudolite is simply designed to transmit a certain percentage of the time. According to Cobb, most existing receivers would track both GPS satellite and pseudolite signals given the proper percentage [4, pg. 62].

One other limitation of pseudolites is geometry. While tropospheric errors aren't a concern due to the relatively short distances involved, the need for signals from high above the horizon is still present. Using exclusively ground based pseudolites, altitude could not be determined, and an altitude would need to be assumed to determine the two-dimensional position.

Pseudolite receivers are also susceptible to multipath error. In reflective environments, such as the flight deck of an aircraft carrier, the effect of multipath error on the position solution may be increased, depending on the transmission power and frequency used.

2.4 Blue Force Tracking

The persistent monitoring system proposed by this research shares many features of the U.S. Army's Blue Force Tracking (BFT) system. BFT uses GPS and satellite communications to relay the positions of U.S. and coalition forces to each other as well as command headquarters [45]. Similarly, the persistent monitoring system proposed here would provide Flight Deck Control with an accurate measurement of the state of the flight deck. There are significant differences in scale, communication range, and accuracy required.

The Army planned to field 40,000 tracking systems by 2008 [45]. Each of these systems communicate via L-band communication satellites to provide near real-time

information to commanders anywhere in the world [50]. This presents a significant use of the military's available satellite communications capacity. To meet the goals of BFT, precise GPS measurements are not required; the accuracy provided by pseudorange measurements is sufficient. Additionally, since not all combat operations take place outdoors, BFT units utilize an inertial measurement system when GPS is unavailable.

One significant issue with BFT has been the lack of interoperability [45]. Systems used by ground vehicles and rotary-wing aircraft often can't communicate [50]. An entirely different project, the Movement Tracking System (MTS), locates supply and maintenance vehicles and was not compatible with most BFT systems. The United States Marine Corp (USMC) used the Mobile Data Automated Communications system and had to install BFT systems during Operation Iraqi Freedom so they would be visible to coalition command centers [45].

The principle of BFT is "that if you could display your location, your buddies' locations and, with intelligence, enemy locations, commanders and soldiers could achieve a level of communication and information integration that would let you focus on your real jobs - commanding and warfighting." [49]. Users of the system, from the Army, USMC, and United Kingdom claim it saved lives and simplified coordination [45].

2.5 Determining Position and Orientation

The position and orientation of an aircraft relative to a fixed location on the deck can be determined using two GPS receivers mounted on the wingtips. Since the aircraft is not flying, its roll and pitch can be ignored and the problem can be treated as two-dimensional. In Figure 2.7, the position of each receiver on the wingtips is denoted by (x_1, y_1) and (x_2, y_2). The length of the wingspan b applies a constraint to the receiver positions given by
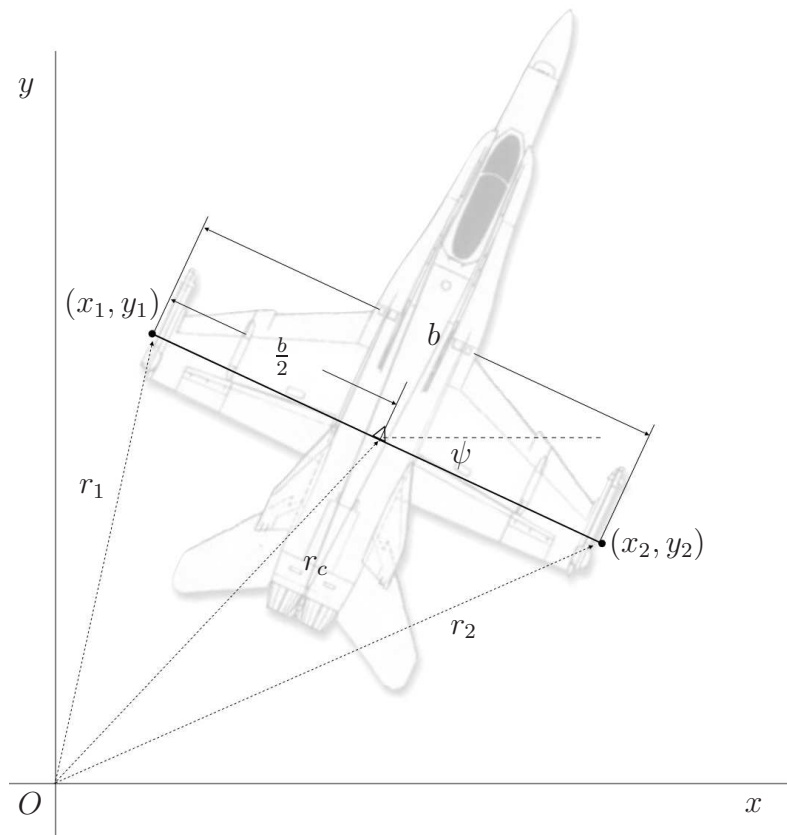
Figure 2.7:   Determining Position and Orientation: Applicable to an aircraft with wingtip mounted receivers.

$$b^2 = (x_2 - x_1)^2 + (y_2 - y_1)^2 . \tag{2.9}$$

Using vector addition, the following relationships can be derived from Figure 2.7

$$(x_1, y_1) = (x_a, y_a) - \frac{b}{2} (\cos \psi, \sin \psi) \tag{2.10}$$

and

$$(x_2, y_2) = (x_a, y_a) + \frac{b}{2} (\cos \psi, \sin \psi) \tag{2.11}$$

where (x_a, y_a) is the location of the aircraft's center and ψ is the aircraft's heading measured from the x-axis. Subtracting Equation 2.10 from Equation 2.11 yields

$$(x_2 - x_1, y_2 - y_1) = (b \cos \psi, b \sin \psi) . \tag{2.12}$$

Rearranging Equation 2.12 provides

$$\frac{b \sin \psi}{b \cos \psi_n} = \tan \psi = \frac{y_2 - y_1}{x_2 - x_1} \tag{2.13}$$

and

$$\psi = \arctan \left(\frac{y_2 - y_1}{x_2 - x_1} \right) . \tag{2.14}$$

With ψ calculated by Equation 2.14 the center position (x_a, y_a) can be calculated by rearranging Equation 2.10 which yields

$$(x_a, y_a) = (x_1, y_1) + \frac{b}{2} (cos\psi, sin\psi) . \tag{2.15}$$

2.6 Determining Distance - The Nearest Neighbor Problem

Given coordinate sets (x_1, y_1, z_1) and (x_2, y_2, z_2) describing the location of two points in three-dimensional Euclidean space relative to some reference frame, the distance between the points can be calculated by the Euclidean- or two-norm from

$$r = \sqrt{(x_2 - x_1)^2 + (y_2 - y_1)^2 + (z_2 - z_1)^2}. \tag{2.16}$$

When determining the distance between two three-dimensional objects, one must first determine which point(s) describing the object should be used. For objects whose size is much smaller than the distance between them, it may be desirable to use the center of mass. For the case where personnel are moving in close proximity to an aircraft, using the aircraft's center of mass does not provide a useful solution. A more useful calculation of distance between personnel and the aircraft requires the determination of the closest point on the aircraft to the personnel. This is a common problem in algorithms known as the Nearest Neighbor or Post Office Problem [1]. Figure 2.8 illustrates the concept of the Nearest Neighbor Problem in two dimensions.

To issue warnings to personnel in hazardous situations, it is necessary to know when personnel are dangerously close to hazardous regions around an aircraft, such as exhaust plumes, engine intakes, etc. Determining which point describing the outline of an aircraft to use for the distance measurement creates a challenging problem. A simple first approach at a solution, best described as a "brute force" approach, is to calculate the distance to every point using Equation 2.16 and then use the smallest resulting value as the distance between the personnel and aircraft. This is usable for aircraft outlines with relatively few points, but as the resolution of the outline increases, the computing power required for this solution will grow with it.

2.6.1 Nearest Neighbor Computation Time. According to Arya, *et al.* [1] the amount of computation time required for the "brute force" approach is on the order of $O(dn)$ where d is the dimension of the vector representing each point, n is
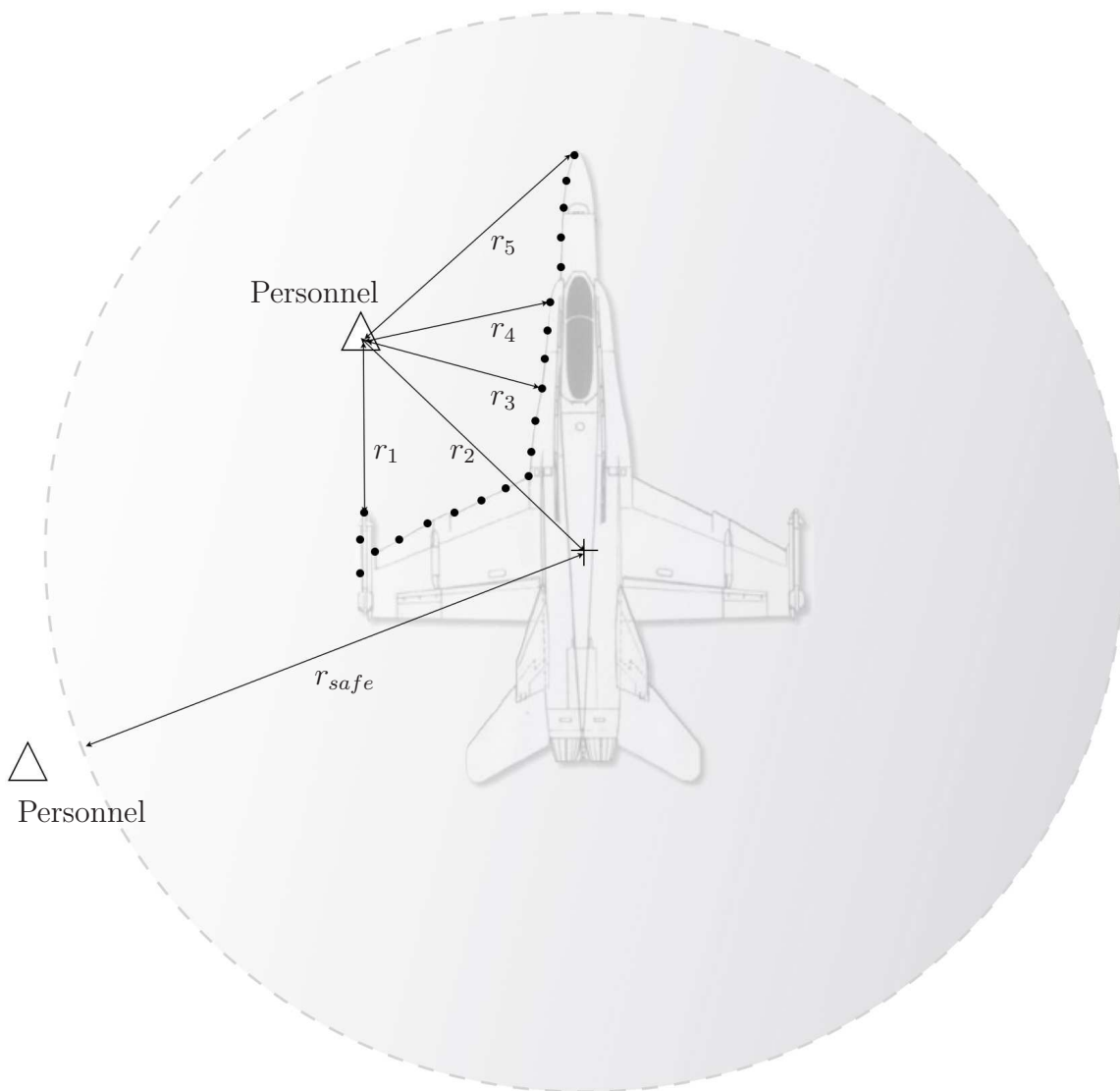
Figure 2.8:   The Nearest Neighbor Problem: How to find which point on the aircraft to use for distance calculation.
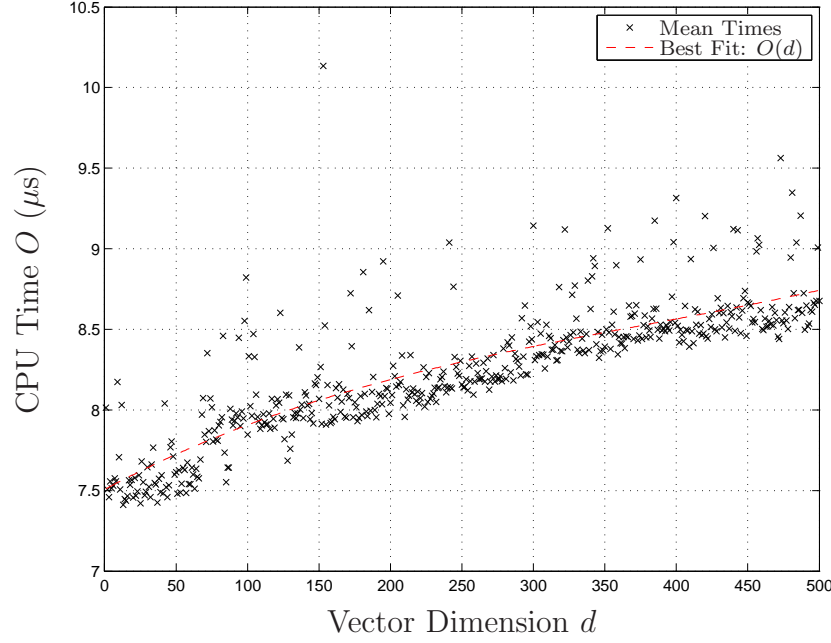
Figure 2.9:   Time to Calculate Euclidean Norm

the number of points to be evaluated, and $O(d)$ is the time required to compute the distance between two points. To determine $O(d)$ for the MATLAB® norm function, a series of 500 norms were computed for vectors of increasing dimension and the time to calculate measured and stored. This process was repeated 1,000 times, and the mean calculation time for each size vector was computed. The results are presented in Figure 2.9[3]. Listing B.1 on page 151 provides the MATLAB® source for this operation.

Fitting a polynomial to the collected data in a least-squares sense provides the equation for $O(d)$ plotted in Figure 2.9. The nonlinear coefficients of $O(d)$ are extremely small, so the mean computation time required for a single distance calculation measured in μs can be approximated by a linear function, given by

$$O(d) \simeq 0.0047 \cdot d + 7.5063. \tag{2.17}$$

This research is primarily concerned with planar and spatial positioning, so only the two- and three-dimensional nearest neighbor solutions are to be evaluated. From

---

[3]Calculations performed on 1.6 GHz Intel Core 2 Duo with 2 GB SDRAM

Equation 2.17, the mean computation times for the two- and three-dimensional cases are 7.5157 and 7.5204 μs, respectively. The three-dimensional case represents a 0.06% increase in computation time. This is a trivial increase, so the use of three-dimensional models does not incur a significant performance decrease over two-dimensional models.

The number of points used to describe the aircraft can have a significant impact on the calculation time. For an aircraft model with n points, the time required for the "brute force" approach is described by $O(dn)$, and while the linear approximation of Equation 2.17 holds for $dn \leq 500$, for two- and three-dimensional models that is only 250 and 166 points, respectively. Given a higher resolution three-dimensional model, where $n = 100,000$, the mean computation time would be significant. Clearly, when the motion of approximately 100 personnel around 65 aircraft is considered, this may require extensive computational power.

2.6.2 Nearest Neighbor Algorithms. The Nearest Neighbor problem has been discussed in computer science literature for decades, with much of the early work being done by Friedman, *et al.* in 1975 [12]. Before discussing algorithms in detail, it is important to describe the terms used and their relation to this research. *Prototypes* are the set of points from which the nearest is desired, or in this research the set of points describing the geometry of an aircraft or hazard. The *test point* is the point from which the nearest neighbor distance is to be calculated, or in this research the personnel on the flight deck.

The work of Friedman, *et al.* [12] provides an algorithm which projects each point along one coordinate axis. Each prototype is examined based on its projected distance, along the sorted coordinate, from the test point. If the distance of a prototype from the test point along this axis is greater than the full-dimensional distance of previously analyzed prototypes, then no more prototypes need be considered.

As an example, consider the two-dimensional case with a test point at the origin $(x, y)_{tp} = (0, 0)$. The prototypes described by projected points $(x, y)_p = (-3, 3)$, $(-1, 0)$, $(0.5, 0.5)$, $(2, 3)$, and $(3, 2)$ are sorted in order of their x-values. It is possible

to start the algorithm with any point, but for this example the second point will be selected. Computing the distance of the second prototype from the test point using the Euclidean norm of Equation 2.16 yields a distance of 1. Now any prototypes for which $abs(x) > 1$ can be eliminated. This leaves only one other prototype to consider, $(0.5, 0.5)$. Compute the distance of all remaining prototypes from the test point and the prototype with the smallest distance value is the nearest neighbor. Clearly $(0.5, 0.5)$ is the nearest neighbor as its Euclidean distance from the origin is $\sqrt{\frac{1}{2}}$. The efficiency of this algorithm comes from eliminating, in this example, three of the five prototypes after only one distance calculation.

The result of tests performed by Friedman, *et al.* show that in a two-dimensional case only 20% of the CPU time needed for a "brute force" search is required for 100 prototypes and 4.5% for 1000 prototypes. In the three dimensional case the percentages of the "brute force" times required are 30% and 10%, respectively. Clearly, this provides significant savings as the resolution of aircraft model geometry increases.

Current research on the Nearest Neighbor problem focuses on high-dimension searching. Friedman, *et al.* showed in 1977 that computation times of $O(\log n)$ are achievable, but only for lower dimensions. [1]. Since higher dimensions are not relevant to this research, well established algorithms for lower dimension nearest neighbor analysis can be used without sacrificing computational efficiency.

2.7 Path Planning

Path planning refers to the process of using a computer to calculate a path from one state to another while following specified rules. For a persistent monitoring system to warn of pending hazards, it would need to be able to predict the path of aircraft taxiing or being towed on the deck. Path planning is usually presented in literature as a two-dimensional translational motion problem. As an example, a vehicle lies on a plane, such as a car in a parking lot, and starts at point $(0, 0)$. It is desired for the vehicle to go to point $(100, 100)$. The obvious solution is a straight line, but it is not always possible as there may be obstacles or boundaries the straight
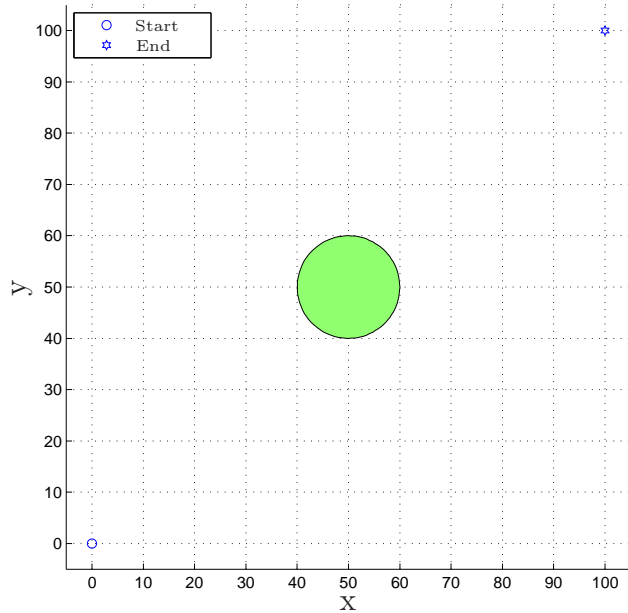
Figure 2.10:   Path Planning Example Scenario

line crosses. For this example, there exists a circular obstacle of radius 10 with its center at point $(50, 50)$. This scenario is depicted by Figure 2.10.

This section will present an overview of path planning algorithms. A simple example will be provided and its limitations will be discussed. A more robust and powerful method, developed by Ross, *et al.* [29] will also be discussed.

2.7.1   Simple Example.   Given the scenario depicted by Figure 2.10, it is possible to plan a simple path which avoids the obstacle and attains the desired state $(x, y)_f = (100, 100)$. The method presented here is described by Fox, *et al.* [11]. This example will illustrate many of the basic principles of path planning as well as the limitations of linear approaches.

The first step is to generate an initial path. This is simply a line from the start point to the end point, described by $y = mx + b$ where m is the slope of the line and b the y intercept. It is clear that in this simple example $m = 1$ and $b = 0$.

Next, the initial path must be checked for collisions with any obstacles. A series of test points are chosen along the initial path. Starting with the test point nearest

60
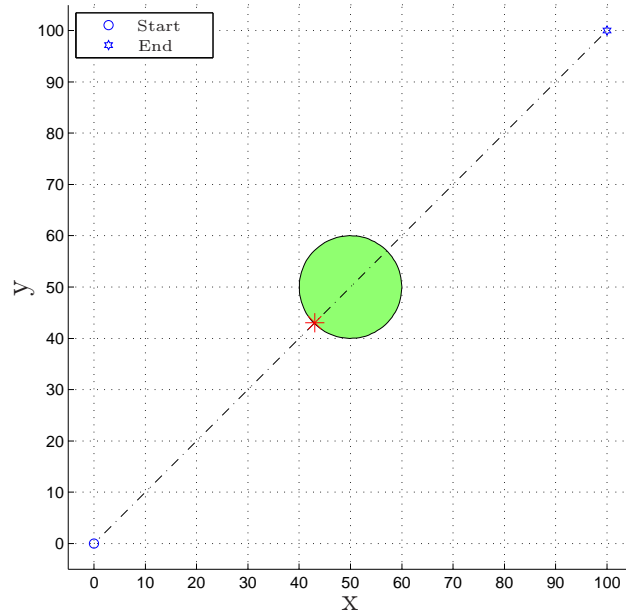
Figure 2.11:   Path Planning Example Scenario: First Collision

the start point, the Euclidean distance, calculated using Equation 2.16, between each test point and the center of each obstacle is calculated. If the calculated distance for any point is less than or equal to the radius, then a collision has occurred at that point. Figure 2.11 shows the first collision detected along the initial path for the example scenario.

Since a collision was detected the initial path cannot be used and an alternative must be found. The next step in this simple method is to attempt a navigation of the object by setting a re-routing point some step distance from the detected collision point along a line perpendicular to the initial path. For this example, the step distance is 60% of the obstacle radius. For this, the obstacle size must be known *a priori*. Then two straight lines are formed: one which connects the start and re-routing point, and one which connects the re-routing point and the end point. The latter line must then be checked for collisions with the obstacle. This is shown in Figure 2.12.

This process is repeated until no more collisions are detected. For this example, only one more iteration is required using the same step distance. The final path is shown in Figure 2.13. This algorithm can be extended to operate in three dimensions
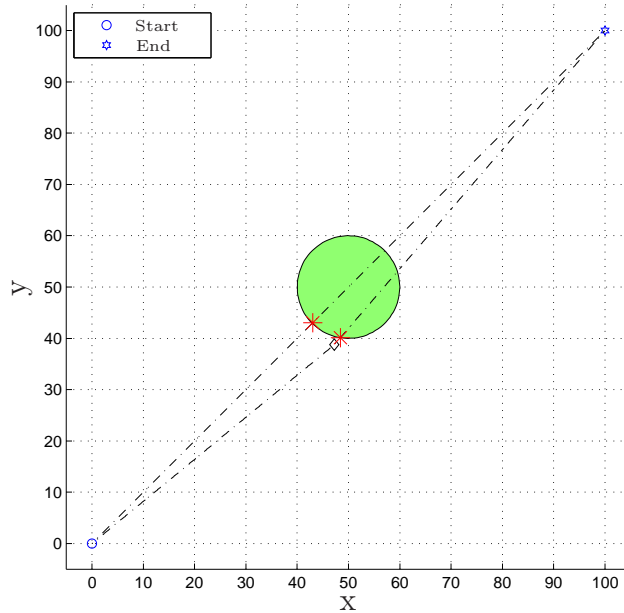
Figure 2.12:   Path Planning Example Scenario: Second Collision

and with obstacles other than circles. It will find a path for a sufficiently simple arrangement of obstacles.

This simple algorithm has many disadvantages and limitations. It requires complete knowledge of the environment, and the environment must be stationary, and yet this knowledge is not used to its full extent. It also makes no consideration for vehicle dynamics. The step distance can be arbitrarily large or small, and may have no basis in the capabilities of the vehicle for which the path is being planned. Additionally, the inability of this simple algorithm to find a path which avoids all obstacles is insufficient to prove a path does not exist.

2.7.2   Proposed Methods.   The focus of much path planning research is in the area of robotics. Areas of focus include wheeled mobile robots [28] and UAVs [56]. The algorithm illustrated in Section 2.7.1 is used in the Strategic-Tactical-Execution Software Control Architecture (STESCA) created by Fox, *et al.* [11]. Other approaches utilize probabilistic knowledge of hazardous areas [10] or pick control inputs at ran-
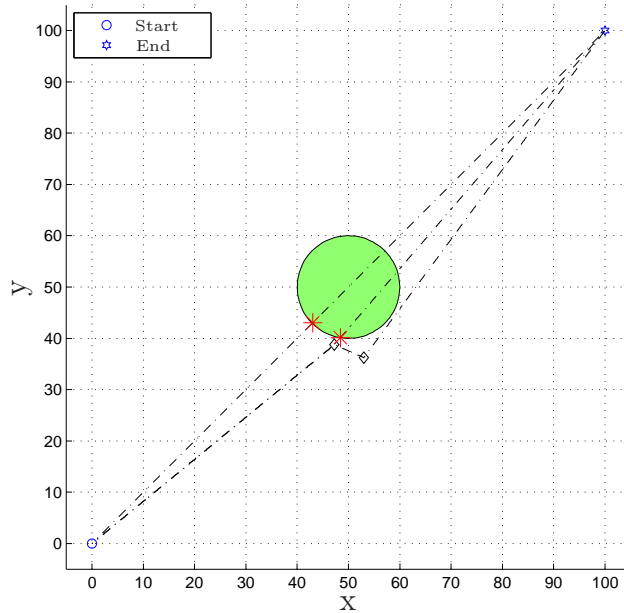
Figure 2.13:   Path Planning Example Scenario: Collisions Avoided

dom [19]. Extensive research has been conducted to determine the optimal, or near-optimal, path for vehicular travel [26, 56].

One of the best known path planning algorithms, introduced by Stentz in *Optimal and Efficient Path Planning for Partially-Known Environments* [48], is known as D*. The path generated by D* will have the minimum cost associated with its traverse. This cost can be defined in virtually any manner; travel time, fuel consumption, and route distance are all valid components of cost.

2.7.3 DIDO.   A similar approach to the path planning problem, solving for the optimal path and the associated controls based upon vehicle dynamics, is proposed by Ross, *et al.* [14, 29]. This method allows obstacles to be of arbitrary size, number, and shape. It approaches the path planning problem as a constrained nonlinear optimal control problem and solves it using pseudospectral computational methods [29]. Ross, *et al.* have developed a MATLAB® toolbox, called DIDO, to determine the optimal path for a given scenario.[4]

---

[4]DIDO is available from `http:\\www.elissar.biz`.

DIDO allows for the computation of an optimal state trajectory through an n-dimensional state space. The states are not limited to location on a Cartesian plane but can be any parameters used to describe the configuration of a dynamic system such as angles, quaternions, and energy levels [46]. Given the dynamics of the states, DIDO minimizes a cost function $J(\bar{x}, \bar{u}, t)$ such that $h_i(\bar{x}) > 0$ where $\bar{x}$, $\bar{u}$, and t represent the states, inputs, and time, respectively. For the two-dimensional translational motion problem with states $x(t)$ and $y(t)$, Ross *et al.* represent an obstacle by [30]

$$h_i(x(t), y(t)) = \ln\left(\left|\left(\frac{x(t) - x_o}{a}\right)^p\right| + \left|\left(\frac{y(t) - y_o}{b}\right)^p\right|\right) \qquad (2.18)$$

where x_o and y_o are the center location of the obstacle, a and b are its width and height, and p determines its shape. For $p = 1$, the resulting obstacle is a diamond, $p = 2$ yields a circle, and $p = \infty$ results in a square [30]. Any point outside of the obstacle areas will have a value of $h > 0$ [29].

The example problem of Section 2.7.1 can be solved quite easily by DIDO. The optimal path as computed by DIDO is shown in Figure 2.14. This path was computed using a set of MATLAB® scripts provided in Appendix B. The problem definition file, Listing B.2 on page 152, sets the constraints on the states as well as the location of the obstacle. The events file, Listing B.3, sets the initial and final states. Path constraints are determined by Listing B.4 and the system dynamics are set by Listing B.5. The cost J to minimize is determined by Listing B.6 on page 157. For this example, the goal is simply to minimize the final time as given by

$$J(\bar{x}, \bar{u}, t) = t_f \qquad (2.19)$$

64
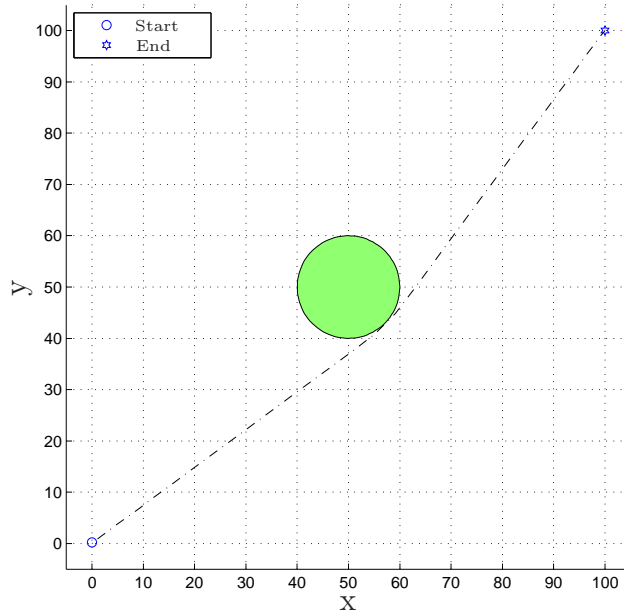
Figure 2.14:　Path Planning Example Scenario: DIDO Sample

2.8　Articulated Vehicle Kinematics

When an aircraft is being towed, it is essentially a passive trailer of the tow tractor. Its nose wheel is linked by a tow bar to the rear hitch of the tow tractor. The system, comprised of the aircraft, tow bar, and tow tractor, is a three-body articulated vehicle. As this research aims to study path planning for the towed aircraft system it is vital to develop an expression for its kinematics.

2.8.1　Single-body.　　When an aircraft is taxiing, the motive force is provided by engine thrust, and its direction is controlled by the angle of the nose wheel. Similarly, a tow tractor is propelled by the rear axle and its direction of travel is controlled by the forward wheel turn angle. The kinematics of each of these vehicles can be represented as a tricycle, with a velocity input applied at the rear axle and a nose wheel angle input to provide heading control. It is assumed that the wheels roll without slipping, to provide a non-holonomic constraint. This kinematic representation, depicted in Figure 2.15, allows the aircraft's motion to be analyzed without a need for the analysis of thrust levels, frictional forces, or inertial properties.
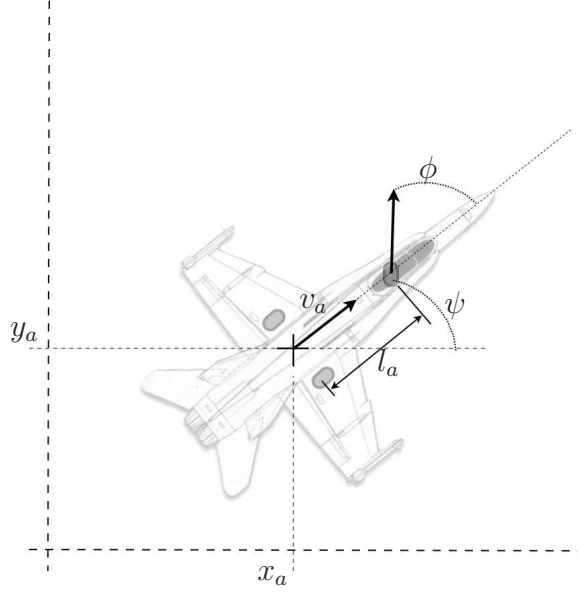
Figure 2.15:   Moving Aircraft Free Body Diagram

The aircraft's ground kinematics can be represented by the set of first order, nonlinear differential equations

$$\dot{x}_a = v_a \cos \psi$$
$$\dot{y}_a = v_a \sin \psi \qquad (2.20)$$
$$\dot{\psi} = \frac{v_a}{l_a} \tan \phi$$

where ϕ is the steering angle of the nose wheel relative to the heading angle ψ, l_a is the aircraft wheel base length, and v_a is the velocity of the aircraft.

When an aircraft is being towed, the input force is not being applied to the aircraft's center, but is instead applied at the nose wheel. This makes the aircraft the trailing member of an articulated vehicle, much like a trailer being pulled by a truck. The location of the nose wheel (x_w, y_w) is calculated by

$$(x_w, y_w) = (x_a + l_a \cos \psi, y_a + l_a \sin \psi) \qquad (2.21)$$

66

and if a velocity v_w is applied at the nose wheel, then the resulting aircraft velocity can be found by

$$v_a = v_w \cos \phi. \tag{2.22}$$

The aircraft kinematics given an input velocity at the nose wheel are given by

$$\begin{aligned}
\dot{x}_a &= v_a \cos \psi \\
\dot{y}_a &= v_a \sin \psi \\
\dot{\psi} &= \frac{v_w}{l_a} \sin \phi.
\end{aligned} \tag{2.23}$$

2.8.2   Multi-body.   The study of the control of articulated vehicles requires an understanding of their kinematics. There are numerous areas of research utilizing articulated vehicle kinematics. Ng *et al.* propose a vehicle following system utilizing a virtual trailer link [36]. Bolzern *et al.* have performed extensive studies of articulated vehicles with off-axle hitching [3] and *n*-body articulated vehicles [2] where the independent variable is distance traveled. Larsson *et al.* propose a nonlinear state space representation of a two-body system (a tractor and one trailer) [27]. The two-body system is insufficient to represent the towed aircraft system ashore, as a tow bar is used. Onboard an aircraft carrier, towing is often performed by a tow tractor which attaches directly to the nose wheel creating a two-body system.

Park *et al.* propose a kinematic representation of an *n*-body articulated vehicle with time as the independent variable [41]. Utilizing and adapting this representation allows for the development of kinematics to represent the three-body articulated towed aircraft system as shown in Figure 2.16.

The kinematics of the three-body articulated towed aircraft system can be developed by combining the single-body kinematics of each component. Given the forward

Figure 2.16:   Three-Body Articulated Towed Aircraft System

velocity of the tow tractor v_c[5] applied at its rear axle and the steering angle of the front wheels α as the system inputs, the tow tractor's motion can be described by

$$\dot{x}_c = v_c \cos \beta$$
$$\dot{y}_c = v_c \sin \beta \qquad (2.24)$$
$$\dot{\beta} = \frac{v_c}{l_c} \tan \alpha$$

where (x_c, y_c) gives the location of the tow tractor, β is the heading of the tow tractor measured from the x-axis, and l_c is the length of the tow tractor's wheel base.

The tow bar, attached to the tow tractor's rear hitch, is the first passive vehicle in the three-body articulated towed aircraft system. As this research is concerned with only simulating the towed aircraft system, for simplification it is assumed that the tow tractor's rear hitch is at the center of the rear axle. To attempt dynamic control of a towed aircraft system, it should be modeled with off-axle hitching which is fairly straightforward to accomplish [3]. With the tow bar hitched to the tow tractor's rear axle, the tow bar's input velocity v_c, and the tow bar steering angle ζ the velocity at the nose wheel v_w is given by

$$v_w = v_c \cos \zeta \qquad (2.25)$$

where v_w is aligned with the direction angle of the tow bar θ and the nose wheels are assumed to rotate or translate without slipping. The tow bar's kinematics are then described by

$$\dot{x}_w = v_w \cos \theta$$
$$\dot{y}_w = v_w \sin \theta \qquad (2.26)$$
$$\dot{\theta} = \frac{v_c}{l_b} \sin \zeta.$$

---

[5]The subscript c is utilized to denote *cart*.

69

where θ is the heading of the tow bar measured from the x-axis and l_b is the length of the tow bar. Combining the towed aircraft kinematics of Equation 2.23, the tow bar kinematics of Equation 2.26, and the tow tractor kinematics of Equation 2.24 it is straightforward to describe the motion of the three-body articulated towed aircraft system by

$$\bar{x} = \begin{bmatrix} x_c \\ y_c \\ \beta \\ x_w \\ y_w \\ \theta \\ x_a \\ y_a \\ \psi \end{bmatrix}, \frac{d}{dt}\bar{x} = \frac{d}{dt}\begin{bmatrix} x_c \\ y_c \\ \beta \\ x_w \\ y_w \\ \theta \\ x_a \\ y_a \\ \psi \end{bmatrix} = \begin{bmatrix} v_c \cos \beta \\ v_c \sin \beta \\ \frac{v_c}{l_c} \tan \alpha \\ v_w \cos \theta \\ v_w \sin \theta \\ \frac{v_c}{l_b} \sin \zeta \\ v_a \cos \psi \\ v_a \sin \psi \\ \frac{v_w}{l_a} \sin \phi \end{bmatrix}, \text{and } \bar{u} = \begin{bmatrix} v_c \\ \alpha \end{bmatrix} \tag{2.27}$$

where $\bar{x}$ is the state vector, $\bar{u}$ is the input vector, and

$$\zeta = \beta - \theta$$
$$\phi = \theta - \psi. \tag{2.28}$$

It is also desired to implement some physical constraints of the towed aircraft system. The tow bar can only rotate about the tow tractor's hitch so far before it collides with the tow tractor's structure. Similarly, the structure of the aircraft's nose wheel places a constraint on its maximum rotation angle. DIDO is capable of enforcing bounds on parameters, but it requires that they be represented as states. The heading of each element of the towed aircraft system should also be able to make

70

as many complete revolutions, in either direction, as the path requires. Representing the headings simply as angles will force DIDO to "unwind" the headings if they are a full rotation from the goal. To enable this, the headings can be represented by two states containing the sin and cos of the angle. The nonlinear kinematics are then given by

$$
\frac{d}{dt}\bar{x} = \frac{d}{dt}
\begin{bmatrix}
x_c \\
y_c \\
\sin\beta \\
\cos\beta \\
x_w \\
y_w \\
\sin\theta \\
\cos\theta \\
\zeta \\
x_a \\
y_a \\
\sin\psi \\
\cos\psi \\
\phi
\end{bmatrix}
=
\begin{bmatrix}
v_c \cos\beta \\
v_c \sin\beta \\
\cos(\beta)\dot{\beta} \\
-\sin(\beta)\dot{\beta} \\
v_w \cos\theta \\
v_w \sin\theta \\
\cos(\theta)\dot{\theta} \\
-\sin(\theta)\dot{\theta} \\
\dot{\beta} - \dot{\theta} \\
v_a \cos\psi \\
v_a \sin\psi \\
\cos(\psi)\dot{\psi} \\
-\sin(\psi)\dot{\psi} \\
\dot{\theta} - \dot{\psi}
\end{bmatrix}
=
\begin{bmatrix}
v_c \cos\beta \\
v_c \sin\beta \\
\cos(\beta)\frac{v_c \tan\alpha}{l_c} \\
-\sin(\beta)\frac{v_c \tan\alpha}{l_c} \\
v_c \cos\zeta \cos\theta \\
v_c \cos\zeta \sin\theta \\
\cos(\theta)\frac{v_c \sin\zeta}{l_b} \\
-\sin(\theta)\frac{v_c \sin\zeta}{l_b} \\
\dot{\beta} - \dot{\theta} \\
v_c \cos\zeta \cos\phi \cos\psi \\
v_c \cos\zeta \cos\phi \sin\psi \\
\cos(\psi)\frac{v_c \cos\zeta \sin\phi}{l_a} \\
-\sin(\psi)\frac{v_c \cos\zeta \sin\phi}{l_a} \\
\dot{\theta} - \dot{\psi}
\end{bmatrix}
, \text{ and } \bar{u} =
\begin{bmatrix}
v_c \\
\alpha
\end{bmatrix}.
$$

(2.29)

These equations could enable a persistent monitoring system to propagate the motion of a towed aircraft forward in time based upon the measured locations and orientations of the vehicles involved. They can also be used with DIDO, providing the dynamics upon which to plan the optimal path to the desired position on the flight deck.

71

2.9 Aircraft Tow Procedures

Towing aircraft on the flight deck or hangar bay of an aircraft carrier is a carefully planned procedure with standardized practices outlined by the CV NATOPS Instruction (00-80t-120) [6]. This instruction calls for the following minimum personnel when towing an aircraft:

1. Director

2. Tractor Driver

3. Plane Captain

4. Two Plane Handlers

5. Two Wing Safeties (when required)

6. Tail Safety (when required)

For a fixed-wing aircraft, such as an FA-18C Hornet, this means that nine personnel are required to move the aircraft. The Director is responsible for the entire procedure. The Plane Captain provides braking control for the aircraft. The Plane Handlers insert the chocks whenever the aircraft is at rest[6]. The Wing and Tail Safeties walk in a fixed position relative to the wingtip or tail to ensure that no collisions occur in that area [6].

The Director is required to maintain visual contact with the Plane Captain at all times and all personnel are equipped with whistles, which they must hold in their mouths, to signal each other [6].

---

[6]The Plane Handler and Wing Safety roles are typically fulfilled by the same personnel when ashore.

III. Data Collection

This chapter describes a series of tests conducted at the Air Force Institute of Technology (AFIT) and Naval Air Station (NAS) Oceana designed to determine if position and velocity measurements provided by the Global Positioning System (GPS) are capable of supporting a system to monitor the position, orientation, and velocity of aircraft, equipment, and personnel on the flight deck of a U.S. Navy aircraft carrier. The equipment used in these tests is also described.

3.1 AFIT Tests

This section describes the tests conducted at AFIT. These tests were performed to gain experience using the hardware, analyzing the collected data prior to testing with aircraft, and to provide the data necessary to create and evaluate simulations. Conducting these tests at AFIT allowed for an estimate of the requirements and risks associated with the tests, prior to performing them with actual aircraft.

3.1.1 Vehicle Measurements.   The first test was designed to determine the position and orientation of a small vehicle using two GPS receivers. From the recorded GPS data, the geometry of the vehicle, and the location of each receiver on the vehicle, the position of the vehicle and its orientation can be calculated.

The goal of this test was to determine the level of precision that can be achieved in the position and orientation calculations and to observe the effect of measurement noise of the resulting calculations. Additionally, the software written to analyze the recorded data can be used again with data recorded at NAS Oceana. Figure 3.1 illustrates the notional setup of this test.

3.1.1.1 Requirements.   The following equipment was required for this test:

1. Golf cart

2. Mobile GPS recorders (quantity: 2)
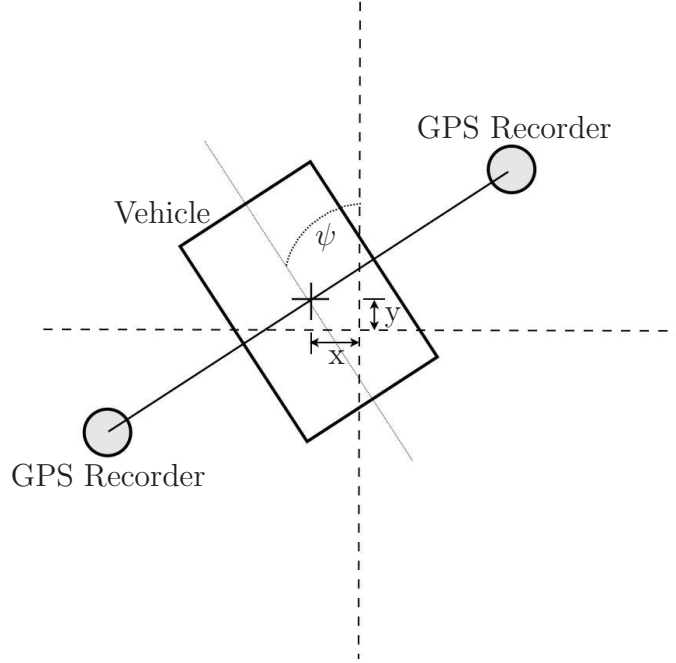
Figure 3.1:   Notional Setup of AFIT Vehicle Measurements Test

3. Dual-frequency GPS antenna (quantity: 2)

4. Stationary GPS recorder

The GPS recorders were attached to right and left side of the golf cart with the antennae supported away from the body of the golf cart. The stationary GPS recorder measured the position of the AFIT Advanced Navigation Technology (ANT) center roof antenna for differential corrections.

3.1.1.2 Procedure.   This test was conducted in two phases. The first phase, static measurements, tests the accuracy and precision of the recorders' measurements while at rest. The second phase, dynamic measurements, tests the recorders while in motion.

For static measurements, the vehicle was kept in a parked position for at least five minutes. The dynamic phase involved driving the vehicle around the field behind AFIT at a walking pace in straight lines or smooth curves. The recorded data can
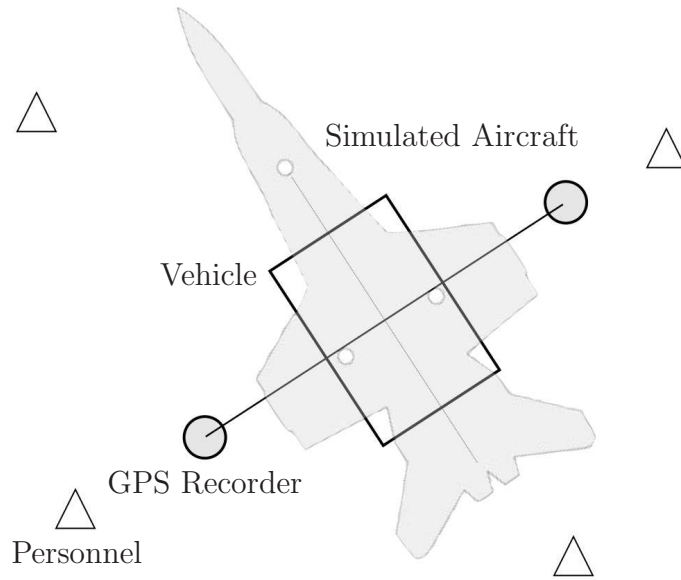
Figure 3.2:   Vehicle and Personnel Simulating Aircraft Movement

be used to analyze the noise in the measurement signal and the ability of software to predict the path of the vehicle.

3.1.1.3 Expected Results.   This test provides results for the accuracy of the position (eg: ± 2 cm) and orientation (eg: ± 2 degrees) of the GPS data as well as its precision (eg: ± 1 cm 97% of time). Additionally, it should allow observation of the effect of multipath error on measurements.

3.1.2 Vehicle and Personnel Movement.   This test recorded the movements of both the vehicle used in Section 3.1.1 and personnel simultaneously. It was designed to simulate the towing of an aircraft with its required personnel, allowing the development of analysis software prior to conducting the test in Section 3.2.1. Figure 3.2 illustrates the configuration for this test. Images recorded from the test are provided in Figure 3.3.

Figure 3.3:   Photographs from Simulated Aircraft Move at AFIT

3.1.2.1   Requirements.   The following equipment was required for this test:

1. Golf cart

2. Helmet (quantity: 4)

3. Backpack (quantity: 4)

4. Mobile GPS recorder (quantity: 6)

5. Stationary GPS recorder

6. Dual-frequency GPS antenna (quantity: 6)

The golf cart was configured with two mobile GPS recorders as in Section 3.1.1.1. The backpacks, helmets, and remaining mobile GPS recorders were carried by personnel wearing the helmets with dual-frequency antenna attached. This test required four personnel to walk with the vehicle, all volunteers were AFIT students or faculty.

3.1.2.2 Procedure. For this test the golf cart was driven slowly along a path behind AFIT. The personnel walked with the cart in an imitation of an aircraft movement crew, as depicted in Figure 3.2.

3.1.2.3 Expected Results. From the data collected in this simulation, software was developed which will be used to analyze the data collected at NAS Oceana, described in Section 3.2.1.

3.2 NAS Oceana Tests

The tests to be performed at NAS Oceana build upon those described in Section 3.1. The purpose is to observe the movement of U.S. Naval aircraft and sailors as they perform tasks similar to those performed on the flight deck of an aircraft carrier. By observing these tasks, a better understanding of the motion of aircraft, equipment, and personnel on the flight deck can be gained. These tests were conducted at a shore installation, but the differences in aircraft handling between sea and shore are minimal.

Collecting data with aircraft presents a greater risk than the simpler tests conducted at AFIT. Even without power being applied to the aircraft, it is vital that proper flight line procedures be observed for the safety of both the aircraft, SE, and personnel involved.

The Naval Aviation Maintenance Program (NAMP) [5] requires that tools used on aircraft be accounted for at all times. This is done to prevent Foreign Object Damage (FOD) from occurring to aircraft or personnel. During these tests, AFIT property was placed temporarily on and around Naval aircraft and personnel. All equipment used for this test was therefore inspected before and after each test to ensure that no parts, such as nuts or bolts, were lost during testing.

3.2.1 Aircraft Towing Observation. This test recorded the position, orientation, and velocity of an aircraft as it was towed from one spot to another on the NAS

Oceana flight line as well as the position and velocity of the personnel required for the towing. This procedure is virtually identical to that performed onboard an aircraft carrier. Figure 3.4 illustrates the towing procedure to be observed. A photograph of the test being conducted is presented in Figure 3.5 depicting the antennae mounted on USN cranials[1] and wingtip mounted GPS recorders.

The purpose of this test was to gather data which fully describes the motion of an aircraft being towed and the personnel around it. This data can then be analyzed for a better understanding of flight deck operations and used in simulations for hazard prediction and UAV incorporation.

3.2.1.1 Requirements. The following equipment was required for this test:

1. Cranial (quantity: 6)

2. Backpack (quantity: 6)

3. Nylon GPS recorder pouch (quantity: 2)

4. Mobile GPS recorders (quantity: 8)

5. Stationary GPS recorder

6. Dual-frequency GPS antenna (quantity: 9)

7. Video camera (quantity: 2)

8. Aircraft (quantity: 1)

9. Tow Tractor and bar

10. Elevated support platform (B-1 stand)

11. Laptop computer

---

[1]Cranial is the term used to describe the helmet used in Naval Aviation which contains hearing and vision protection.
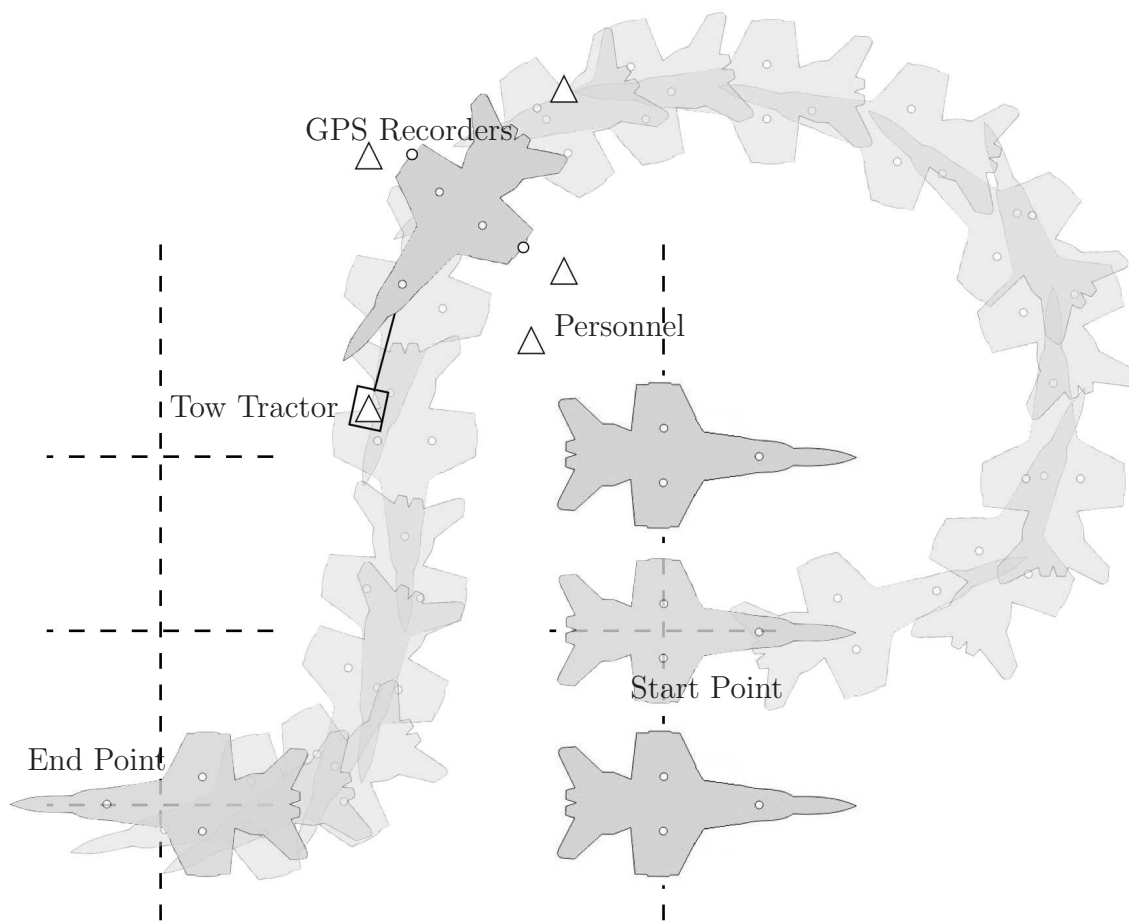
Figure 3.4:   Example Aircraft Tow Plan

Figure 3.5:   Photograph of Aircraft Being Towed at NAS Oceana

79

Two mobile GPS recorders were affixed on the wingtips of the aircraft using the nylon pouches made by squadron personnel, depicted in Figure 3.6. This mounting was designed to be completely non-permanent involving no modification to the aircraft or metal on metal contact.

The remaining mobile GPS recorders were provided to the tow personnel to record their movements with cranial mounted antennae and backpacks. The Plane Captain in the cockpit was not provided with a GPS recorder as their position was fixed relative to the aircraft during the entire procedure. The Tow Tractor and bar was used to move the aircraft. A video record of the test was made with a video camera placed atop the elevated support platform and another was used at ground level.

The stationary GPS recorder was used to record data for differential correction in post-processing. It was placed near the flight line atop the elevated support platform. The laptop computer was used to store the recorded data after each portion of the test.

A sufficient number of trained USN personnel were needed to perform the towing procedure. NAS Oceana instructions require a minimum of six trained personnel to tow an aircraft. The squadron's maintenance department provided a sufficient number of qualified volunteers to perform the tow procedure.

3.2.1.2 Procedure.   After mounting the GPS recorders as described in Section 3.2.1.1, the aircraft was towed from one spot to another on the flight line, similar to the tow plan depicted in Figure 3.4. The tow personnel were directed to park the aircraft multiple times, with both forward and reverse motion. This test was conducted with two different groups of personnel: one group during the day, the other at night.

3.2.1.3 Expected Results.   The data provided by this test allows a more thorough understanding of the movement of aircraft, equipment, and personnel

Figure 3.6: Nylon Pouch Made for Leica Recorder With Antenna Mount: Nylon webbing with velcro bands was used to lash the recorder to aircraft wingtip pylons. Pouches were made and provided by sailors of Strike Fighter Squadron Three Four - The Blue Blasters.
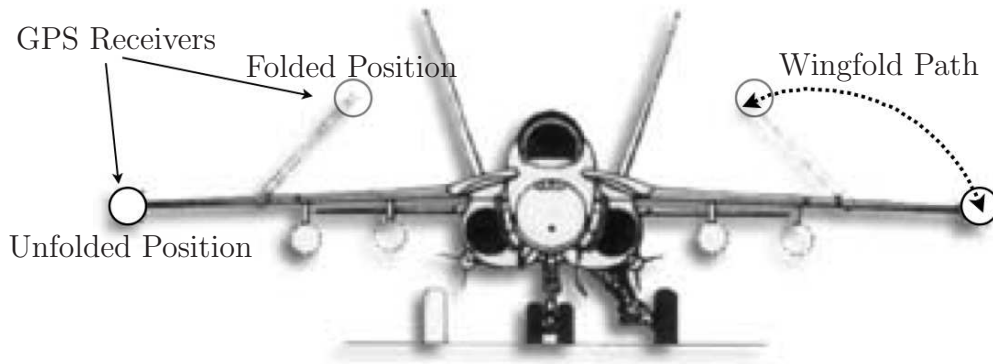
Figure 3.7:   GPS Receiver Placement and Desired Motion of Wingfold Test

involved in Naval Aviation. By analyzing this data, it should be possible to develop a system to predict the motion of aircraft under tow and the personnel involved.

3.2.2   Wingfold Detection.   At the conclusion of the evening aircraft tow, the personnel were directed to fold and unfold the wings. This allowed the mounted recorders to observe the motion of an aircraft's wingtips as they fold and unfold. Folding the wings of an aircraft leads to a reduced footprint on the deck of an aircraft carrier, but if they unfold inadvertently they can damage nearby aircraft. The goal of this test was to collect data on the folding and unfolding of wings so that an algorithm can be developed to detect this motion. Figure 3.7 illustrates the placement of GPS recorders and wingfold process of an FA-18C Hornet.

3.2.2.1   Requirements.   The following equipment was required for this test:

1. Cranial (quantity: 6)

2. Backpack (quantity: 6)

3. Nylon GPS recorder pouch (quantity: 2)

4. Mobile GPS recorders (quantity: 8)

5. Stationary GPS recorder

6. Dual-frequency GPS antenna (quantity: 9)

7. Video camera

8. Aircraft (quantity: 1)

9. Speed Handles (quantity: 2)

10. Laptop computer

Two mobile GPS recorders were affixed to the wingtip of an aircraft in the same manner described in Section 3.2.1.1. The stationary GPS recorder was used for differential correction. The laptop computer was used to record the data from the receivers. A visual record of the test was made with the video camera. Speed handles were used to manually fold and unfold the wings.

3.2.2.2   Procedure.   This test was started with the wings in the unfolded position at the conclusion of the evening aircraft tow procedure. Personnel on either side of the aircraft were directed to use the speed handles to fold and then unfold the wings. Following the test, the GPS recorders were removed from the wingtips, and the aircraft was returned to its normal parking configuration.

3.2.2.3   Expected Results.   Analysis of the data collected in this test helps in the development of an algorithm to detect a change in the wingfold status of an aircraft.

3.2.3   Personnel Tracking Near Aircraft.   During flight operations on an aircraft carrier, it is routine for authorized personnel to approach a powered aircraft quickly and remain in close proximity. This test explores the ability of GPS position data to monitor such motion of personnel. The motion of personnel near an aircraft and the hazardous areas near it is depicted by Figure 3.8. The preparations made to tow an aircraft provide many opportunities to record the motion of personnel near the aircraft.
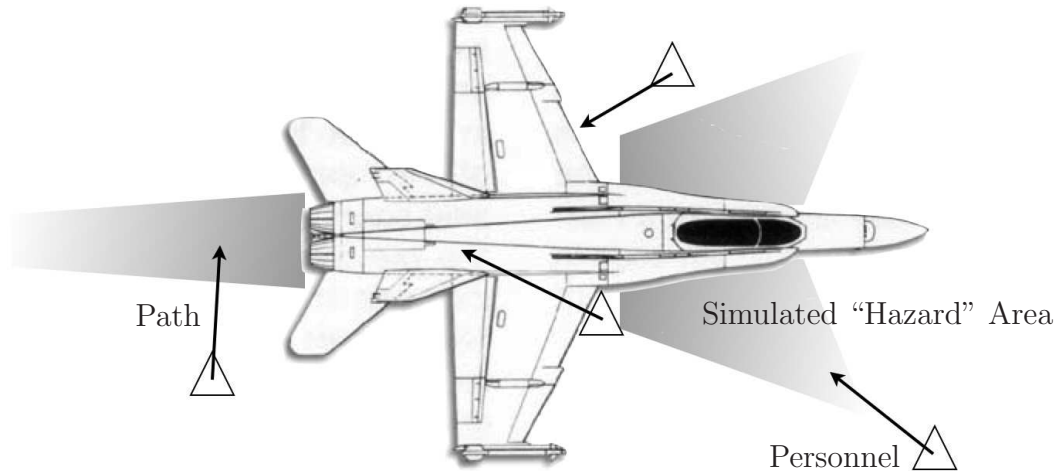
Figure 3.8:   Tracking Personnel Near an Aircraft

3.2.3.1 Requirements.   The following equipment was required for this test:

1. Cranial (quantity: 6)

2. Backpack (quantity: 6)

3. Nylon GPS recorder pouch (quantity: 2)

4. Mobile GPS recorders (quantity: 8)

5. Stationary GPS recorder

6. Dual-frequency GPS antenna (quantity: 9)

7. Video camera (quantity: 2)

8. Aircraft (quantity: 1)

9. Tow cart and bar

10. Elevated support platform (B-1 stand)

11. Laptop computer

Six mobile GPS recorders were carried by personnel, as in Section 3.1.2, who were involved in the aircraft tow procedure. Two mobile GPS recorders were affixed to the aircraft wingtips. A stationary GPS recorder was used to collect data for

differential correction. The video camera was used to create a visual record of the test. The computer was used to collect data from the GPS receivers.

3.2.3.2 Procedure. Throughout the test described in Section 3.2.1, it was often necessary for the personnel involved to approach the aircraft closely. The recorded data in these situations allows the simulation of maintenance personnel approaching hazard areas, such as the engine intake and exhaust.

3.2.3.3 Expected Results. As maintenance personnel often get very near aircraft, even crawl underneath them, during pre-launch procedures it is expected that the accuracy of the GPS solution will degrade significantly due to the effect of multipath and other factors. At times, the GPS receivers may even lose lock and be unable to compute a solution.

The final result of this test demonstrates the ability of small GPS receivers to track the motion of personnel near aircraft on the flight deck of an aircraft carrier. The algorithms developed from data collected in the test described by Section 3.1 should be able to determine if personnel enter the simulated engine "hazard" areas.

3.3 Equipment

This section describes the GPS equipment used during the tests of Sections 3.1 and 3.2.

3.3.1 Custom GPS Recorders. Two of the GPS recorders provided by the ANT center, referred to as the Custom GPS Recorders, are comprised of a NovAtel OEMV-3 card, a Gumstix computer, and a 12V lithium-polymer battery. They are contained within an aluminum enclosure with power switch, status indicator light, Ethernet port, and antenna jack as depicted in Figure 3.9.

The system is wired so that the NovAtel OEMV-3 and Gumstix computer are both started when the switch is turned to the on position. The OEMV-3 takes
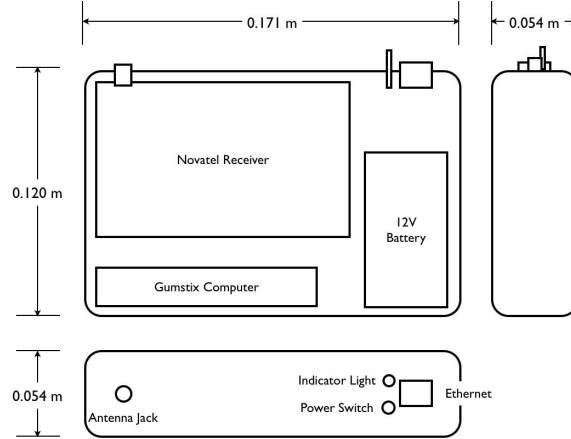
Figure 3.9:   Diagram of Custom GPS Recorder

Figure 3.10:   NovAtel OEMV-3

approximately five seconds to begin transmitting messages, while the computer takes approximately 30 seconds to boot and run the logging software.

3.3.1.1   NovAtel OEMV-3.   The NovAtel OEMV-3, depicted in Figure 3.10 [39, pg. 28] is a triple frequency GPS receiver capable of computing code and carrier phase solutions as well as processing differential GPS error corrections. It can utilize GPS signals broadcast on L1, L2, and the upcoming L5 as well as the Russian GLONASS L1 and L2 signals. For these tests, it was configured to track only GPS L1 and L2. It is capable of tracking 14 GPS satellites simultaneously. [39, p. 27].

For this research, the NovAtel OEMV-3 is configured to transmit satellite ranging (RANGECMPA) and ephemeris (RAWEPHEMA) data as well as its best position

Table 3.1:   NovAtel ASCII Message Header Format

Field	Name	Description
1	Sync	"#" symbol starts every message.
2	Message	Type of message. For this research only RANGECMPA, RAWEPHEMA, or BESTPOSA.
3	Port	Communications port transmitted on. For this research only COM2.
4	Sequence Number	Used for multiple related logs. Normally 0.
5	Percent Idle Time	Minimum percent of time processor is idle between successive logs.
6	GPS Time Status	Indicates the quality of GPS time solution.
7	Week	GPS Week Number.
8	Seconds	Seconds since start of GPS week.
9	Receiver Status	Eight digit hexadecimal number reporting status of hardware/-software components.
10	Reserved	Not described by NovAtel.
11	Version	Receiver software build number.
12	;	Semi-colon describes end of message header.

solution (BESTPOSA) to its second serial communications port (COM2). This information is transmitted in an ASCII message, and is therefore directly human readable. Each of the messages is transmitted with a header using the format described in Table 3.1 [38, pg. 22].

Following the message header, the RANGECMPA, RAWEPHEMA, and BESTPOSA message each contain different information. RANGECMPA contains hexadecimal information on the calculated range to each satellite, on each frequency the receiver has acquired. RAWEPHEMA is an ephemeris message for each satellite the receiver has acquired. BESTPOSA is the best possible position the receiver can cal-
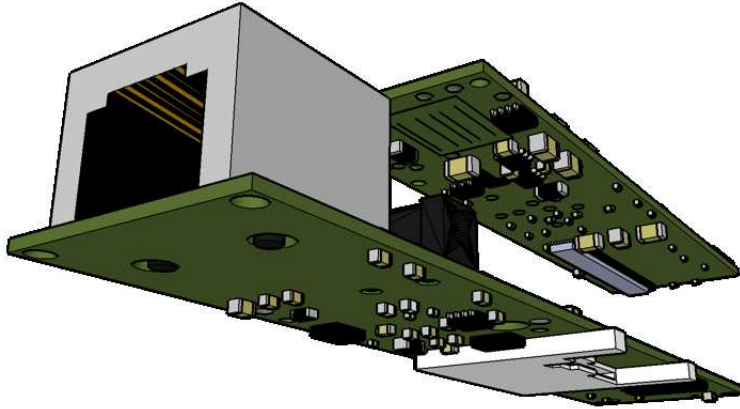
Figure 3.11:   Onboard Computer, Exploded View

culate from available data. RANGECMPA is transmitted at 5 Hz, BESTPOSA at 1 Hz, while RAWEPHEMA is transmitted every five minutes.

A description of the contents of each navigation message is provided by the OEMV Family Firmware Reference Manual [38, pgs. 250, 401, 408].

3.3.1.2 Onboard Computer.   The onboard computer runs an embedded version of the Linux operating system. It executes the program provided in Listing B.14 on page 178 to record the data transmitted by the NovAtel receiver on COM2 to a file located on a removable MultiMediaCard (MMC) flash chip.

The motherboard is a Gumstix "Connex" series with a Marvell® PXA-255 400 MHz processor, 64 MB of RAM, and onboard Flash storage of 16 MB for the operating system. It is configured with two daughterboards: a "breakout-gs" for serial communications and a "netMMC" for Ethernet and MMC connections. Figure 3.11 provides an exploded view of the Gumstix computer and its daughterboard with Ethernet and MMC connections [17].

It is possible to communicate with the onboard computer over its serial port or its Ethernet port. When connecting over Ethernet, the computer is configured to

announce which remote connection services are running using the Network Zerconf Protocol[2] software. Conveniently, this means a computer connected to it can tell if its remote connection processes are running. The Secure Shell[3] allows for both a remote terminal connection and copying of files over the network.

The computer is configured to boot the Linux® OpenEmbedded operating system from its onboard Flash storage. The startup scripts of the operating system have been configured to execute the logging program of Listing B.14 at the conclusion of the boot sequence.

The logging program runs from and only manipulates files on the MMC storage. It first determines which run number it is on to create sequential file names for the recorded data. It reads this data from *run_file.txt*, and each receiver is configured to start at a different number (1000, 2000).

3.3.2 Leica GX1210.   The ANT center also provided six Leica GX1210 GPS receivers. The default GX1210 is only capable of single frequency (L1) measurements, but the six units owned by the AFIT ANT center have been upgraded to support dual frequency (L1 and L2) measurements. They have 14 channels for each frequency.

There are two RX1200 controllers which attach to the GX1210 and provide a touch-screen graphical user interface. Figure 3.12 shows a GX1210 with an attached RX1200.

Measurements are stored to an internal 2 GB CompactFlash card. Technical specifications claim 20 mm accuracy when differential corrections are applied in post-processing. They are powered by up to two rechargeable Lithium Ion batteries (4.2 Ah / 7.4 V). One battery powers the receiver for approximately 30 hours.

---

[2]`http://avahi.org`
[3]`http://openssh.com`

Figure 3.12:   Leica GX1210 With RX1200 Interface

3.3.3   Antennae.   Three different models of antenna were used during testing at AFIT and NAS Oceana. Every antenna used was capable of dual-frequency reception. During the NAS Oceana tests personnel were equipped with one of two antennae: the ANT-A72GA-TW-N or the ANT-35C2GA-NW, both distributed by NovAtel and manufactured by Antcom. The primary difference is the connector: the former using a TNC connector and the latter a N-connector. The Leica recorders mounted on the aircraft wingtips were equipped with a Leica AX1202 GG antenna, also using a TNC connector.

IV. Results

This chapter describes the results of the tests conducted in Chapter III. The AFIT tests were designed to demonstrate the capacity of mobile GPS recorders mounted at fixed distances to allow the position and heading of a moving vehicle to be calculated. Algorithms used to calculate the results are also explained in this chapter. The NAS Oceana tests provide highly accurate measurements of procedures very similar to those performed aboard U.S. Navy aircraft carriers. Results from the tests at NAS Oceana include aircraft tow velocities (translational and rotational) as well as the distance personnel maintain from the aircraft.

4.1   AFIT Test Results

This section provides the results of preliminary testing conducted at AFIT. The performance differences between the Custom and Leica GPS recorders are discussed.

4.1.1   Test Vehicle Antenna Distance.   With two GPS antennae mounted on a rigid aluminum bar on the test vehicle, as described in Section 3.1.1 on page 73, the first data collected was analyzed to determine the accuracy and precision of the measurements. As an initial test, the two Custom GPS recorders were attached to the test vehicle antennae. Figure 4.1 shows the distance between the antennae, made using the BESTPOSA solution, for both static and kinematic regimes, provided by the Custom GPS Recorders, described in Section 3.3.1 on page 85. The BESTPOSA solution, referred to as a Single Point Solution (SPS), is calculated solely by the receiver and does not include any differential corrections, so ephemeris and tropospheric errors should be present. Additionally, without a base station present only code phase measurements can be computed. The measured distance (using a tape measure) between the antennae phase centers was 0.464 m.

When a third receiver was made available, the same two receivers were mounted to the test vehicle but a stationary receiver was used to collect data for differential correction. From this point forward the data collected in all tests has differential
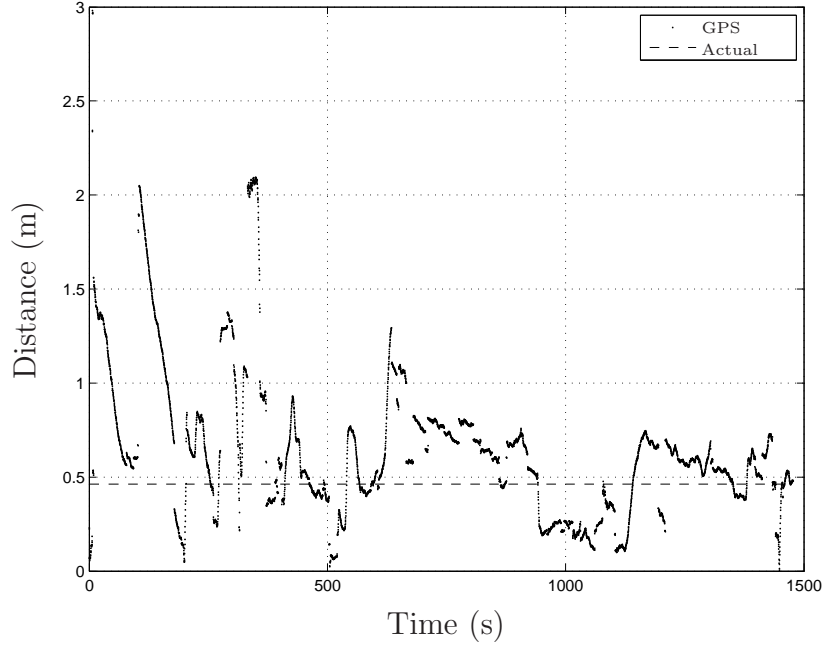
Figure 4.1:   Custom GPS Fixed Antenna Distance - SPS

corrections applied. Figure 4.2 shows the antenna distance with differential corrections applied by the NovAtel Waypoint GrafNav[TM] [40][1] software in post-processing.

There is a large region of accurate distance measurement in Figure 4.2, made when the test vehicle was stationary. From this information, it is clear that once the test vehicle began its motion the accuracy of the solution for the position of each custom GPS receiver was no longer reliable. Table 4.1 provides the error statistics, including the max, mean, and standard deviation, for each portion of the tests conducted at AFIT.

There are many possible explanations for the high levels of measurement error in Figure 4.2. The first place to look is the number of satellites used for the solution and the quality of the satellite geometry, or DOP, represented numerically as D. These are presented in Table 4.2, and are well within the range of values expected for a good solution. Multipath is the next most likely cause as the worst variations occur when the test vehicle is near the AFIT building or driving through the AFIT parking lot,

---

[1]The NovAtel Waypoint GravNav[TM] software is hereafter referred to simply as Waypoint.

(a) Static Regime   (b) Kinematic Regime
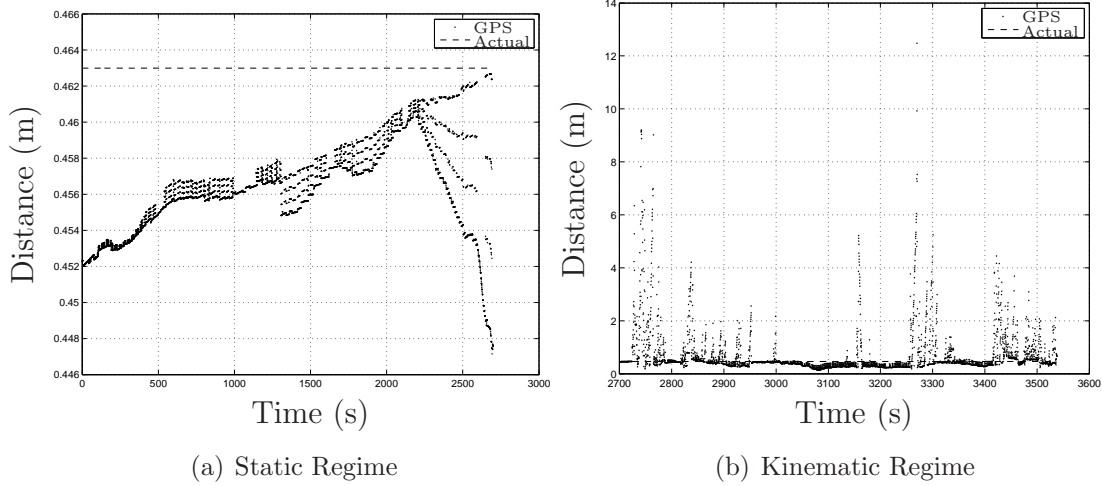
Figure 4.2:   Custom GPS Fixed Antenna Distance - CDGPS

both being highly reflective areas. This is an unlikely cause as multipath error should be fairly random, and in a video playback of the recorded data the measurement errors are consistently in the direction of motion. Another possibility considered was that the NovAtel OEMV receivers were changing which satellites were used in the solution during the kinematic phase, a common practice for receivers with a small number of channels. This possibility was discarded as the OEMV has 14 channels on each frequency which is more than sufficient for the number of available satellites. Additionally, the determination of which satellites to use in the solution is performed by Waypoint during post-processing, which should eliminate discontinuities.

Another possibility, inherent to the receiver construction and not the calculation of the solution, is a constraint in available bandwidth in the system bus linking the MMC card and the serial port. While the serial port was capable of handling RANGECMPA message at 5 Hz, BESTPOSA messages at 1 Hz, the bursting of RAWEPHEMA every five minutes may have overloaded the bus and caused ephemeris messages to be lost. This does not appear to be the case, as valid solutions are obtained with multiple satellites as depicted in Table 4.2, but it should be left open as a possibility.

94

Table 4.1:   AFIT Antenna Distance Measurement Statistics

Date	Regime	Device	e_{max} (m)	$\bar{e}$ (m)	σ_e (m)
21-Oct-2008	All	Custom	2.5184	0.2877	0.3096
22-Oct-2008	Static	Custom	0.0159	0.0068	0.0024
22-Oct-2008	Kinematic	Custom	12.0174	0.3941	0.8969
23-Oct-2008	Static	Leica	0.0467	0.0134	0.0102
23-Oct-2008	Kinematic	Leica	0.0763	0.0098	0.0104

Table 4.2:   AFIT Antenna Distance Satellite Statistics

Date	Regime	Device	D_{max}	$\bar{D}$	k_{max}	$\bar{k}$
22-Oct-2008	Static	Custom	1.7300	1.3759	11	9.7926
22-Oct-2008	Kinematic	Custom	2.1900	1.3557	9	8.9045
23-Oct-2008	Static	Leica	6.0300	3.5071	8	6.8342
23-Oct-2008	Kinematic	Leica	6.3100	2.7097	9	7.5575

The results from the Leica recorders are depicted in Figure 4.3 with the error statistics in Table 4.1. There is much less disparity between the static and kinematic solutions using the Leica recorders. With the low error measurements, it was decided to use Leica recorders for the aircraft wingtips in the NAS Oceana tests.

The results of the tests using the Custom GPS recorders were disturbing. The high level of inaccuracy when corrected using Waypoint made their measurements almost useless. It was decided, as a total of eight mobile GPS recorders were necessary to record all personnel involved in towing an aircraft at NAS Oceana, that they would be provided to those personnel whose distance relative to the aircraft varies the most during the procedure.

The relative accuracy of the Leica receivers also merits some discussion. There are many possible explanations, but among the most likely are multipath rejection and data message format. The Leica recorders, being commercial products designed for surveying, likely include advanced multipath rejection algorithms which reduce (but not eliminate) the effect of multipath on its measurements. Given the high demand for precision in the surveying industry and the high cost of these receivers, it is difficult

(a) Static Regime   (b) Kinematic Regime
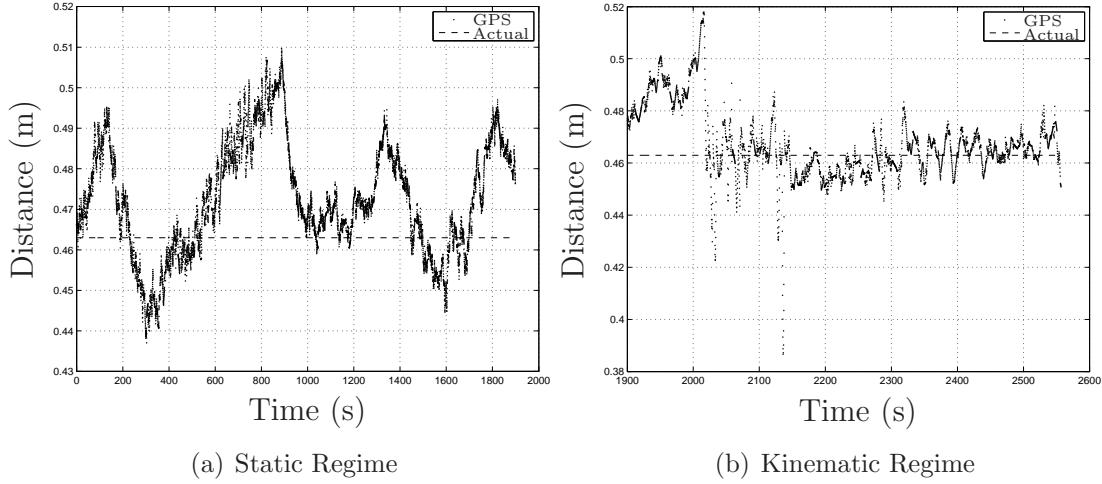
Figure 4.3:   Leica Fixed Antenna Distance - CDGPS

to imagine multipath rejection is not incorporated. Another possible explanation is the use of a binary message format, alleviating the bandwidth concerns. The ASCII message used by the NovAtel receivers is a relatively inefficient method of transmitting the measurement data.

4.1.2 Test Vehicle Heading.   The heading of the test vehicle is calculated using the equations derived in Section 2.5 on page 52. The MATLAB® script created to perform this calculation is provided as Listing B.7 in Appendix B on page 158. The MATLAB® command *atan2* is used to provide quadrant resolution when determining the heading.

Considering the inaccuracy of the position measurements from the Custom GPS recorders, it was expected that the heading calculation would contain significant levels of noise, making it unusable for proper attitude determination. As seen in Figure 4.4, the actual heading is virtually impossible to determine at any given time due to the rapid fluctuations. When the same calculations are performed using the Leica recorders the results contain significantly less noise. This allows the heading at any given moment to be accurately measured. In fact, using the Leica recorders allows the turns taken by the test vehicle to be clearly identified.
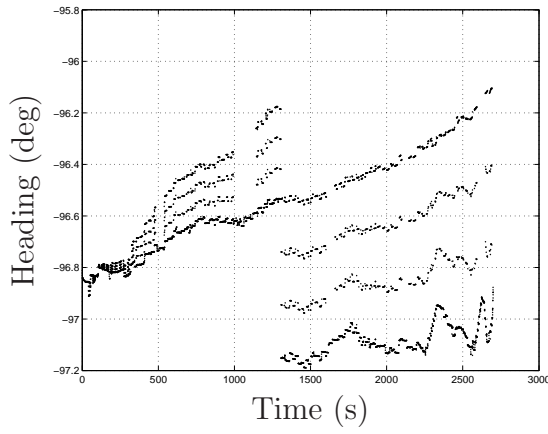
(a) Static Regime - Custom GPS Recorder
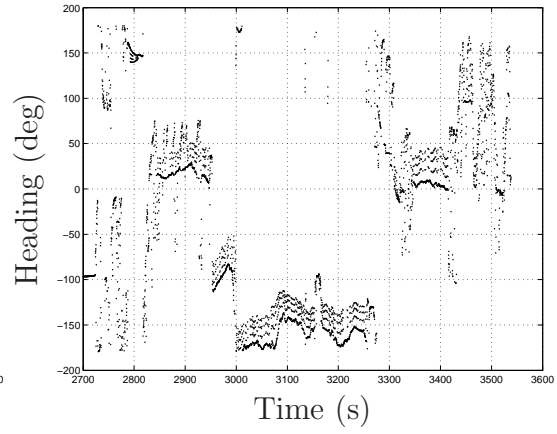
(b) Kinematic Regime - Custom GPS Recorder
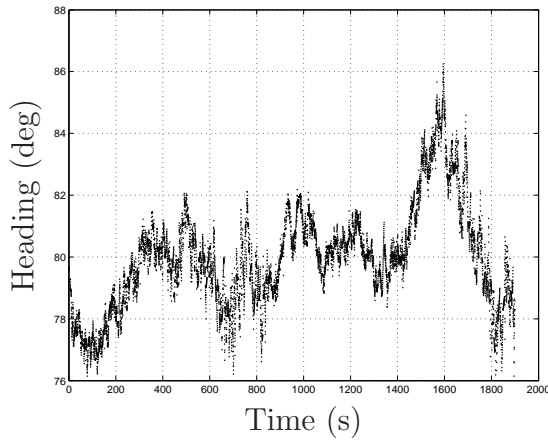
(c) Static Regime - Leica Recorder
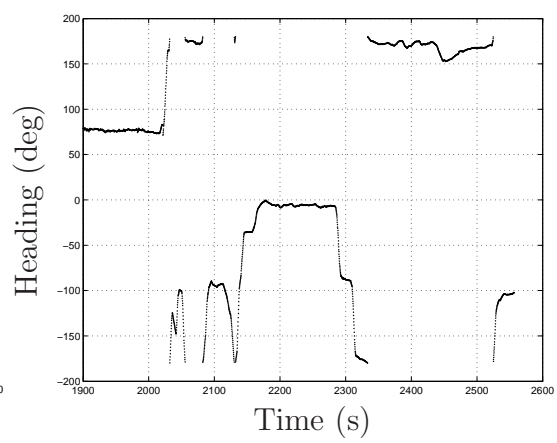
(d) Kinematic Regime - Leica Recorder

Figure 4.4:   AFIT Test Vehicle Heading

4.2 NAS Oceana Test Results

This section describes the results of the tests conducted at NAS Oceana, VA. Topics include the measurement of aircraft wingspan b, calculation of position (x_a, y_a) and heading ψ, and the path along which the aircraft was towed.

4.2.1 Aircraft Wingspan. The two Leica recorders mounted on the wingtips provide an excellent indicator of the accuracy and precision of the GPS solution. The recorders were strapped to the inboard side of the wingtip missile pylons using the nylon pouches made by squadron personnel depicted in Figure 3.6 on page 81. The distance between these pylons is fixed when the wings are spread, so the only variation should result from the placement of the recorders along the length of the pylon. According to *Jane's All the World's Aircraft*, the wingspan of an FA-18C Hornet is $b = 11.43$ m [23].

Figure 4.5 shows the wingspan measurements taken during the morning and evening tow procedures. Of note is the increased noise level in the latter phase of the evening test. In this portion, the wingspan measurement varies about the actual, but does approach it. The difference in distance measurements may also be attributable to the location of the phase center of the antennae.

The morning and evening wingspan error statistics are provided in Table 4.3. There are many factors which may explain the increased error during the evening portion, but the most likely explanation is increased multipath due to the increased number of aircraft on the flight line. During the day portion, there were approximately four total aircraft on the area of flight line used. Twice that number were present during the evening portion.

4.2.2 Aircraft Heading and Heading Rate. The heading of the aircraft ψ is determined by the same algorithm as the AFIT test vehicle, with the MATLAB® script provided in Listing B.7 on page 158. To determine the heading rate, it was necessary to numerically differentiate the calculated heading data, a process which
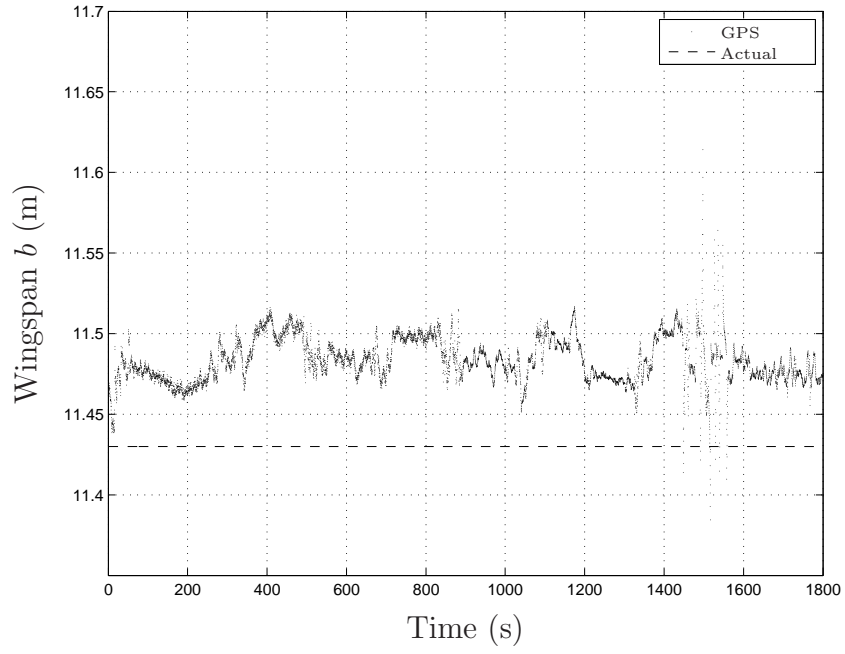
(a) Morning
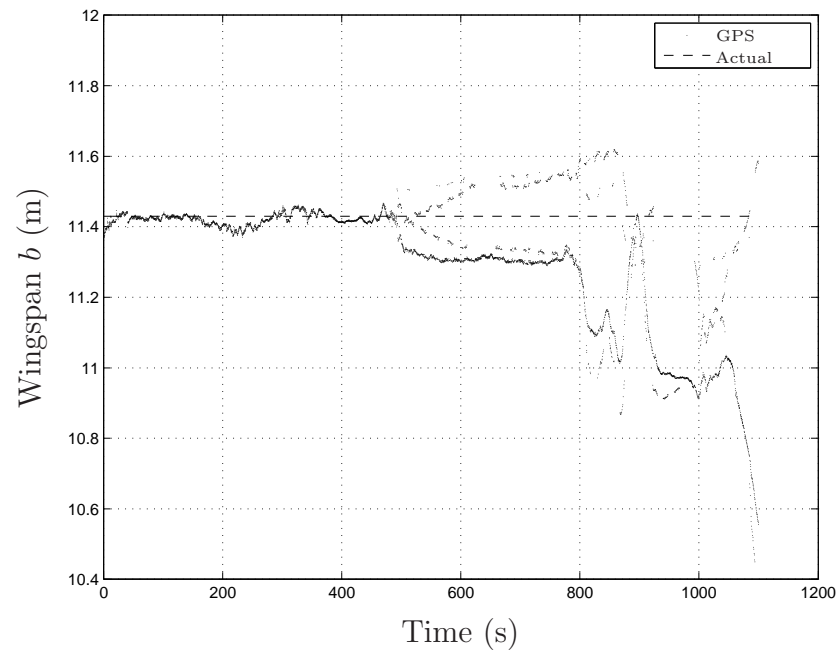
(b) Evening

Figure 4.5:   NAS Oceana Aircraft Wingspan Measurements

99

Table 4.3:   NAS Oceana Aircraft Wingspan Measurement Statistics

Time	e_{max} (m)	$\bar{e}$ (m)	σ_e (m)
Morning	0.1842	0.0535	0.0140
Evening	0.9808	0.1333	0.1727

often introduces noise into measurements. The *diff* command, included with MATLAB® was used for the heading rate calculation and the resulting array was padded with a leading zero to maintain array length. Since the aircraft was initially at rest this leading zero does not affect the results.

One potentially useful element of information that can be derived from the observation of an aircraft tow procedure is the maximum turn rate used. This can be used to provide a motion planning algorithm with more realistic estimates of the vehicle capabilities. The maximum turn rate is a function of the nose wheel angle and the maximum tow cart velocity. While the maximum turn rate used in these tests ashore may not be the maximum capable, it should be on the same order of magnitude. The heading and heading rate of the tow procedure conducted at NAS Oceana are provided in Figure 4.6.

By calculating the heading rate of an aircraft, it would be possible to predict the change of hazard areas with time. As an example, the motion of the area behind a taxiing aircraft containing hazardous exhaust can be predicted. If the hazard area will intersect a sailor within a short time horizon, a warning could be issued to the sailor and pilot.

4.2.3 Aircraft Position and Velocity.   Analyzing the route taken with the towed aircraft allows for analysis of safe distances between aircraft (ashore) and route preferences. Figure 4.7 shows the path taken for both morning and evening tow procedures. It is clear from this data that there are set routes between the rows of aircraft parking spaces, and that during this test two of them were used. There were in fact painted taxiway markings on the flight line which were used between rows of
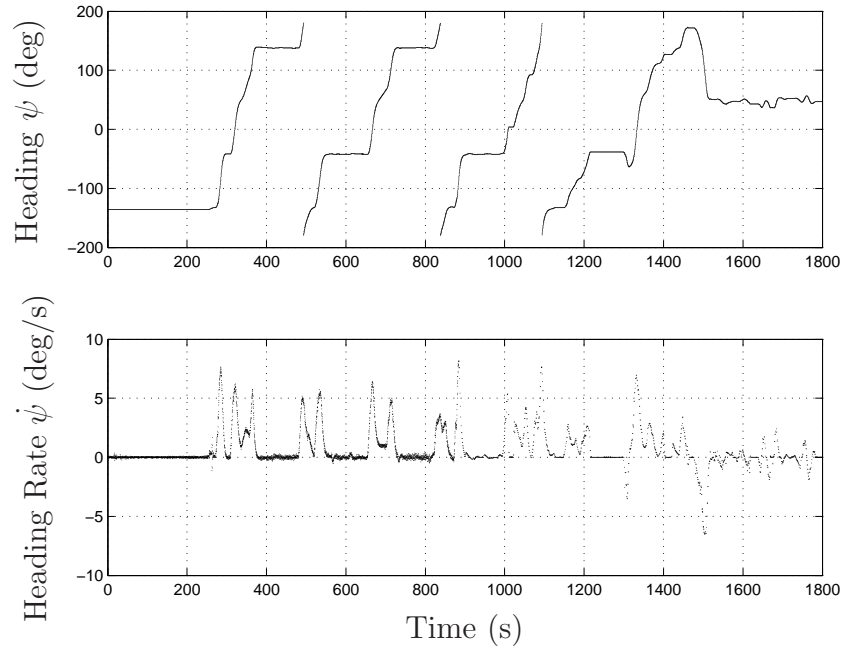
(a) Morning
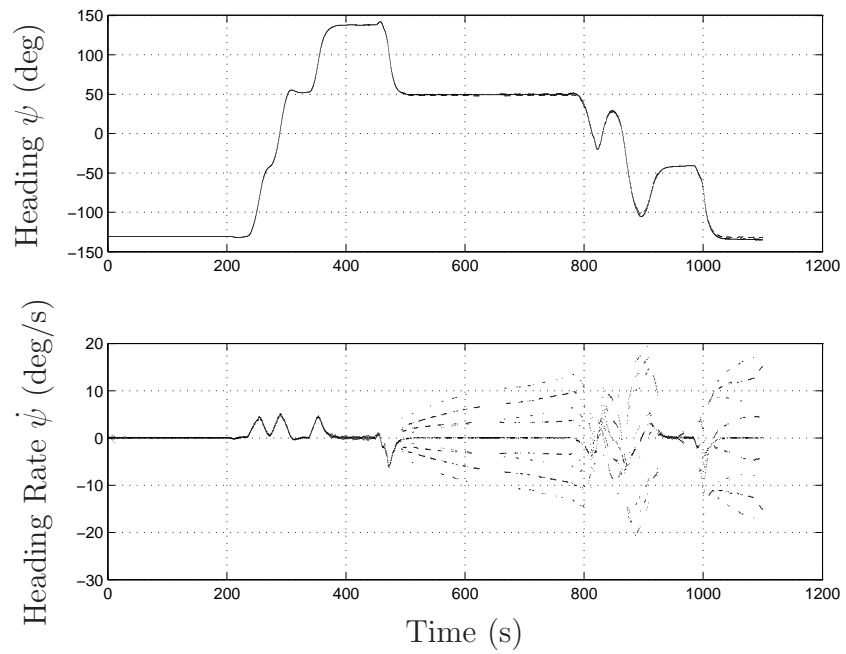
(b) Evening

Figure 4.6:   NAS Oceana Towed Aircraft Heading and Heading Rate

Table 4.4:   NAS Oceana Aircraft Motion Statistics

Time	$\dot{\psi}_{max}$ (deg/s)	$\bar{\dot{\psi}}$ (deg/s)	$v_{a,max}$ (m/s)	$\bar{v}_a$ (m/s)
Morning	8.1480	0.7015	0.5117	0.1338
Evening	8.5982	0.2999	0.5929	0.1146

Table 4.5:   NAS Oceana Personnel Roles

Personnel	Equipment	Morning Role	Evening Role
p_1	Leica	Director	Tail Safety
p_2	Leica	Wing Safety	Wing Safety
p_3	Leica	Tail Safety	Wing Safety
p_4	NovAtel	Tractor Driver	Tractor Driver
p_5	NovAtel	Supervisor	Director

aircraft. The location of parked aircraft is an estimate based upon visual observations of the aircraft present.

The velocity of the towed aircraft v_a, calculated by numerical differentiation of the position data, is provided in Figure 4.8. Aircraft motion statistics are presented in Table 4.4. Note that the heading rate statistics presented for the evening tow procedure are only for the first 600 s. Following that period the increased position error causes rapid variations in the heading rate.

4.2.4 Personnel Position.   The accuracy of the measurements taken presents an opportunity to analyze the behavior of trained personnel performing a routine procedure. The distance p_n maintained by the nth personnel from the towed aircraft, in the nearest neighbor sense, is presented as Figure 4.9. This calculation is performed by the script provided in Listing B.8 on page 159. The role fulfilled by each person during the move, discussed in Section 2.9 is presented in Table 4.5. The Supervisor role listed for p_5 in the morning is an additional role required by the squadron when the Director is below the rank of E-6.
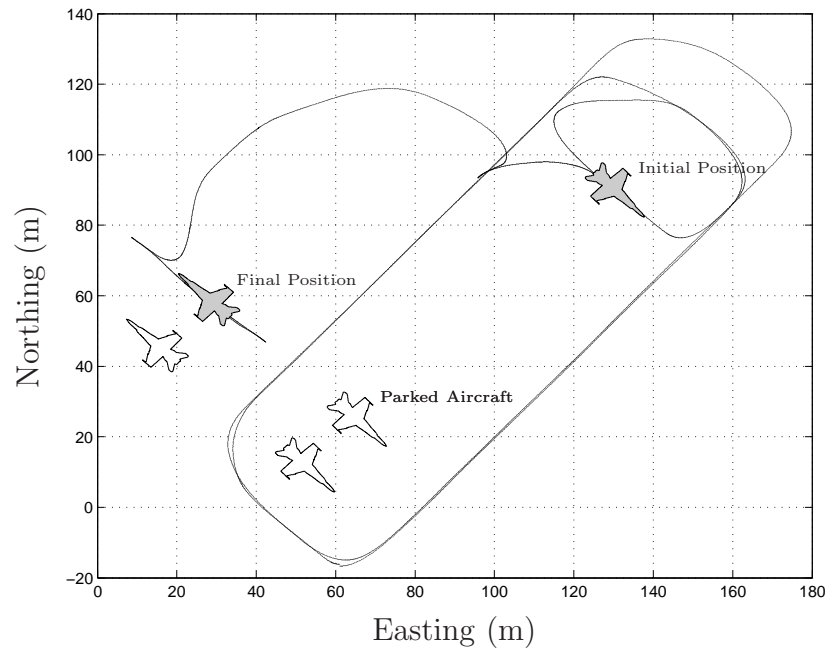
(a) Morning
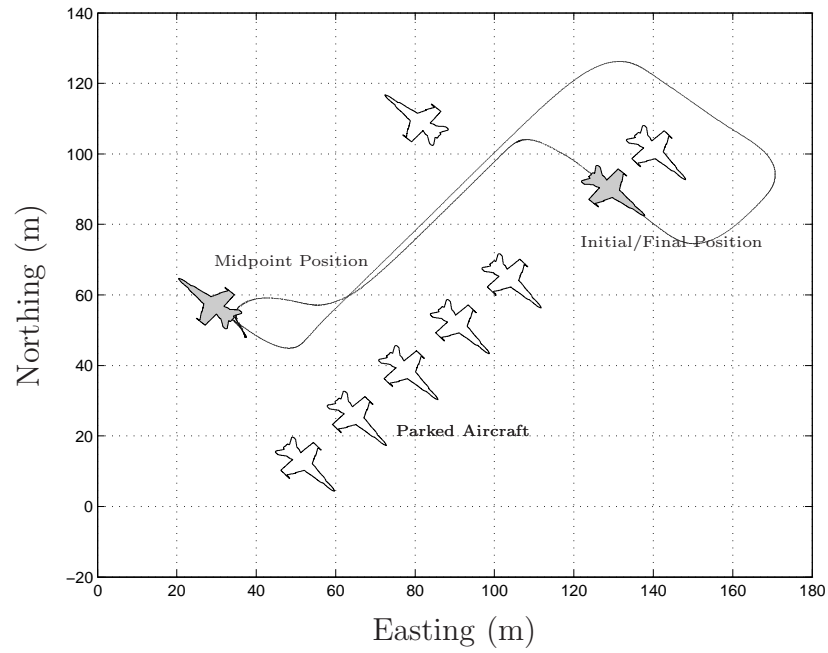
(b) Evening

Figure 4.7: NAS Oceana Aircraft Tow Route: Locations of parked aircraft are estimates.
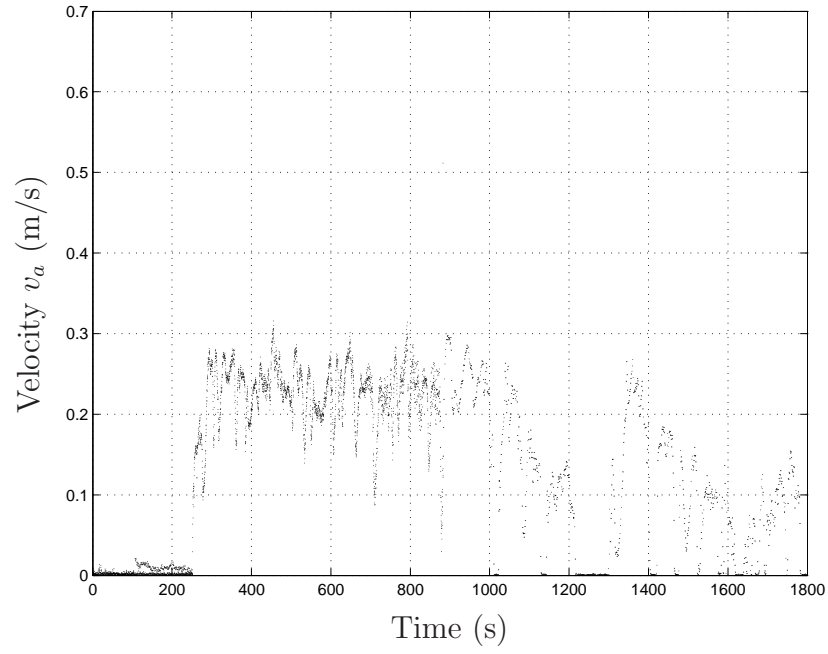
(a) Morning
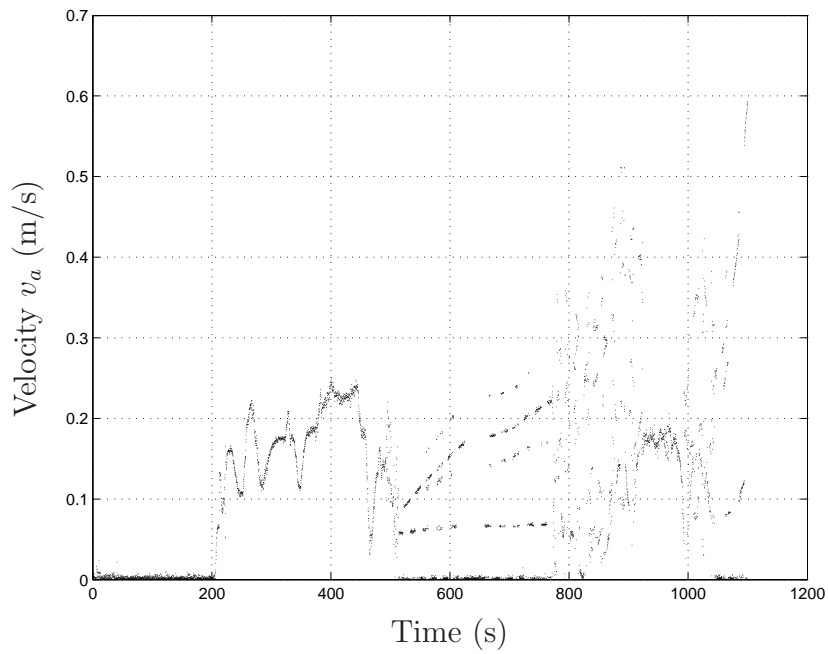
(b) Evening

Figure 4.8:   NAS Oceana Aircraft Tow Velocity

104

Table 4.6:   NAS Oceana Personnel Distance Statistics

Time	Type	p_1 (m)	p_2 (m)	p_3 (m)	p_4 (m)	p_5 (m)
Morning	Max	27.0057	4.5079	8.2550	26.5641	16.9151
	Mean	7.3512	2.3953	4.2892	2.8061	7.2944
Evening	Max	5.9548	3.7441	4.0742	7.9871	30.4477
	Mean	3.8124	1.8905	2.5317	2.3566	6.4603

While six personnel were equipped with receivers during both the morning and evening tow procedures, one of the Leica recorders failed to record its measurements. This recorder had been provided to the starboard wing safety for the morning procedure, so there are no measurements available for this position. This failure was noticed following the morning procedure and the device was reconfigured in hopes of providing functionality for the evening procedure. In anticipation of a repeated failure, the malfunctioning recorder was provided to a trainee acting as a secondary in the wing safety role. The reconfiguration was unsuccessful and no evening data was recorded by the malfunctioning device either.

It is also useful to observe the position of personnel involved relative to the aircraft. Many of the mishaps discussed in Chapter I involve personnel being injured by contact with aircraft landing gear or standing in a jet exhaust area. Figures 4.10 through 4.16 show the relative position for each phase of the morning tow procedure. During this procedure, there were three phases where no motion of the aircraft occurred. Figure 4.10 shows the motions of personnel preparing the aircraft to be towed while Figures 4.12 and 4.14 show periods where the Director was consulting with the Supervisor on the best course to take. The relative positions for the evening tow procedure are provided in Figures 4.17 through 4.20.
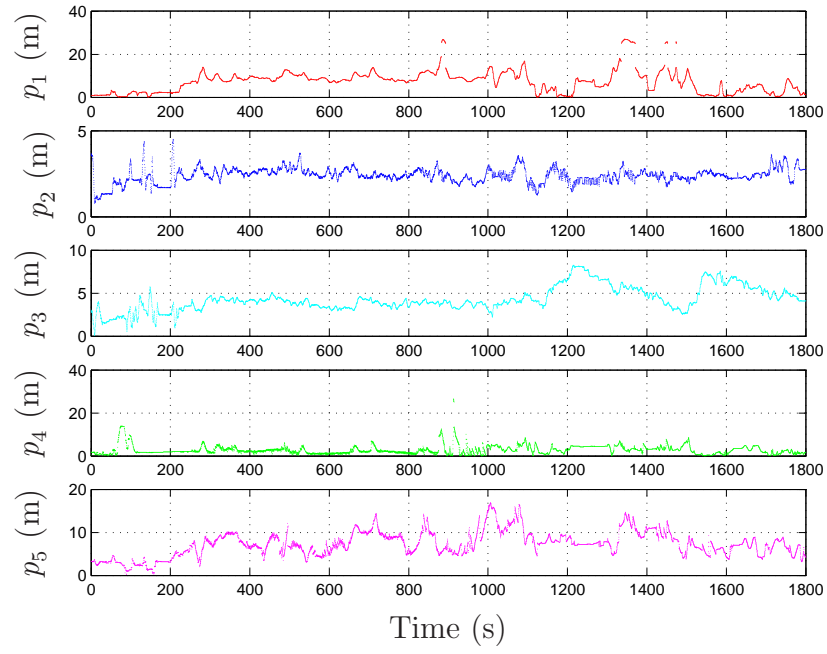
(a) Morning
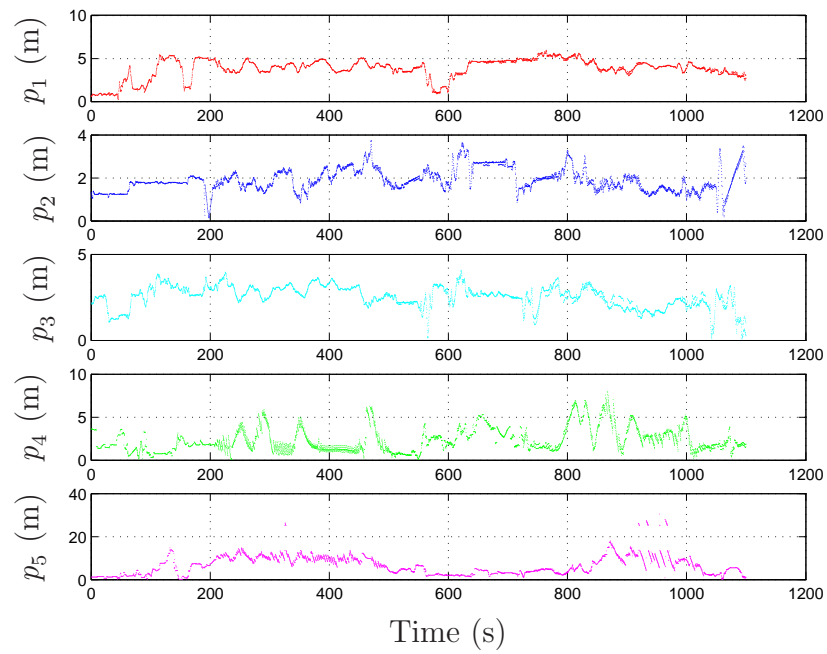
(b) Evening

Figure 4.9:   NAS Oceana Personnel Distance

106
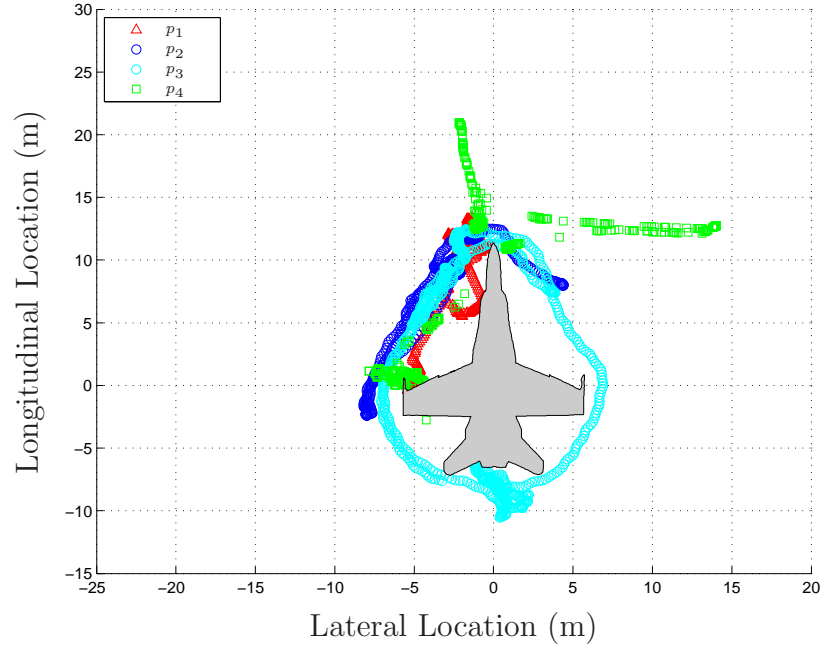
Figure 4.10:   Relative Personnel Position - Morning - Setup
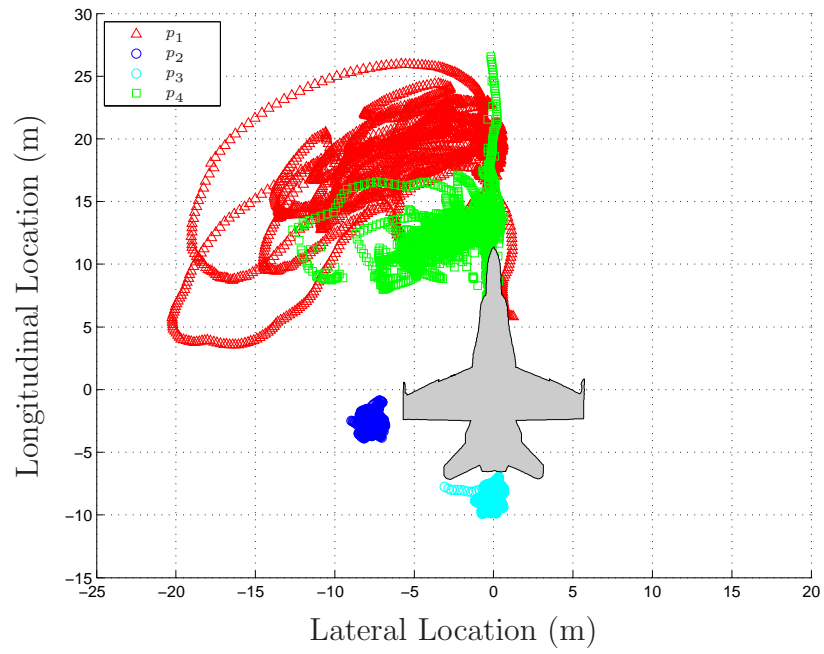
Figure 4.11:   Relative Personnel Position - Morning - First Move
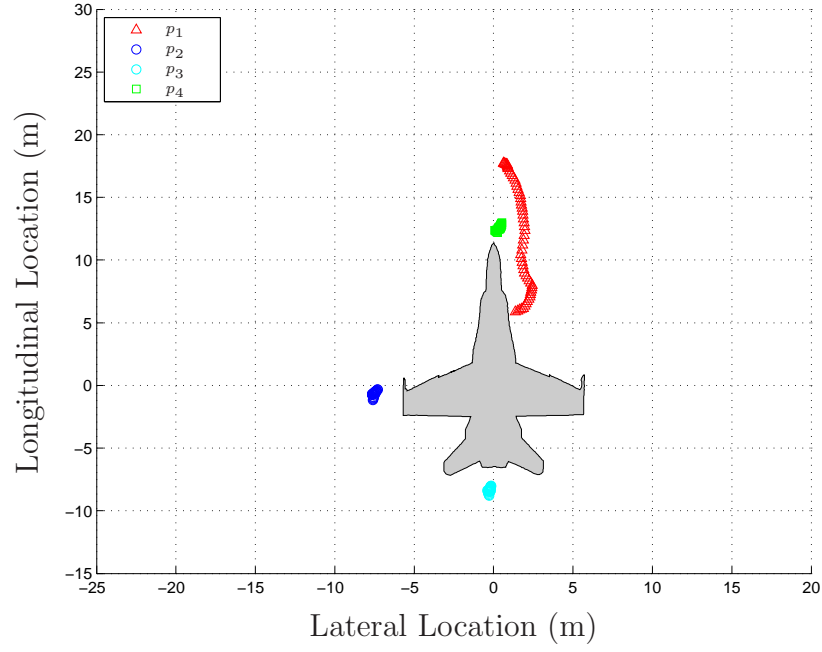
Figure 4.12:   Relative Personnel Position - Morning - Preparing to Reverse
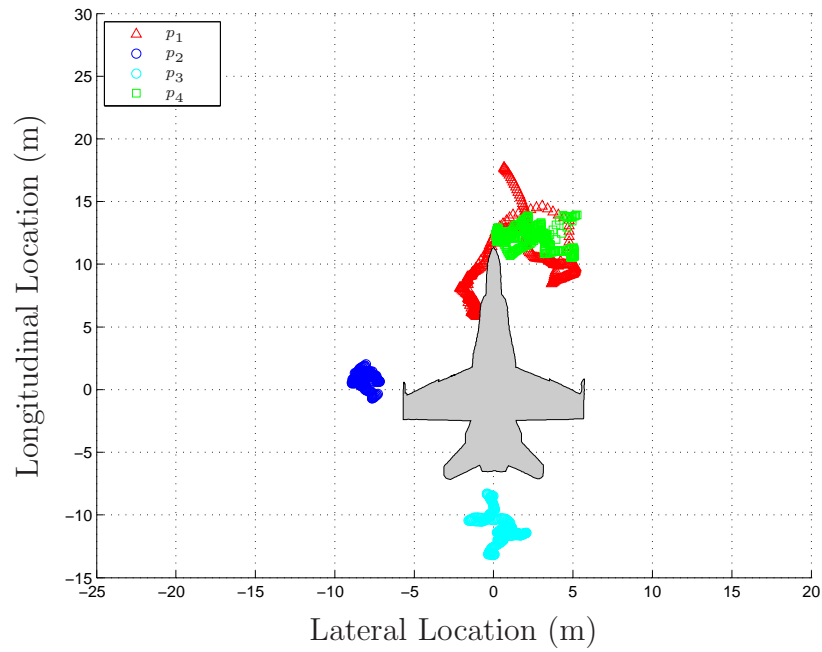
Figure 4.13:   Relative Personnel Position - Morning - Reversing
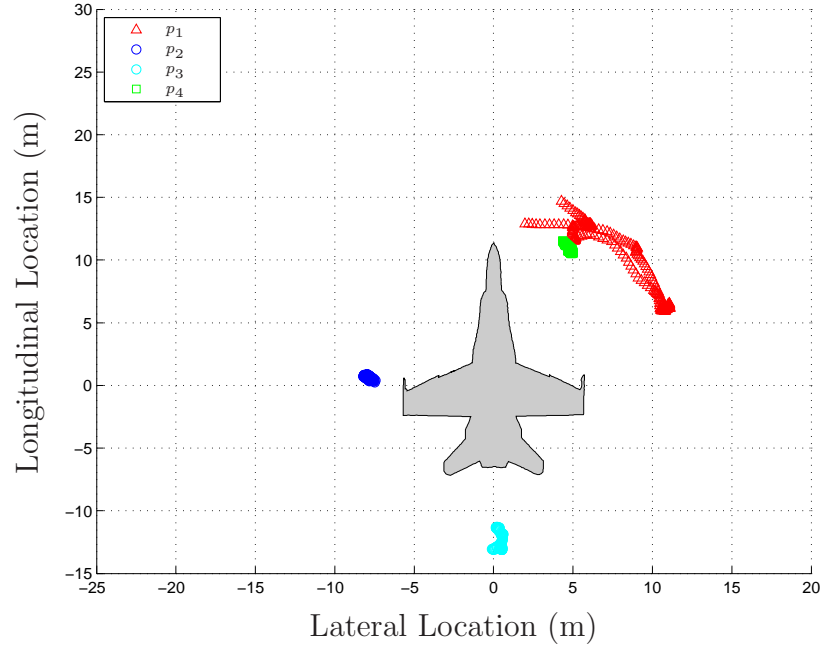
Figure 4.14:   Relative Personnel Position - Morning - Deliberating
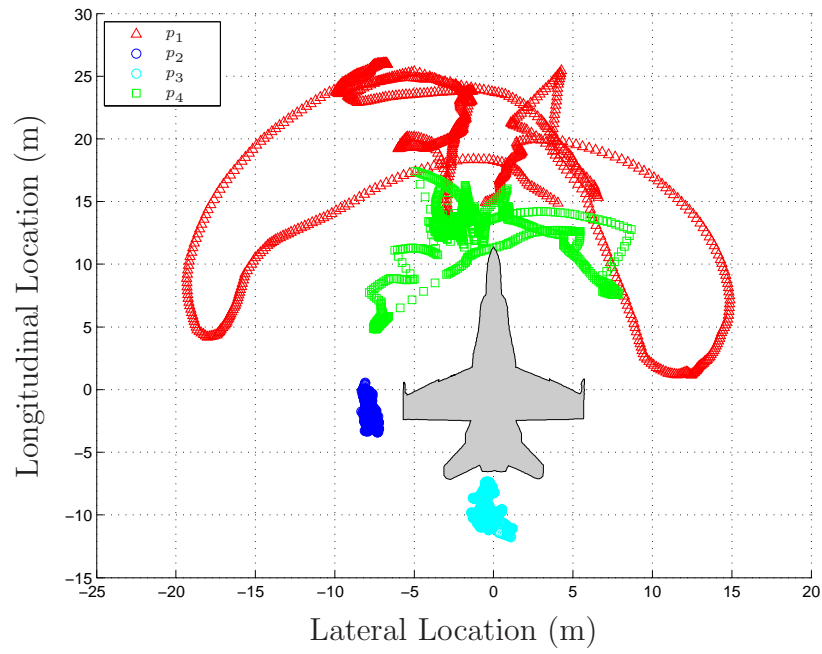
Figure 4.15:   Relative Personnel Position - Morning - Moving Forward
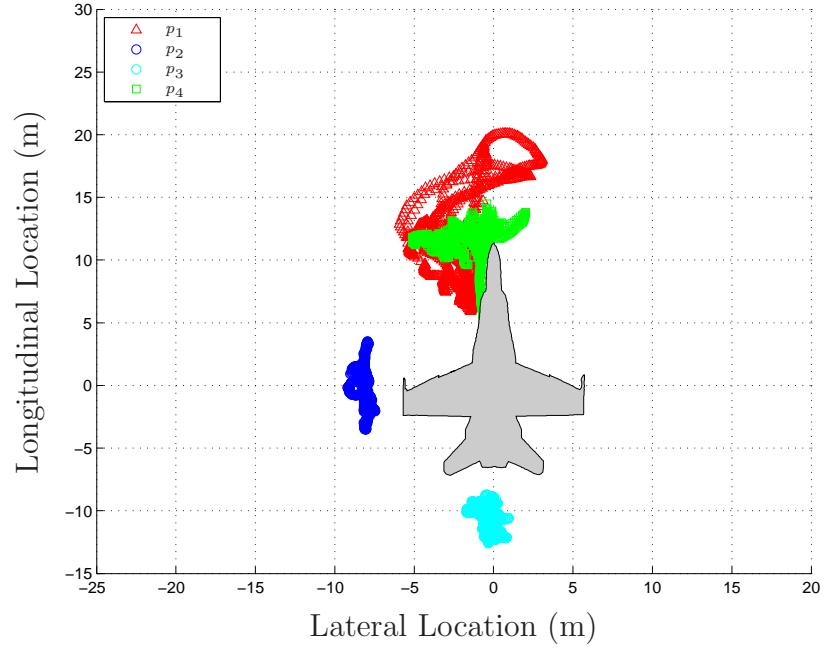
Figure 4.16:   Relative Personnel Position - Morning - Reverse Parking
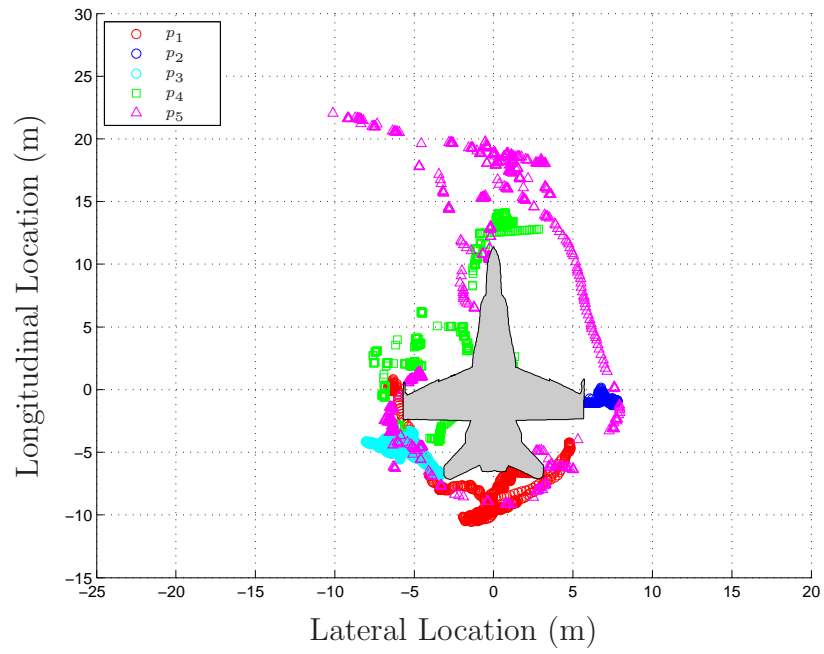
Figure 4.17:   Relative Personnel Position - Evening - Setup
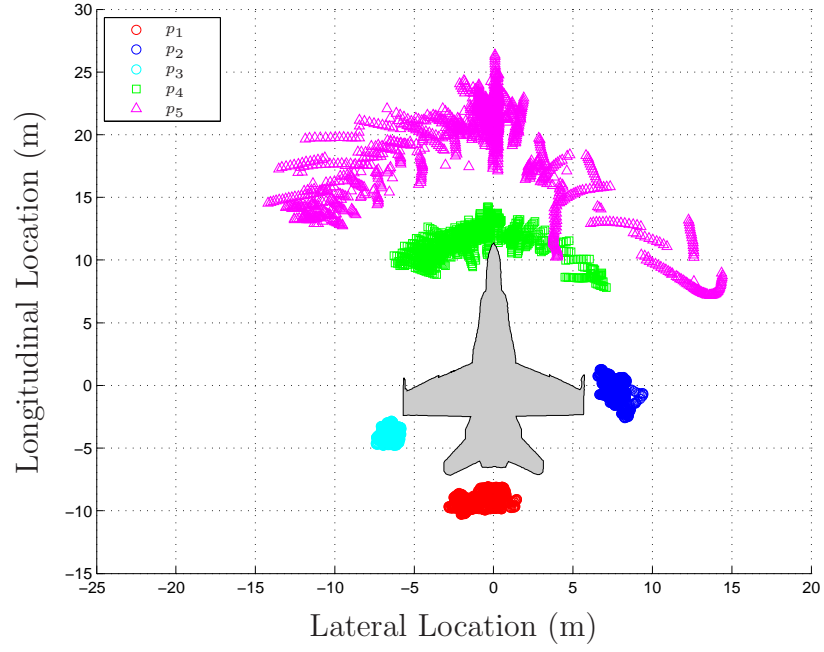
Figure 4.18:   Relative Personnel Position - Evening - First Move
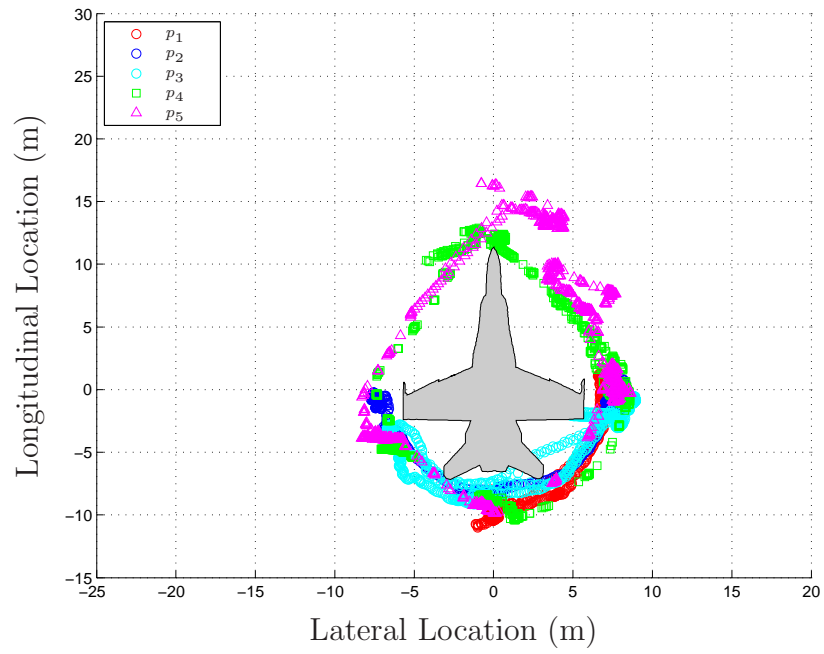
Figure 4.19:   Relative Personnel Position - Evening - Deliberating
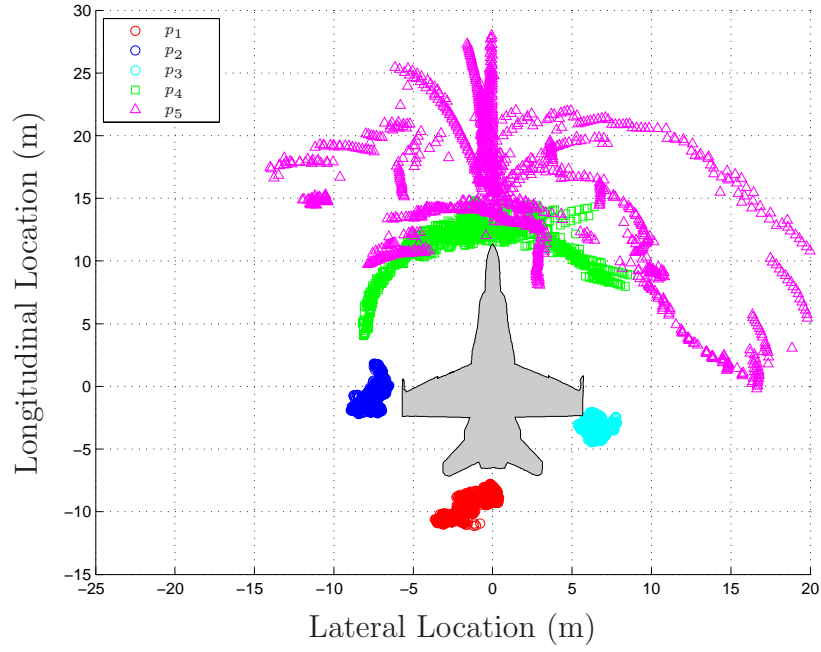
Figure 4.20:   Relative Personnel Position - Evening - Second Move
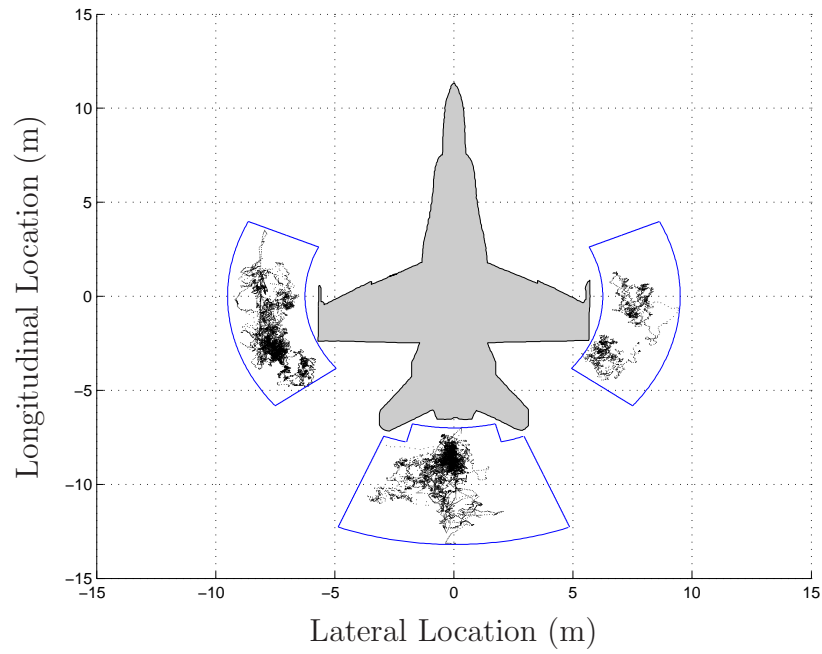
Figure 4.21:   Relative Personnel Position - Wing and Tail Safeties

112

It is also possible to examine the relative position of both the Wing and Tail Safeties throughout all the movement phases. The position of the Tractor Driver is excluded as, during motion, they never leave the cart and the relative inaccuracy present in the NovAtel measurements would cause too many errors in a similar analysis. The Director is excluded as only one individual fulfilling that role was measured with a Leica recorder and as seen in Figures 4.10 through 4.20 their position can vary greatly. The Supervisor is excluded as the position is not required onboard a U.S. Navy aircraft carrier.

Figure 4.21 provides the relative location of the Wing and Tail Safeties throughout all movement phases, both morning and evening. The data shows the aggregate positions of five personnel, three as Wing Safety and two as Tail Safety. Using this data it was straightforward to create bounding boxes as shown. With further study, these bounding boxes could be treated as required positions for personnel towing an aircraft. Bounding boxes for the Director and Tractor Driver could be created with more data on their positions during an aircraft tow procedure. If a sailor leaves the bounding box while the aircraft is in motion, the Director could be alerted.

4.2.5 Measurement Quality. The measurement quality statistics for both the morning and evening phases are presented as Table 4.7. The mean DOP $\bar{D}$ is fairly consistent across the devices during each phase. This is to be expected as the satellite geometry shouldn't have changed dramatically during each phase, but may have between the phases. The high maximum DOP D_{max} seen for some devices corresponds to the personnel traveling underneath the aircraft's wings.

4.2.6 Aircraft Wingfold. Following the conclusion of the evening tow procedure, the personnel involved manually folded the wings of the aircraft. The wingspan calculated from the recorder positions during this period are presented in Figure 4.22. It is difficult, due to the noise in this data, to pick out the exact moment when the wingfold procedure started. While it is possible to get a better approximation of the

Table 4.7:   NAS Oceana Measurement Quality Statistics

Device	Time	D_{min}	D_{max}	$\bar{D}$	σ_D	k_{min}	k_{max}	$\bar{k}$	σ_k
Left	Morning	1.72	2.90	2.33	0.37	6	7	6.54	0.50
Right	Morning	1.72	2.90	2.35	0.37	6	7	6.52	0.50
p_1	Morning	1.77	7.28	2.45	0.54	4	7	6.48	0.56
p_2	Morning	1.43	2.90	2.22	0.32	6	8	6.74	0.45
p_3	Morning	1.30	8.06	2.45	0.78	4	8	6.49	0.57
p_4	Morning	1.77	10.95	2.79	0.92	4	7	6.44	0.60
p_5	Morning	1.77	7.17	2.86	0.66	6	7	6.51	0.50
Left	Evening	1.78	6.07	3.64	1.46	5	8	6.47	0.79
Right	Evening	1.47	3.81	2.81	0.93	5	8	6.24	0.95
p_1	Evening	1.46	13.08	2.95	1.61	4	9	6.24	1.29
p_2	Evening	1.62	9.82	3.02	1.44	4	9	6.47	1.05
p_3	Evening	1.46	10.98	3.03	1.38	4	9	6.53	1.09
p_4	Evening	1.40	9.69	3.55	1.51	4	9	6.31	1.02
p_5	Evening	1.40	9.98	3.93	1.78	4	9	6.04	0.96

Table 4.8:   Wingfold Measurement Quality Statistics

Location	D_{min}	D_{max}	$\bar{D}$	σ_D	k_{min}	k_{min}	$\bar{k}$	σ_k
Left	4.11	11.99	5.46	1.27	4	6	5.37	0.56
Right	3.70	13.32	4.42	0.89	4	7	5.22	0.70

time from personnel positions, this is of little use as the wingfolds this research is concerned with are not performed manually.

Table 4.8 provides the measurement quality statistics for the wingfold procedure. The mean DOP $\bar{D}$ is significantly higher during this procedure than during the movement phases. This is likely due to the antenna direction as the wings are folded. With the wings fully folded, the antennae pointed towards the center of the aircraft rather than towards the sky.

4.2.7 Path Planning.   In order for a persistent monitoring system to provide early warnings of hazardous situations, it must be capable of predicting the path of objects on the flight deck. If DIDO, the path planning software discussed in Sec-
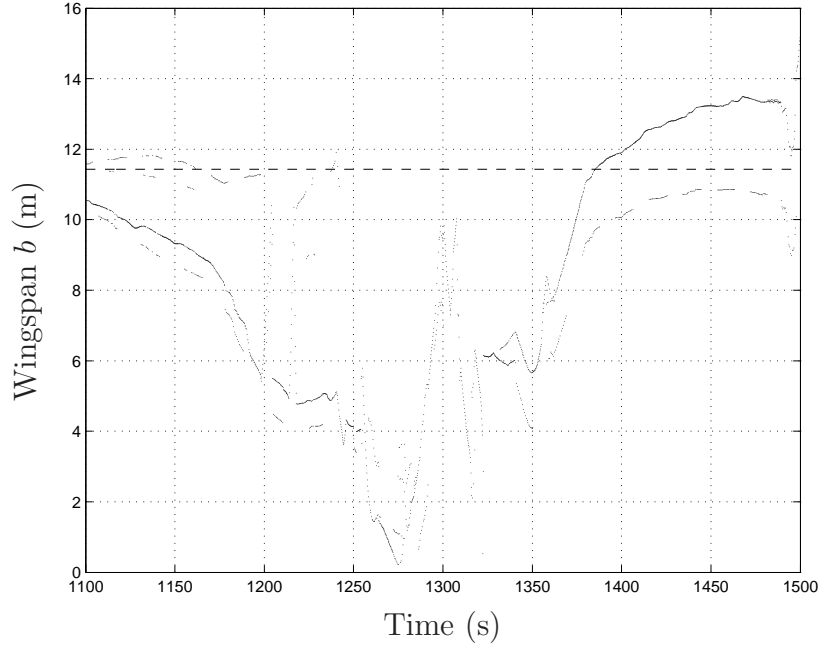
Figure 4.22:   Wingfold Wingspan Measurements

tion 2.7.3 on page 63, is provided a cost function $J(\bar{x}, \bar{u}, t)$ which, when minimized, simulates the objectives of the personnel involved in the towing procedure, then DIDO should predict a path similar to the one taken. In the simulation, only forward motion of the aircraft was allowed for simplification, however, this constraint could easily be removed. The desired path, taken from the first portion of the evening phase, is shown in Figure 4.23 and contains only forward motion. It is the first half of the movement shown in Figure 4.7 but with the coordinate axes rotated so that the rows of parked aircraft are aligned with the figure's x-axis.

The procedures for towing aircraft are designed to minimize the risk to aircraft and personnel. The decisions made by the personnel performing the tow procedure should also be to minimize risk. From the path shown in Figure 4.23, it was observed that straight paths are desired over long curves. This is likely due to greater risk of collision with other aircraft or personnel during turns. The motion of the aircraft, two articulated linkages behind the trailer, is more difficult for the Director and Tractor Driver to predict while the system is turning. It is also more challenging for the Wing and Tail Safeties to walk in a curve, rather than a straight line. So the tow tractor

Figure 4.23:   Path Planning: Desired Path

steering angle as a function of time $\alpha(t)$ should be minimized. A cost function which simulates this desire for straight paths is given by

$$J\left(\bar{x}, \bar{u}, t\right) = \int |\alpha(t)| \ dt. \tag{4.1}$$

Other parameters could be used in the cost function as well. Minimizing ζ and ϕ may provide even closer results. Using DIDO to find a path and minimizing this cost provides the path shown in Figure 4.24. This path was generated by the MATLAB® scripts provided as Listings B.9 through B.13 on pages 160-177. The scripts used for this problem were based on work by Hurni, *et al.* [20–22]. Over 30 minutes of computation time was required to solve for the optimal path. While the paths do not match exactly, this system can be used to warn personnel of potential mishaps outside their field of view.

Figure 4.24:   Path Planning: Predicted Path

4.3   Summary

The ability of a radio-navigation based positioning system to measure the state of the flight deck has been demonstrated using precision GPS recorders. The errors observed in the measurements taken at NAS Oceana are consistent with expected GPS errors. The position errors on the wingtips observed in the evening portion caused measurement noise in the heading of the vehicle. Having observed the consistency of personnel positions relative to the aircraft it is straightforward to envision how a persistent monitoring system could recognize a potential mishap involving personnel. The optimal path planning results, which closely match the actual path taken, could enable a persistent monitoring system to recognize mishaps further ahead in time than distance measurements alone.

V. Conclusions

The subject of this research was the feasibility of a persistent monitoring system originally discussed in Section 1.3. Such a system would continually monitor the position and orientation of all aircraft and support equipment, the position of all personnel on the flight deck, and the state of critical flight deck systems such as the up/down status of the jet blast deflectors. Such a system would provide this information in a format easily understandable by decision makers, such as the Aircraft Handling Officer, so that they can improve the safety and overall efficiency of flight deck operations. The system should also autonomously notify personnel if they are approaching a hazardous area or situation. The goal of such a system is a more efficient flight deck which can

1. reduce the occurrence of flight deck mishaps and

2. provide accurate recordings of flight deck operations for analysis.

This chapter presents an overview of the research performed, how the knowledge gained can be applied to the development of a persistent monitoring system, and recommendations for future work in this area.

5.1   Overview

Chapter I provided a detailed analysis of the aviation mishap records provided by the Naval Safety Center. This study showed that *Interest Mishaps*, those which are potentially preventable by a persistent monitoring system, account for $92,486,469, or 5.55% of the cost of all recorded mishaps in the data provided. These *Interest Mishaps* were categorized by cause and four successive levels of monitoring were proposed to help mitigate their occurrence.

Prior research towards improving flight deck operations was explored in Chapter II as well as related topics such as GPS, pseudolite positioning, and Blue Force Tracking. Algorithms necessary to implement a persistent monitoring system were discussed including position and orientation determination as well as the nearest neighbor

problem. Multiple path planning methods were presented with the goal of predicting the trajectory of a towed or taxiing aircraft.

The data collected for this research, discussed in Chapter III, involved measuring the position and orientation of a towed aircraft as well as the position of the personnel required for the procedure. Preliminary tests were conducted at AFIT to ensure the proper operation of the GPS recorders and their ability to provide precision measurements.

An analysis of the data collected, presented in Chapter IV, demonstrated the ability of precision GPS recorders to measure the position and orientation of an aircraft, both stationary and in motion, as well as the positions of personnel around it. Significant error was observed in the evening tests, most likely caused by multipath. The path planning software DIDO was used to find an optimal trajectory for the towed aircraft system based upon the measured data.

From the results of this research, some overall conclusions can be made about the feasibility of a persistent monitoring system:

1. Due to a number of factors, such as the high multipath error observed, the high cost of dual frequency GPS receivers, the need for indoor functionality, and the risks involved in relying on satellite transmissions, the measurement system should not exclusively rely on GPS for the highly accurate measurements required.

2. Substantial computing power is required to predict the path of a towed aircraft and process state information from potentially hundreds of positioning devices. The ability to closely match the actual path could significantly improve the system's ability to recognize potential mishaps.

5.2 Preventing Mishaps

With the knowledge and experience gained from the tests at NAS Oceana described in Chapter III, it is possible to discuss how a persistent monitoring system
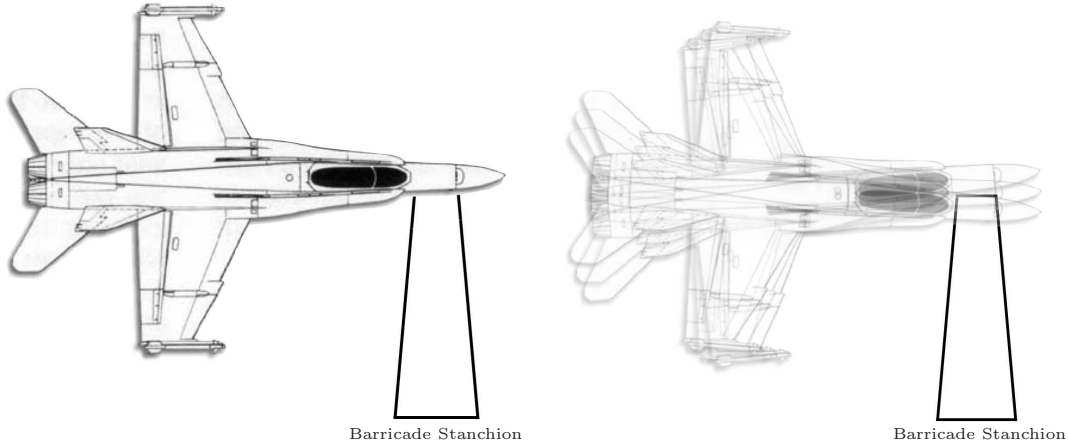
(a) Precise Measurement: The barricade stan-
chion will impact the aircraft when raised.

(b) Imprecise Measurement: It is unknown if
the barricade stanchion will impact the aircraft
when raised.

Figure 5.1:   Recognizing Spotting Mishaps

could be designed in order to prevent mishaps. Recalling the primary mishap classifi-
cations of Section 1.2.2, this section provides an example for each classification. Each
example is taken from the narratives of Table 1.4 on page 12.

5.2.1   Spotting Mishaps.   An extremely common spotting mishap is a parked
aircraft being struck by a Jet Blast Deflector (JBD) or Barricade Stanchion. Fig-
ure 5.1 illustrates an aircraft parked such that the raising of a Barricade Stanchion
will impact the aircraft. A Level One system, one which measures aircraft position
and orientation, could potentially prevent such a mishap if the measurements are
sufficiently accurate.

A distance measurement between the aircraft and the barricade stanchion could
be used to recognize a potential mishap. If the distance between an aircraft's center
and the barricade stanchion is below a certain threshold, then a nearest neighbor
search should be conducted to determine if any point on the aircraft is near zero
distance, in two-dimensions, from any point on the stanchion. If this is true, then a
persistent monitoring system could be set to handle the situation in different ways.

Having determined there is potential for a spotting mishap, the system could warn the Taxi or Tow Director that the aircraft is parked in an undesirable location. Alternately, the system could warn Flight Deck Control that the aircraft was parked in a hazardous location, leaving it to the Handling Officer to determine whether it should be moved. If the decision is made to park the aircraft in a potentially hazardous position, for whatever reason, then the system could alert Flight Deck Control of this hazard again if the Barricade Stanchions are set to be raised.

Considering the prevention of this type of mishap also allows an analysis of the level of accuracy required for both position and orientation measurements. Figure 5.1 shows the effect of just 5° of heading angle measurement error. With this error a monitoring system could not determine whether the stanchion would collide with the aircraft.

The results of the heading calculations, presented in Figure 4.6 on page 101, demonstrate the ability of precision GPS to provide accurate and low-noise headings. Any radio navigation system with centimeter-level accuracy should be able to provide similar results.

5.2.2 Towing Mishaps.   Potential towing mishaps, such as a collision with a parked aircraft in the hangar bay, could be recognized by a Level One system. A path planning system, such as one that uses DIDO, discussed in Section 2.7.3 on page 63, could continuously compute a reasonably close prediction of the path of the towed aircraft system. If a Level Two system is implemented, it could monitor both aircraft and support equipment.

Many towing mishaps listed in Appendix A involve a towed aircraft being parked in close proximity to a stationary aircraft. Figure 1.16 on page 32 provides a visualization of this close proximity. In this case, the persistent monitoring system could continuously calculate the nearest neighbor distance to surrounding aircraft, equipment, and personnel. If this distance is less than a pre-determined threshold, the system could alert all personnel involved to the risk of collision.

Recognizing towing mishaps will be dependent upon the position measurement accuracy of the system. As increased multipath errors were seen in the measurements during the evening phase of the tests at NAS Oceana, described in Sections 4.2.1 and 4.2.2, this type of mishap may also dictate the requirements for maximum allowable multipath error. Figure 4.7 on page 103 shows that GPS can accurately measure the location of the aircraft while Figure 4.9 on page 106 and Figure 4.21 on page 112 demonstrate the ability of GPS measurements to be utilized for personnel position and nearest neighbor determination.

5.2.3   *Taxiing Mishaps.*   A Level One system, measuring the position and orientation of all aircraft on the flight deck, should be able to recognize a potential taxiing mishap. Typically, this type of mishap involves a collision between two aircraft. While it could be possible to warn of such a potential mishap simply by calculating the distance between the aircraft and their relative velocity, the use of a path planning system, such as one that uses DIDO, discussed in Section 2.7.3 on page 63, could significantly increase the time that personnel would be given to react to the warning and reduce the occurrence of false warnings.

If a potential mishap is detected, the pilot of one aircraft could be directed to stop while the other moves beyond the collision event horizon. In the case of a path becoming obstructed, the Taxi Director and pilot could be provided with a new path to follow.

5.2.4   *Exhaust Mishaps.*   With the heading rate and personnel position measurements from Sections 4.2.2 and 4.2.4 it is possible for a Level Three system to recognize a potential exhaust mishap. In a typical scenario, the system could watch for a taxiing aircraft performing a turn on deck with a sailor standing still in a location the exhaust will pass through. Such a scenario is depicted in Figure 5.2.

To prevent injury or damage from resulting from this type of mishap, the system could utilize not only the position and orientation measurements, but a desired
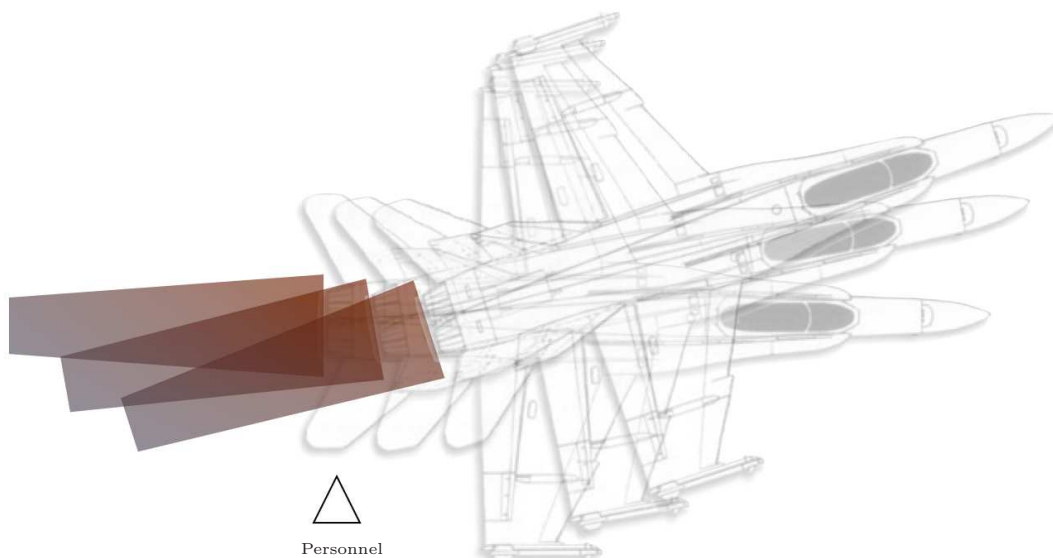
Figure 5.2:   Recognizing Exhaust Mishaps

location as determined by Flight Deck Control. A taxiing aircraft is generally heading towards a catapult, a de-arming location, or a parking spot, and the desired locations are set by Flight Deck Control. Starting from the aircraft's measured position and orientation a path planning system, such as DIDO, should provide a reasonable estimate of the path if a desired final position and orientation are known. The heading rate calculations can be used to determine the speed with which the exhaust hazard is approaching the sailor. With this information, it would be possible to determine the amount of time before the aircraft's exhaust poses a hazard to the sailor. The sailor could be alerted to this hazard with time to move out of the way or duck to avoid the exhaust. In a Level Four system, where the status of aircraft systems is reported to the persistent monitoring system via a datalink, the actual throttle status could be utilized to determine the dimensions of the exhaust hazard area.

The ability of a persistent monitoring system to predict this kind of mishap would depend greatly upon the position measurement accuracy and precision. If position measurements are noisy, the heading rate calculations would be useless. Ad-

ditionally, the rapid pace of events on the flight deck could require the system to have a particular measurement update rate to be fully effective.

5.2.5 *Contact Mishaps.* The contact mishap presented in Table 1.4 on page 12 describes a Plane Handler, identified by the color of jersey worn, being run over by the main mount of an aircraft. If a Level Three persistent monitoring system is implemented it could issue warnings of such a situation. One potential prevention method is to use the personnel bounding boxes shown in Figure 4.21 on page 112. These bounding boxes are areas surrounding the aircraft where the personnel involved are expected to remain throughout the procedure. The system could inform the Director, Tractor Driver, and Plane Captain when all personnel are positioned within the bounding boxes, and only then would they start moving the aircraft. If the pilot is operating the aircraft, then the pilot could be given permission to move once all personnel are positioned within their respective bounding boxes.

Preventing this type of mishap imposes requirements on the accuracy of both aircraft and personnel position measurements. As personnel often travel underneath the wing or fuselage of an aircraft during flight deck operations, it also presents requirements for signal re-acquisition time for radio measurements or drift rate for inertial measurements.

5.2.6 *Engine Mishaps.* As previously discussed, it is easy for a sailor to walk directly into a turning propeller. With a Level Three system monitoring the movements of personnel, the distance between a person and the propellor could be measured and a warning issued if the distance is below a certain threshold. It would also be possible to create a hazard zone directly in front of the propeller. If a person enters the zone then the system would alert them to leave it immediately. Figure 5.3 illustrates notional hazard zones around the propellers of an E-2C Hawkeye.

The propeller hazard zones only exist when the propellers are turning. Maintenance must be performed on the propellers, so the persistent monitoring system must
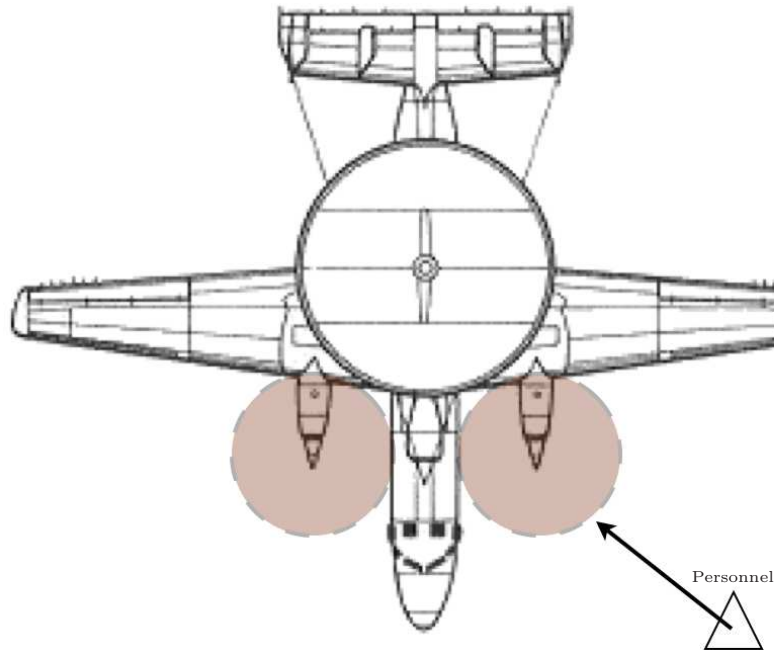
Figure 5.3:   Recognizing Engine Mishaps

somehow be aware of this status. An aircraft scheduled for a flight within a speci-fied time, for instance, could automatically be checked for engine hazard violations. Alternately, a supervisor on the flight deck could be required to inform Flight Deck Control to disable the engine hazard violation warnings for maintenance purposes. If a Level Four system is in place, then the engine status reported by the aircraft could be utilized to determine hazard zone status.

5.2.7 Wingfold Mishaps.   One method to potentially prevent wingfold mishaps is a Level Four system, where the aircraft have been modified to report their wingfold switch status to the persistent monitoring system. If the measured position and orientation of the aircraft would force its unfolding wings to impact an-other object, then the system would not allow the wings to unfold. This modification could be prohibitively expensive, but future aircraft could have it included earlier in the acquisition process at a reduced cost.

125

Another method to detect a potential wingfold mishap is to measure the distance between wingtip mounted receivers as part of a Level One system. The rate at which the wings were folded at NAS Oceana, presented in Section 4.2.6, was slow because the fold was performed manually. When an FA-18C is powered, the wingfold process is significantly faster. The magnitude of the wingspan measurement slope in Figure 4.22 on page 115 would be greater for a powered wingfold, and therefore easier to detect.

A persistent monitoring system's performance specifications such as accuracy and update rate will greatly affect its ability to recognize this type of mishap. Using wingtip mounted receivers to detect the wingfold motion may also impose constraints on the physical design of the receiver. Significant multipath was observed when the wings were folded and the antennae were pointed towards the aircraft.

5.2.8 Non-aviation Mishaps. A non-aviation mishap, such as an aircraft being struck by a forklift during an underway replenishment, is very similar to a towing mishap. The same processes to recognize a potential mishap, path prediction and distance calculation, should be applicable.

The challenge inherent to non-aviation mishaps is that they don't exclusively involve aviation assets or personnel. The forklifts and pallet jacks used by the supply department would need to be monitored, and the personnel operating them would have to be trained to respond to hazard warnings. Attempting to prevent this type of mishap leads to considerations on the pervasiveness and simplicity of a persistent monitoring system, as non-aviation personnel would only occasionally be required to use it.

5.3 Measurement System Implementation

This section discusses the requirements for implementing methods to measure the position and orientation of objects on the flight deck based upon the research described in Chapter III. The equipment necessary to measure position and communicate hazard warnings is discussed.

5.3.1 Position Measurement.   As discussed in Section 2.1.2 on page 36, the Navy currently plans to use video analysis to measure the position and orientation of each aircraft on the flight deck, although with less accuracy than the measurements made in this research using GPS. To reduce the occurrence of flight deck mishaps, one of the major goals of a persistent monitoring system, it is vital to not only have accurate measurements of aircraft position and orientation but to measure the position and orientation of support equipment as well as the position of personnel. It may be possible to use additional cameras to measure these positions, but there are numerous challenges. One challenge is identifying, via video recordings, a person who may be standing up straight, crawling under an aircraft, or lying injured on the deck. If this can be achieved, it is likely to require extensive computational power. Radio navigation provides a simpler alternative and, as shown in Chapter IV, the accuracy is significantly better than that expected of the planned video analysis system. This section will focus on the methods of implementing a radio navigation system to measure the location of aircraft, equipment, and personnel on the flight deck and hangar bay.

5.3.1.1 Measurement Source.   This research focused on using GPS for position measurements. As discussed in Section 5.1, the exclusive use of GPS is not desirable for a persistent monitoring system. The functionality of a system reliant on GPS is at risk of degradation from multiple sources: satellite constellation issues, atmospheric disturbance, as well as jamming or spoofing by an opposing force. Furthermore, it is desired for this system to measure locations both on the flight deck and the hangar bay. Given that the hangar bay is essentially one large Faraday cage, and external radio transmissions cannot be received inside, it is impossible to use GPS inside of it.

To achieve centimeter-level accuracy it is required to use a dual frequency GPS receiver. Dual frequency antennae are expensive (each of the antennae used in this research cost approximately $1,000), and a dual frequency receiver must either have

the classified decryption key for P(Y) code or, like the receivers used in this research, advanced algorithms to utilize the L2 signal without decrypting P(Y), potentially costing thousands of dollars per receiver. These costs are currently decreasing and could potentially be further reduced given the mass production required to equip the fleet.

Pseudolite positioning provides a promising alternative. With multiple transmitters mounted on the flight deck and in the hangar bay the persistent monitoring system should have observability of both areas. Pseudolites also provide the ability to select the frequency and chipping rate of the transmission. With a higher chipping rate or frequency transmission than GPS, highly accurate measurements could be made using either code or carrier phase solutions, even on a single frequency. The system would be organic to the ship enabling these parameters to be reconfigured as the mission requires as well as eliminating the dependency on satellites. With sufficient pseudolite transmitters around the perimeter of the flight deck, it could be possible to avoid most scenarios where a receiver would be prevented from receiving a signal due to another object's obstruction.

Both GPS and pseudolite measurements are susceptible to multipath errors, as observed in the wingspan and heading measurements of Chapter IV. This error will likely be amplified onboard an aircraft carrier due to the large metal deck, metal superstructure, and prevalence of other aircraft. To mitigate this, it may be necessary to integrate inertial measurements with the code or carrier phase measurements through a Kalman filter.

While this research has addressed the measurement accuracy needed for mishap recognition, the measurement integrity of the system is critical to the proper operation of a persistent monitoring system. Since the system is intended to enhance the safety of personnel, it is vital that it be aware of any significant errors in the measurements.

5.3.1.2 Measurement Device. Position measurements are to be made for three different objects: aircraft, support equipment, and personnel. If orientation

measurements are also desired, then the object would require two devices (or at least two antennae). A common core device could be designed with additional components specific to each object. The core device needs to make position measurements and communicate these to a central computer onboard the ship wirelessly and in near real-time. It would be possible for the core device to simply make pseudorange measurements and transmit them via a packetized network protocol (such as IEEE 802.11) which would allow for the use of public/private key authentication to prevent spoofing and allow identification. A centralized computer could then apply any error corrections and calculate the actual relative flight deck positions and velocities. The measurement device used must not add significant complication to flight deck operations. Battery management is likely to be a major user concern unless addressed early in the design phase.

Simplifications can be included in the design of the measurement devices because they will operate primarily onboard the aircraft carrier. When a device can communicate with the central onboard computer it needs only transmit the range information: no position computations need to be performed in the device. Offloading computations would reduce the device's processing power requirement and power consumption. This centralization will also allow updates to the measurement algorithm, including error corrections, to be applied centrally.

For aircraft position and orientation, the Navy must decide whether it is more effective to modify the aircraft and install permanent receivers or to temporarily mount them while the aircraft is on deck, similar to the method described in Section 3.2.1 on page 77. In either case, it is vital that they are capable of transmitting measurements whether the aircraft is powered or not. Support equipment presents a unique challenge, as there are dozens of different types. It may be advantageous to measure position and orientation only for SE over a certain threshold size. Position measurements may also be needed for smaller SE such as ordnance carts and aircraft jacks.

129

To enhance the safety of personnel, their device would require the largest number of features. It must not only collect and transmit range measurements but be capable of providing warnings to the person using it. The device should not hinder the movements of personnel any more than current flight deck protective equipment does. The ideal device would integrate into existing helmets and/or float coats. Aural warnings could be provided through noise-cancelling headphones, which could even enable the wearer to be steered away from a hazardous area. The Navy and Air Force are currently investigating active noise cancelling technology for use in high-noise aviation environments which could be adapted to support this capability [55].

5.3.2   *Flight Deck Status.*   It would be necessary to measure the elements of flight deck state presented in Table 1.8 on page 23. Many of these are already measured but it would be necessary to tie all of the measurements to a centralized system.

5.3.3   *Obstacles to Implementation.*   The single greatest obstacle to physical implementation would likely be training personnel to use it properly. If decision makers are not familiar with its capabilities, they will not use it to the full extent. If sailors are not aware of its limitations they may rely on it too much for their safety.

Shipboard frequency allocation is a significant obstacle which would need to be resolved. With multiple frequencies needed for pseudolite and wireless packetized data transmission, it is vital that the system not interfere with existing systems or pose a risk to electromagnetically sensitive equipment, such as ordnance.

5.4   *Monitoring System Implementation*

With a computer capable of collecting the position and state measurements of objects on the flight deck, it is essential that software be created to fully utilize this information. Many of the methods and algorithms discussed to recognize mishaps, such as path planning and nearest neighbor searching, are computationally inten-

sive, requiring a high-performance computing infrastructure. The monitoring system will also need to be highly reliable and survivable, able to withstand malfunctioning components and damage. The monitoring system must be able to clearly and effectively communicate with personnel in a variety of ways such as accepting inputs for flight schedules and maintenance requests, displaying the current status and projected configuration, and alerting personnel concerned to potential hazards.

5.4.1 Computational Requirements. Modern computers are significantly more advanced than when CADOCS, discussed in Section 2.1.1, was proposed. The tasks CADOCS was to perform, such as storing flight schedules, displaying a map of the flight deck, and recording aircraft fuel and maintenance information, pushed the limits of computational capacity. For a modern computer, these tasks are trivial.

Providing the ability to recognize and potentially prevent mishaps for a large number of aircraft, equipment, and personnel requires a significant amount of computing power. The central computer must calculate positions and orientations from the ranges reported by each measurement device, perform hundreds of nearest neighbor searches, and update path predictions at a rate which enables these calculations to be useful. The measurements data for this research was collected at 5 Hz, which is a reasonable requirement for the onboard computer system. As discussed in Section 2.6.1, the nearest neighbor calculation time is dependent upon the number of points composing the model, so the system developers will have to trade model resolution, calculation rate, and computational power.

The path planning algorithm is orders of magnitude more computationally intensive than the other algorithms discussed. Using DIDO in MATLAB® to calculate the results presented in Section 4.2.7 required over 30 minutes on a computer with a dual-core processor. Implementing this for a real-time operational system will require rewriting an optimal solver in a lower-level language, such as C or C++, utilizing multiple computers in a massive parallel system, or both. While this is the most com-

putationally intensive portion of the hazard recognition process, it has the potential to provide the greatest benefit.

Another consideration that should be taken into account in the development of a persistent monitoring system is the need for redundancy, reliability, and maintainability. If the central computer ceases to function, for whatever reason, the entire system would cease to function. Parallel computing provides a straightforward solution to this problem. Multiple spaces, spread throughout the ship, could be utilized to house the computers for this system. This has the added advantage of making the system highly maintainable as a single faulty computer could be replaced without disabling the system.

5.4.2 Human-Computer Interaction. No matter how well the system is able to recognize and potentially prevent mishaps, it won't be used if the personnel concerned can't fully interact with it. The input method for providing schedules, requests, and orders must be intuitive. A user should be able to immediately recognize and understand the information provided by a display. Warnings need to be effective without hindering flight deck operations.

A touch-sensitive table computer, depicted in Figure 2.3 on page 36, seems to be the perfect method for human-computer interaction within flight deck control. Movement orders can be provided simply by touching, dragging, and rotating the icon for an aircraft. Multiple users can even use the system simultaneously. Critical information, such as fuel state, maintenance status, and next scheduled flight could be accessed with the touch of a finger.

Maintenance personnel throughout the ship could be provided with flight deck and hangar bay information through a web browser based system. This could allow maintenance requests to be communicated effectively to flight deck control and aircraft movement schedules to be accessed directly by the personnel directed to perform maintenance. The web browser based interface would allow access without any special software and updates to be applied only to a central computer.

5.4.3 Data Recording. Part of preventing mishaps is studying the exact events that occurred. The monitoring system could record all of its information for later access in the case of a mishap, much as an aircraft records data to the "black box." This data could be archived with organizations concerned, such as the Naval Safety Center and Naval Air Systems Command, for thorough study to improve not just safety, but the performance of flight deck operations.

In the event of a mishap, the ship or squadron would be able to review the events in detail with the personnel involved. This provides an objective recording of mistakes from which to learn. Simply reviewing the data collected could potentially be of greater value than the real-time monitoring provided by the system.

5.5   Future Work

The persistent monitoring system proposed by this research is complex, and no off-the-shelf product can provide its capabilities. Since the proposed system is modular, with independent subsystems for measurement and monitoring, future work in this area can explore each simultaneously.

The development of the measurement system requires more study of radio positioning in an environment similar to the flight deck. Further research into integrating inertial and radio navigation measurements for multipath error mitigation should be performed. The use of pseudolites, near ground level, to provide two-dimensional positioning on a moving platform also requires significant research.

Further research in using path planning to match the movements of aircraft on the flight deck is critical to the monitoring system. Determining the correct parameters to calculate the cost function could significantly improve the accuracy of the predicted path. Other research should focus on the best methods of interacting with personnel, and what functionality experienced personnel would find useful.

5.6 Final Thoughts

This research set out to determine the feasibility of utilizing a persistent monitoring system to potentially prevent mishaps onboard a U.S. Navy aircraft carrier. From the data collected it is clear that radio navigation can provide the accuracy to collect the information necessary to recognize a hazardous situation. Actually implementing a system to provide this functionality is a complex and challenging task. Arguments have been provided that significant cost savings could be achieved by implementing such a system. It is up to Naval leadership to determine if the operational and safety benefits outweigh the costs.

Appendix A. Interest Mishaps

The records provided by the Naval Safety Center contained information on 3,228 mishaps. Those that were identified by the author as potentially preventable, here labelled *Interest Mishaps*, are those in which a persistent monitoring system for the flight deck could have provided some warning.

Many of the data elements provided, described in Table 1.1 on page 6, are provided here. If multiple aircraft were involved in the mishap, only the first is listed under Type/Model/Series. The Fatalities and Major Injuries columns were generated by reading the narratives. A tally was made only when the narrative specifically stated a sailor was injured or killed. The category column represents the mishap classification as described in Section 1.2.2 on page 9.

Narratives are presented exactly as contained in the data provided by the Naval Safety Center. Some commonly used abbreviations not previously explained which may be unclear to readers without Naval experience are:

1. P/C or PC: Plane Captain

2. GSE: General Support Equipment

3. STBD: Starboard

4. MLG: Main Landing Gear

5. SQN: Squadron

6. ABH-2: Aviation Boatswain's Mate (Handling) Second Class

7. CQ: Carrier Qualifications

8. LEF: Leading Edge Flap

Event Serial	Fiscal Year	Event Class	Type Model Series	Total Event Cost ($)	Fatalities	Major Injuries	Narrative	Category
31164	1980	A GROUND	F004N	2,679,830	0	0	ACFT ROLLED OFF FLT DECK AND SANK WHILE SHIP WAS PERFORMING PORT TURN.	Spotting
31266	1980	B GROUND	F014A	34,000	0	1	CHOCK WALKER SUSTAINED MAJ INJURY WHEN FOOT WAS RUN OVER BY TOWED ACFT	Contact
31656	1980	B GROUND	E002B	34,000	0	1	P/C SUSTAINED MAJOR INJURIES WHEN HE WALKED INTO ARC OF TURNING PROP.	Engine
31708	1980	B FLIGHT	A007E	273,102	0	0	CHOCK CART AND CHOCKS BLOWN INTO TURNING PROPS BY JET BLAST.	Exhaust
31720	1980	B FLIGHT	A007E	151,789	0	0	A/C TAXIING ON CV STRUCK SECOND A/C AND 2 FLT DK PERSONNEL CAUSING INJ	Taxi
31739	1980	B GROUND	S003A	120,064	0	0	ACFT BACKED INTO PARKED ACFT WING BUTT DURING DECK RESPOT.	Towing
31740	1980	B GROUND	S003A	128,636	0	0	ACFT BACKED INTO WING BUTT OF PARKED ACFT DURING DECK RESPOT.	Towing
29567	1981	A FLIGHT	S003A	106,937	1	0	ACFT JET ENG INGESTED MAINT TROUBLESHOOTER DURING TURN-UP ON CV. FATAL	Engine
29757	1981	C GROUND	F014A	22,760	0	0	ACFT SUSTAINED DAMAGE TO A/B SUPPORT DURING DECK RESPOT.	Spotting
29763	1981	C FLTREL	A007E	285	0	0	GSE OPERATOR INJURED WHEN BLOWN OFF POWER CART BY JET BLAST.	Exhaust
30143	1981	A FLTREL	A006E	151,000	0	1	JET BLAST STRUCK FINAL CHECKER ON FLT DECK RESULTING IN MAJOR INJURIES	Exhaust
30222	1981	B FLIGHT	HH046A	337,050	0	0	ACFT ROLLED ONTO SIDE AFTER STBD MLG BECAME FOULED IN CV ELEV COMBING.	Towing
30345	1981	B FLIGHT	TE002A	107,171	0	0	PROP STRUCK BY JBD PANEL AS ACFT TAXIIED INTO POSITION FOR CAT LAUNCH	Taxi
30422	1981	A FLTREL	A007E	37,000	1	0	LINE DIV DAY SUPER BLOWN OVER THE SIDE BY JET BLAST. FATALLY INJURED.	Exhaust
31798	1981	A GROUND	RF008G	500,000	0	0	AIRCRAFT UNDER TOW STRUCK WING OF PARKED AIRCRAFT ON FLIGHT DECK.	Towing
31865	1981	A GROUND	F014A	13,997,000	0	0	ACFT SPOTTING DOLLY LOST OVERBOARD DURING ACFT SPOTTING OP AT SEA.	Spotting
31915	1981	A GROUND	F014A	724,000	0	0	PARKED ACFT SUSTAINED ALPHA DAMAGE WHEN STRUCK BY CLOSING HGR BAY DOOR	Spotting

Event Serial	Fiscal Year	Event Class	Type Model Series	Total Event Cost ($)	Fatalities	Major Injuries	Narrative	Category
31921	1981	B FLIGHT	F004J	136,240	0	0	NOSE OF ACFT STRUCK UNMANNED ACFT DUE TO JET BLAST FROM TAXIING ACFT.	Exhaust
27205	1982	B GROUND	F014A	108,834	0	0	ACFT STRUCK 2 OTHER ACFT DURING FLIGHT DECK RESPOT.	Towing
27299	1982	A FLTREL	F004N	47,000	1	0	FLT DECK COORDINATOR BLOWN INTO PARKED A/C BY JET EXHAUST.FATAL INJS.	Exhaust
27355	1982	B GROUND	F004	43,000	0	1	CHOCK WALKER SUSTAINED INJ TO BOTH FEET WHEN RUN OVER BY TOWED ACFT.	Contact
27475	1982	B FLTREL	A007E	0	0	1	FLT DECK PERS SUSTAINED LEG INJ WHEN LEG WAS TRAPPED UNDER TAXIING A/C	Contact
30779	1982	B GROUND	F014A	186,518	0	0	TRACTOR DRIVER INJURED, 3 ACFT DAMAGED DURING NIGHT FLT DECK RESPOT.	Towing
24867	1983	B GROUND	SH003H	98,643	0	1	UNMANNED TOW TRACTOR ROLLED ACROSS FLT DECK CAUSING INJURY/DAMAGE.	Spotting
25348	1983	B GROUND	F014A	43,000	0	1	CHOCK HANDLER HAD FOOT RUN OVER BY MOVING ACFT.	Contact
25439	1983	B FLTREL	F014A	43,000	0	1	FLIGHT DECK PERSON LEG WAS RUN OVER BY ACFT.	Contact
25489	1983	B FLTREL	A007E	43,000	0	1	ORDNANCEMAN LEFT FOOT RUNOVER AS AIRCRAFT WAS BEING TAXIED TO CATAPULT	Contact
26044	1983	A GROUND	A007E	47,000	1	0	AIRMAN LOST AT SEA AFTER BEING BLOWN FROM FLT DECK BY TURNING ACFT.	Exhaust
26193	1983	B FLIGHT	EA006B	177,669	0	0	ACFT STRUCK OTHER ACFT DURING NIGHT CATAPULT SHOT	Spotting
28890	1983	A FLIGHT	S003A	137,638	1	0	MAINT PERSON FATALLY INJURED WHEN HE WAS SUCKED INTO ENGINE INTAKE.	Engine
23104	1984	A GROUND	S003A	190,000	0	1	GND PERSON RUN OVER BY ACFT MLG DURING RESPOT. PERM TOTAL DISABILITY.	Contact
23628	1984	A GROUND	F014A	16,250,225	0	0	ACFT ROLLED OVERBOARD SHIP FROM ELEVATOR DURING FLIGHT DECK RESPOT.	Spotting
26976	1984	A FLTREL	A007E	47,000	1	0	PHONE TLKR BLWN OVRBRD BY JET BLAST.VICTIM LOST AT SEA DURING RESCUE.	Exhaust
27085	1984	B FLIGHT	S003A	147,458	0	0	ACFT ON FLT DECK WAS HIT BY AN ACFT BEING RAISED TO DECK ON ELEVATOR.	Spotting
21424	1985	B GROUND	E002C	43,000	0	1	CHOCK WLKR INJURED AS HE FELL WHEN FOOT WAS RUN OVER BY PUSHED ACFT.	Contact

Event Serial	Fiscal Year	Event Class	Type Model Series	Total Event Cost ($)	Fatalities	Major Injuries	Narrative	Category
24264	1985	B GROUND	F014A	257,102	0	0	ACFT STRUCK PARKED ACFT DURING RESPOT EVOLUTION.	Taxi
24447	1985	A GROUND	KA006D	47,000	1	0	GND PERSON RECEIVED FATAL INJ WHEN BLOWN OVERBD DURING NIGHT LAUNCH.	Exhaust
17534	1986	A FLTREL	A007E	47,000	1	0	FLT DECK PERS BLOWN OVERBOARD BY JET BLAST DUR LAUNCH W/FATAL INJURY.	Exhaust
18846	1986	A FLIGHT	S003A	209,954	1	0	ACFT HIT GROUND PERSON DURING NIGHT CATAPULT LAUNCH WITH FATAL INJURY.	Contact
18952	1986	B GROUND	A006E	43,000	0	1	ACFT UNDER TOW ROLLED OVER ORDNANCEMAN'S L LEG DURING DECK RESPOT.	Contact
19051	1986	C FLIGHT	F018A	89,142	0	0	ACFT UNDER TOW RUNS OVER ACFT HANDLER'S LEG.	Contact
22273	1986	B GROUND	SH003H	129,932	0	0	PARKED ACFT SUSTAINED DAMAGE WHEN BARRICADE STANCHION STRCK HORIZ STAB	Spotting
22622	1986	B GROUND	F018A	43,000	0	1	CHOCK WALKER HAD FOOT RUN OVER BY ACFT DURING SPOTTING OPERATION.	Contact
14396	1987	B FLIGHT	E002C	328,404	0	0	ACFT DAMAGE/PERS INJURIES RESULT FROM DECK RAMP BLOWN BY JET EXHAUST	Exhaust
15008	1987	B FLTREL	A007E	43,000	0	1	ACFT TAXIED OVER FINAL CHECKER'S LEGS.	Contact
15258	1987	B GROUND	KA003B	43,000	0	1	ACFT HANDLING CREWMAN'S LEG WAS RUN OVER DURING ACFT RESPOT ON CV.	Contact
15881	1987	A GROUND	F014A	553,839	0	0	ACFT HIT MULTIPLE ACFT WHILE BEING PUSHED TO RESPOT POSITION.	Towing
19749	1987	A FLIGHT	A007E	2,839,435	0	0	ACFT WENT OVER PORT SIDE OF SHIP DURING TAXI. ACRW EJECTED.	Taxi
7671	1988	A GROUND	A007E	2,877,000	1	0	DUR RESPOT SLID OFF FLT DECK WHILE UNDER TOW. P/C MISSING.	Towing
8158	1988	A FLIGHT	C002A	78,204	1	0	SQN PLANE CAPTAIN WALKED INTO ACFT PROP FOLLOWING NORMAL RECOVERY.	Engine
8368	1988	B FLIGHT	F014A	105,761	0	0	INADVERTENT WINGSWEEP ON DECK. WING STRUCK ANOTHER ACFT.	Wingfold
8739	1988	B FLTREL	EA006B	45,700	0	1	MAIN MOUNT STRUCK SHUTTLE, TIRE EXPLODED INJURING YELLOW SHIRT.	Misc
16200	1988	B GROUND	A006E	43,000	0	1	ACFT RAN OVER PLANE CAPT TRAINEE'S LEG DURING NIGHT FLT DECK RESPOT.	Contact
16384	1988	A FLIGHT	E002C	77,199	1	0	DURING PREP FOR LAUNCH, GROUND PERSON WALKED INTO TURNING PROPELLER.	Engine

138

Interest Mishaps.

Event Serial	Fiscal Year	Event Class	Type Model Series	Total Event Cost ($)	Fatalities	Major Injuries	Narrative	Category
16519	1988	B FLIGHT	E002C	116,404	0	0	ACFT UNDER DIRECTOR CONTROL TAXIIED INTO TURNING PROP. NO INJURIES.	Taxi, engine
1408	1989	B GROUND	E002C	344,390	0	0	ACFT TAXIIED INTO TURNING PROP OF ANOTHER ACFT.	Taxi, engine
5630	1990	A GROUND	EA006B	1,310,570	0	0	ECM POD INADVERTENTLY FIRED DUE TO EXHAUST EXPOSURE.	Exhaust
32216	1991	B GROUND	F014B	320,962	0	0	TAXIING ACFT STRUCK TWO OTHER ACFT ON CARRIER FLIGHT DECK.	Taxi
33679	1991	B GROUND	S003B	294,597	0	0	PARKED ACFT SLID INTO CATWALK DURING SHIPS TURN.	Spotting
40078	1991	C GROUND	F018C	98,524	0	0	ACFT HORIZ STAB, DOORS WERE BURNT BY EXHAUST OF ANOTHER ACFT	Exhaust
35370	1992	A GROUND	F014A	500,000	0	1	BLUE SHIRT RUN OVER BY ACFT MAIN MOUNT.	Contact
35480	1992	B GROUND	EA006B	115,000	0	0	DUR ACFT TAXI JET BLAST BLEW ABH-2 FROM FLT DECK TO LOWERED ELEVATOR.	Exhaust
37767	1993	B GROUND	F014A	115,000	0	1	FLIGHT DECK PERSON PULLED INTO ACFT INTAKE.	Engine
37867	1993	C GROUND	SH060F	31,338	0	0	ACFT WING SPREAD INTO HELO ON HANGAR BAY.	Wingfold
38669	1993	A GROUND	A006E	270,000	0	1	MAINT PERS BLOWN OVERBD BY JET EXHAUST WORKING ON FLT DECK.	Exhaust
38778	1993	C GROUND	EA006B	57,809	0	0	CATAPULT 2 JBD STRUCK ACFT LEFT WING TIPE DURING ACFT TAXI.	Taxi
39865	1994	C GROUND	A006E	13,048	0	1	ACFT TAXIED ONTO FINAL CHECKER'S ANKLE DURING ACFT SPOT ON CATAPULT.	Contact
40106	1994	C GROUND	EA006B	63,166	0	0	PARKED AIRCRAFT STRUCK BY TOW TRACTOR ON FLIGHT DECK.	Spotting
40139	1994	C GROUND	F018C	50,438	0	0	DEPLOY OPS/UNDER FLT DECK DIR/NIGHT POST RECOVERY, ACFT HIT PARKD ACFT	Taxi
40155	1994	C GROUND	F018C	15,828	0	0	PARKED ACFT WAS STRUCK BY ACFT UNDER TOW DURING FLT DECK RESPOT.	Towing
40431	1994	C GROUND	SH003H	155,979	0	0	DURING NIGHT FLT DECK RESPOT ACFT UNDER TOW HIT HELO PARKED ON SPOT 5.	Towing
40688	1994	C GROUND	F014D	50,336	0	0	ACFT UNDER TOW IN HANGAR DECK BAY COLLIDED WITH PARKED ACFT.	Towing
40775	1994	GRND HZ: GENERAL	A006E	0	0	0	ACFT PORT OUTBOARD WING TIP WAS HIT BY JET BLAST DEFLECTOR.	Unknown

Interest Mishaps.

Event Serial	Fiscal Year	Event Class	Type Model Series	Total Event Cost ($)	Fatalities	Major Injuries	Narrative	Category
40832	1994	GRND HZ: GENERAL	E002C+	0	0	0	HYD JENNY ROLLED INTO HAWKEYE DAMAGING FUSELAGE.	Spotting
40910	1994	C GROUND	F018C	15,852	0	0	ACFT UNDER TOW AND CONTROL OF FLT DECK DIRECTORS HIT ANOTHER ACFT.	Towing
41057	1994	GRND HZ: GENERAL	F018C	0	0	0	ACFT WITH CAPTIVE TRNG ORD CONTACTED GSE ON CV FLT DECK ON CQ OPS	Unknown
40888	1995	B GROUND	F018C	115,000	0	1	ACFT UNDER TOW RAN OVER AIRMAN ON FLIGHT DECK.	Contact
40990	1995	B GROUND	EA006B	115,000	0	1	ORDNANCEMAN SUFFERED CRUSHED FOOT FROM TAXIING ACFT ON FLIGHT DECK.	Contact
41428	1995	B GROUND	F014A	456,386	0	0	ACFT BLOWN INTO CATWALK BEHIND CAT 4; AIRCREW EJECTED SAFELY.	Exhaust
41451	1995	C GROUND	C002A	16,569	0	1	ENG NAC PANELS LOST OVRBD & MAINT MAN BLOWN DOWN BY JET BLAST ON DECK.	Exhaust
41501	1995	C GROUND	F018C	40,000	0	0	ACFT RADOME DAMAGED AFTER COLLISION WITH ANOTHER ACFT ON FLT DECK.	Unknown
42144	1995	C GROUND	EA006B	0	0	1	DURING NIGHT FRS CQ AIRCRAFT TAXIED OVER AIRMAN'S FOOT.	Contact
42699	1995	C GROUND	F018C	13,177	0	0	ACFT RADOME STRUCK RIGHT HORIZ STAB OF ANOTHER ACFT DURING TAXI.	Taxi
42963	1996	C GROUND	ES003A	31,904	0	0	GSE HIT ACFT PORT SIDE CAUSING DAMAGE TO ENG INLET COWL & ARS RAT	Spotting
43036	1996	C GROUND	S003B	21,300	0	0	ACFT RUDDER HIT CVN ISLAND, PLAT PLATFORM, WHILE BEING TAXIED ON DECK.	Taxi
43137	1996	FLT HZ: GENERAL	EA006B	0	0	0	FLT DECK HATCH ON UPPER STAGE WEAPONS ELEV 2 OPENED DAMAGING ALQ-99.	Spotting
43424	1996	C GROUND	F018C	94,029	0	0	CAT 2 JBD WAS RAISED INTO LEFT WING OF ACFT IN DEARMING AREA.	Spotting
43473	1996	C GROUND	F018A	48,966	0	0	DURING NIGHT FLIGHT DECK OPERATIONS, ACFT TAXIED INTO PARKED ACFT.	Taxi
43581	1996	C GROUND	F018C	26,930	0	0	AIRCRAFT UNDER TOW ON FLIGHT DECK IMPACTED LSO PLATFORM WINDSCREEN.	Towing
43641	1996	C GROUND	F018C	29,417	0	0	FORKLIFT OPERATOR STRUCK HORIZ STAB OF PARKED ACFT DURING VERTREP.	Misc
43970	1996	B GROUND	F018C	245,252	0	0	CRANE OPERATOR INADVERTENTLY LIFTED ACFT WHILE STILL CHAINED DOWN.	Misc

Interest Mishaps.

Event Serial	Fiscal Year	Event Class	Type Model Series	Total Event Cost ($)	Fatalities	Major Injuries	Narrative	Category
44056	1996	C GROUND	EA006B	1,875	0	0	TAILHOOK LOWERED ONTO FUEL HANDLER MANNING REFUELING STA IN CATWALK.	Contact
44099	1996	GRND HZ: GENERAL	EA006B	0	0	0	TOW TRACTOR COLLIDED WITHALQ-99 POD RADOME.	Towing
44447	1996	GRND HZ: GENERAL	S003B	0	0	0	ACFT CARRIER JET BLAST DEFECTOR RAISED INTO TAXIING ACFT.	Taxi
44458	1996	GRND HZ: GENERAL	E002C+	0	0	0	UHF SATCOM ANTENNA DAMAGED WHILE TOWING ACFT IN HANGAR BAY	Towing
44473	1996	A GROUND	F014A	500,000	0	1	GROUND HANDLER RUN OVER BY ACFT UNDER TOW. PERM TOTAL DISABILITY.	Contact
45407	1996	GRND HZ: GENERAL	EA006B	0	0	0	ACFT TAXIED INTO NOSE RADOME OF ANOTHER ACFT. FOD INGESTED BY STBD ENG	Taxi
45035	1997	GRND HZ: GENERAL	F018C	0	0	0	WINGS WERE INADVERTENTLY SPREAD DURING START UP, DAMAGING CATM9 MISSIL	Wingfold
45403	1997	GRND HZ: GENERAL	F018C	0	0	0	WINGS WERE INADVERTENTLY SPREAD DURING FLT DECK MAINT, DAMAGING AIM9.	Wingfold
45554	1997	GRND HZ: GENERAL	S003B	0	0	0	ACFT STRUCK TOW TRACTOR DURING RESPOT ON SLIPPERY DECK & HIGH SEAS.	Towing
45584	1997	C GROUND	S003B	58,504	0	0	TOW TRACTOR STRUCK ACFT DURING FLIGHT DECK RESPOT.	Towing
45629	1997	C GROUND	F018	25,940	0	0	DURING TAXI, ACFT HIT PARKED ACFT ON FLIGHT DECK.	Taxi
45766	1997	GRND HZ: GENERAL	E002C	0	0	0	MAINT PERSONNEL BLOW INTO FANTAIL SAFETY NET DURING ACFT MAINT TURN.	Exhaust
46014	1997	GRND HZ: GENERAL	E002C	0	0	1	FINAL CHECKER TRAINEE BLOWN OVER JBD DURING AIRCRAFT RUN-UP ON CAT.	Exhaust
46047	1997	C GROUND	F014A	13,110	0	0	DURING HANGAR BAY RESPOT, ACFT COLLIDED WITH ADJACENT CHANIED ACFT.	Towing
46119	1997	C GROUND	F018A	44,528	0	0	ACFT SUSTAINED DAMAGE TO RADOME DURING HANGAR DECK RESPOT.	Towing
46203	1997	GRND HZ: GENERAL	F018C	0	0	0	ACFT AT HIGH POWER DURING TAXI BLEW PREFLIGHTING AIRCREW INTO CATWALK	Exhaust
46269	1997	C GROUND	F018C	54,417	0	0	ACFT SUSTAINED DMG TO LEADING EDGE FLAP WHEN JBD WAS RAISED INTO IT.	Spotting
46536	1997	C GROUND	F018C	199,522	0	0	ACFT RADOME STRUCK BY WING BUTT OF TAXIING ACFT ON FLIGHT DECK.	Taxi

Continued on next page

Interest Mishaps.

Event Serial	Fiscal Year	Event Class	Type Model Series	Total Event Cost ($)	Fatalities	Major Injuries	Narrative	Category
46704	1997	GRND HZ: GEN-ERAL	S003B	0	0	0	TOW TRACTOR HIT AERIAL REFUELING STORE ON FLT DECK.	Towing
46852	1997	C GROUND	E002C+	61,073	0	0	ACFT 01 TAXIED INTO TURNING ACFT 02 PROP DAMAGING BOTH ACFT.	Taxi, engine
47263	1998	C GROUND	F018C	25,940	0	0	ACFT UNDER TOW STRUCK LSO PLATFORM DURING NIGHT FLIGHT DECK RESPOT.	Towing
47376	1998	C GROUND	EA006B	18,965	0	0	TOW TRACTOR COLLIDED WITH ACFT AND INJURED TROUBLESHOOTER	Towing
47618	1998	C GROUND	F018C	66,670	0	0	AIRCRAFT TOWED INTO PARKED AIRCRAFT.	Towing
47643	1998	GRND HZ: GEN-ERAL	E002C+	0	0	1	PLANE CAPTAIN STRUCK BY TURNING PROPELLER.	Engine
47673	1998	GRND HZ: GEN-ERAL	F018C	0	0	0	ACFT RADOME IMPACTED BY AILERON OF SECOND ACFT WHICH WAS TAXIING ON DK	Taxi
47772	1998	GRND HZ: GEN-ERAL	EA006B	0	0	0	CAT CREW RETRACTED SHUTTLE INTO ACFT PORT MAIN TIRE;INADEQ COORDINATIO	Spotting
47870	1998	C GROUND	F018C	45,676	0	0	STARBOARD HORIZONTAL STABILIZER DMGD WHEN STRUCK BY FORKLIFT.	Misc
47904	1998	GRND HZ: GEN-ERAL	F018C	0	0	0	RIGHT HORIZONTAL STAB STRUCK ANOTHER ACFTS LEF DUR FLT CNTRL CAS CKS.	Spotting
48805	1999	C FLIGHT	S003B	22,406	0	0	FLIGHT DECK PERSONNEL DROVE TOW TRACTOR INTO BUDDY STORE OF AIRCRAFT.	Towing
48838	1999	C GROUND	E002C	33,739	0	0	WING TIP OF TAXIING ACFT STRUCK PROP OF PARKED ACFT ON FLIGHT DECK.	Taxi, engine
49159	1999	C GROUND	C002A	23,256	0	0	TAILSKID HIT SCUPPER, BREAKING ACTUATOR FITTING.	Unknown
49612	1999	C GROUND	F018C	16,241	0	0	DUR LOW PWR TURN, INADVERTENT WINGSWEEP CAUSED STBD WING TO HIT AILERO	Wingfold
49753	1999	GRND HZ: GEN-ERAL	C002A	0	0	0	STBD WING TIP HIT TOP OF COMBAT HATCH DURING WINGSPREAD EVOLUTION.	Wingfold
49776	1999	C GROUND	HH060H	22,900	0	0	TAIL ROTOR BLADE OF PARKED AIRCRAFT DAMAGED BY CRASH CRANE.	Misc
49853	1999	GRND HZ: GEN-ERAL	F018C	0	0	0	MISPOSITIONED WINGFOLD HANDLE RESULTED IN INADVERT WINGSPREAD ON START	Wingfold
49899	1999	C GROUND	F014D	177,287	0	0	AIRCRAFT STRUCK BY JET BLAST DEFLECTOR WHILE TAXIING TO CATAPULT.	Taxi

Event Serial	Fiscal Year	Event Class	Type Model Series	Total Event Cost ($)	Fatalities	Major Injuries	Narrative	Category
50089	1999	B FLIGHT	F018C	318,479	0	0	LAUNCHED W/CAT TRACK BUTTON IN PLACE. ENG FODDED. NIGHT BARRICADE.	Misc
50092	1999	C GROUND	MH053E	140,400	0	0	DUR ONBOARD CARGO DELIVERY FORKLIFT LIFTED CAGE & STRUCK ACFT CARGO DR	Misc
50097	1999	A GROUND	F018C	1,202,804	0	0	EXHAUST FM ACFT ON CAT 4 BLEW A TURNING ACFT INTO A PARKED ACFT.	Exhaust
50477	1999	C GROUND	F018C	21,299	0	0	ACFT TAXIING OUT OF LDG AREA STRUCK JET STARTING UNIT.	Taxi
50538	1999	C GROUND	F018C	64,150	0	0	NOSE RADOME DAMAGED WHEN ACFT TAXIED INTO FLIGHT DECK FIRE TRUCK	Taxi
50609	1999	GRND HZ: GENERAL	E002C	0	0	0	MISSILE CARARD ATTACHED TO HORNET HIT PORT PROP WHILE HORNET WAS TOWED	Towing
50631	1999	C GROUND	F018C	64,150	0	0	AIRCRAFT RADOME WAS STRUCK BY P-25 MOBILE FIRE FIGHTING VEHICLE.	Misc
50548	2000	FLT HZ: GENERAL	F018C	0	0	0	UNCOMMANDED WING SPREAD CAUSED WINGS TO STRIKE ACFT IN CLOSE PROXIMITY	Wingfold
50566	2000	C GROUND	C002A	57,116	0	0	DURING CV QUALS, #1 JBD HIT ACFT STBD VERTICAL STABILIZER. NO INJURIES	Spotting
50865	2000	C GROUND	F018C	44,150	0	0	ACFT PORT HORIZ STAB STRUCK LSO WINDSCREEN DURING FLIGHT DECK RESPOT.	Towing
50919	2000	C GROUND	T045C	1,875	0	1	ACFT SAFETY OBSERVER BROKE LEFT ARM WHILE SPOTTING ACFT ON CAT 2 OF CV	Unknown
51020	2000	GRND HZ: GENERAL	UNK	0	0	0	INADVERTENT WING SPREAD CAUSED AIM-9 CONT FIN TO STRIKE ADJACENT ACFT	Wingfold
51046	2000	C GROUND	F014A	40,031	0	0	TWO AIRCRAFT SUSTAINED DAMAGE DURING FLIGHT DECK RESPOT EVOLUTION	Towing
51063	2000	C GROUND	F018C	41,265	0	0	UNINTENTIONAL WING SPREAD/WINGTIP LAU7 STRUCK/DAMAGED ADJACENT AC CPY	Wingfold
51070	2000	C GROUND	F014B	18,105	0	0	AIRCRAFT TAXIING ON FLIGHT DECK COLLIDED WITH PARKED, UNMANNED ACFT.	Taxi
51127	2000	C GROUND	F018C	55,960	0	0	ACFT LEFT LEADING EDGE FLAP STRUCK BELKNAP POLE WHILE TAXIING ON DECK.	Taxi
51154	2000	C GROUND	F014B	16,704	0	0	TOWED AIRCRAFT STRUCK PARKED AIRCRAFT DURING CARRIER FLT DECK RE-SPOT.	Towing
51243	2000	A GROUND	E002C	156,338	1	0	FLIGHT DECK CREWMAN FATALLY INJURED WHEN STRUCK BY ACFT'S TURNING PROP	Engine

143

Event Serial	Fiscal Year	Event Class	Type Model Series	Total Event Cost ($)	Fatalities	Major Injuries	Narrative	Category
51352	2000	C GROUND	F018C	46,004	0	0	PORT LE FLAP HIT STBD HORIZ STAB OF PARKED ACFT DUR TAXI ON FLT DECK.	Taxi
51369	2000	FLT HZ: GENERAL	E002C	0	0	0	TECHNICIAN CROSSED FOUL LINE WITH APPROACHING AIRCRAFT OVER THE RAMP.	Misc
51477	2000	C GROUND	F018C	56,858	0	0	AIRCRAFT SLID WHILE TAXIING AND COLLIDED WITH PARKED AIRCRAFT.	Taxi
51539	2000	B GROUND	SH060F	310,607	0	0	UNMANNED ACFT ROLLED ACROSS FLIGHT DECK COLLIDING WITH PARKED ACFT.	Spotting
51572	2000	C GROUND	E002C	18,318	0	0	PORT STAB OF TOWED ACFT HIT NOSE CAP OF PARKED ACFT ON FLIGHT DECK.	Towing
51673	2000	C GROUND	F018C	38,232	0	0	PORT HORIZONTAL STABILIZER DAMAGED WHEN HIT BY FORKLIFT.	Misc
51676	2000	C GROUND	F018C	34,015	0	0	ACFT 02 CANOPY DAMAGED WHEN ACFT 01'S WINGS WERE SPREAD DURING MAINT.	Wingfold
51691	2000	C GROUND	F018C	73,171	0	0	TAXIING ACFT'S WINGTIM CATM-9 STRUCK & DAMAGED PARKED ACFT'S RADOME.	Taxi
51741	2000	GRND HZ: GENERAL	EA006B	0	0	0	HOT EXHAUST FROM TURNING ACFT CAUSED DAMAGE TO ACFT TAXIING FROM LDG.	Exhaust
51762	2000	C GROUND	F014	0	0	1	CV FLT DECK CAT OFFICER KNOCKED DOWN BY JET BLAST;SUSTAINED BKN FIBULA	Exhaust
51888	2000	GRND HZ: GENERAL	F018B	0	0	0	JBD CONTROL BOX TOGGLE SWITCH INADVERTANTLY ACTUATED.	Spotting
52346	2000	FLT HZ: GENERAL	E002C	0	0	0	DURING THREE EVENTS FLGHT DECK PERSONNEL APPROACHED TURNING PROPS.	Warning
52348	2000	FLT HZ: GENERAL	E002C+	0	0	0	EMBARKED CHOCKING PROCEDURES HAZARDOUS TO CHOCK WALKERS DUR TOW OPS.	Warning
53111	2000	GRND HZ: GENERAL	C002A	0	0	0	TOWED ACFT TAILSKID DAMAGED WHEN ACFT SLID INTO ELEVATOR COMBING.	Towing
51729	2001	C GROUND	S003B	97,030	0	0	RIGHT HORIZ STAB OF TOWED ACFT COLLIDED W/LEFT AILERON OF PARKED ACFT.	Towing
51778	2001	C GROUND	F018C	151,710	0	0	NAVY ACFT TAXIED INTO PARKED NAVY ACFT ON FLT DECK.	Taxi
51788	2001	C GROUND	S003B	22,694	0	0	TAXIING ACFT SLID AND COLIDED WITH A PARKED ACFT.	Taxi
51789	2001	C GROUND	F018C	81,036	0	0	ACFT SUSTAINED STAB DAMAGE WHEN STRUCK BY ACFT UNDER TOW. 1 INJURY	Towing

Interest Mishaps.

Event Serial	Fiscal Year	Event Class	Type Model Series	Total Event Cost ($)	Fatalities	Major Injuries	Narrative	Category
51848	2001	C GROUND	F018C	23,772	0	0	ACFT'S WING STRUCK PARKED AIRCRAFT DURING WING SPREAD EVOLUTION.	Wingfold
51854	2001	GRND HZ: GENERAL	S003B	0	0	0	ACFT W/PARKING BRAKE ENGAGED SLID INTO JBD WHILE OTHER ACFT IN TENSION	Spotting
51862	2001	C GROUND	F018C	76,563	0	0	ACFT #1 TAXIED INTO PARKED ACFT #2 ON FLIGHT DECK.	Taxi
51874	2001	C GROUND	F018C	22,363	0	0	TAXIING ACFT HORIZ STAB STRUCK OUTBD LEF OF PARKED ACFT ON FLT DECK.	Taxi
51892	2001	C GROUND	F014B	39,204	0	0	ACFT 01 STBD WINGTIP STRUCK ACFT 02 RADOME DUR WINDMILL FOR AN OP CHK.	Wingfold
51914	2001	C GROUND	F018C	16,659	0	0	ACFT TAXIED INTO PARKED ACFT FOLLOWING NIGHT CV LANDING	Taxi
51920	2001	C GROUND	F014B	20,000	0	0	STBD HORIZ STAB OF TAXING ACFT STRUCK PORT OTBD LE FLAP OF PARKED ACFT	Taxi
51949	2001	C GROUND	F014D	72,746	0	0	ACFT BEING TOWED ONTO ELEVATOR IN HNGR BAY STRUCK PARKED ACFT.	Towing
51975	2001	C GROUND	F018C	32,570	0	0	AIRCRAFT RADOME WAS STRUCK BY JET BLAST DEFLECTOR.	Spotting
52028	2001	GRND HZ: GENERAL	S003B	0	0	0	ACFT BEHIND RAISED JBD SLID WHEN ACFT ON CAT 3 WENT INTO TENSION.	Spotting
52047	2001	C GROUND	F018A	48,000	0	0	LEFT LEF ACFT 01 TAXIING W/WING FOLDED STRUCK HORIZ STAB OF PARKED A/C	Taxi
52048	2001	C GROUND	F014A	100,921	0	0	AIRCRAFT STRUCK DECK EDGE ELEVATOR CABLES DURING HANGAR DECK RESPOT.	Towing
52070	2001	C GROUND	S003B	64,594	0	0	CATAPULT 3 JBD WAS RAISED INTO ACFT RIGHT WING TIP.	Spotting
52085	2001	C GROUND	F014D	52,072	0	0	DUR CV NIGHT RESPOT, ACFT UNDER TOW COLLIDED WITH PARKED ACFT ON DECK.	Towing
53357	2001	GRND HZ: GENERAL	F018	0	0	1	FLIGHT SURGEON BLOWN OVERBOARD DURING CQ OPERATIONS.	Exhaust
65655	2001	GRND HZ: GENERAL	A006B	0	0	0	WHILE DRIVING ACFT AFT THROUGH HANGAR BAY, TRACTOR STRUCK PARKED ACFT.	Towing
65756	2001	GRND HZ: GENERAL	E002C	0	0	0	DAMAGE TO ACFT DURING SHIPBOARD ACFT TOWING EVOLUTION.	Towing
52207	2002	A GROUND	F014A	2,358,190	0	0	ACFT UNDER TOW STRUCK 2 UNMANNED, CHAINED ACFT DURING DECK ROLL AT NGT	Towing

Event Serial	Fiscal Year	Event Class	Type Model Series	Total Event Cost ($)	Fatalities	Major Injuries	Narrative	Category
52228	2002	C GROUND	S003B	20,000	0	0	HANGAR BAY AMMUNITION ELEVATOR HATCH OPENED AND STRUCK ACFT RADOME.	Spotting
52251	2002	C GROUND	F018C	27,510	0	0	DURING ACFT TIEDOWN, OUTBD WING PYLON HIT ADJACENT ACFT HORIZ STAB.	Towing
52361	2002	C GROUND	F018E	125,318	0	0	ACFT1 STBD AILERON STRUCK ACFT2 STBD HORIZ STAB DUR FLT DECK ACFT MOVE	Towing
52710	2002	C GROUND	S003B	23,865	0	1	FLIGHT DECK TROUBLESHOOTER BLOWN DOWN ON FLIGHT DECK BY ACFT EXHAUST.	Exhaust
52868	2002	C GROUND	F014B	55,950	0	0	TOW TRACTOR IMPACTED STBD DROP TANK DURING RESPOT EVOLUTION.	Towing
52953	2002	C GROUND	F014B	20,000	0	0	ACFT UNDER TOW DURING FLIGHT DECK RESPOT STRUCK BY NR 3 JBD.	Towing
52956	2002	C GROUND	F018E	28,860	0	0	PORT HORIZ STAB DAMAGED BY ENGINE EXHAUST OF LIKE ACFT DUR ENG START.	Exhaust
53356	2003	C GROUND	F018C	22,940	0	0	AIRCRAFT SLID INTO ANOTHER AIRCRAFT DURING CHOCKING & CHAINING.	Spotting
53395	2003	C GROUND	SH060F	37,419	0	0	WHILE MOVING ACFT CRANE FOR FLT DECK DRILLS, SLING HIT MRB AND TRB'S.	Misc
53403	2003	C GROUND	F018E	179,580	0	0	AIRCRAFT #1 TAXIED INTO PARKED AIRCRAFT #2.	Taxi
53447	2003	C GROUND	F018E	90,268	0	0	STBD HORIZ STAB DAMAGED BY LANTERN POD ON SKID BEING MOVED ON FLT DECK	Misc
53482	2003	C GROUND	F018C	47,010	0	0	TOWED AIRCRAFT #1 BACKED INTO RADOME OF AIRCRAFT #2.	Towing
53692	2003	C GROUND	F018C	134,760	0	0	WINDSHIELD DAMAGED AFTER EXPOSURE TO ACFT ENG EXHAUST DUR LAUNCH CYCLE	Exhaust
53695	2003	B GROUND	E002C+	505,760	0	0	ACFT SLID INTO PARKED ACFT DAMAGING BOTH ACFT & DEBRIS HIT 3RD ACFT.	Spotting
64733	2003	C GROUND	EA006B	22,856	0	0	TOW TRACTOR IMPACTED BAND RADOME ON ACFT STA WHILE TRYING TO TRANSIT.	Towing
64749	2003	C GROUND	F018C	79,215	0	0	ACFT #1 TAXIED INTO ACFT #2 ON FLIGHT DECK.	Taxi
64794	2003	B GROUND	C002A	286,298	0	0	2 ACFT PARKED ON SHIP'S ELEVATOR DAMAGED DUR ELEVATOR DOWNWARD TRAVEL.	Spotting
64851	2003	C FLIGHT	F018A	22,021	0	0	AIRCRAFT #1 DAMAGED ON FLIGHT DECK WHEN IT WAS TOWED INTO AIRCRAFT #2.	Towing
64852	2003	C GROUND	F018C	64,610	0	0	ACFT #1 TAXIED INTO ACFT #2 ON FLIGHT DECK UNDER YELLOW SHIRT CONTROL.	Taxi

Event Serial	Fiscal Year	Event Class	Type Model Series	Total Event Cost ($)	Fatalities	Major Injuries	Narrative	Category
64855	2003	C FLIGHT	EA006B	22,856	0	0	TOW TRACTOR COLLIDED WITH AND CRUNCHED ACFT'S ALQ-99 POD RADOME.	Towing
64898	2003	A FLIGHT	S003B	25,877,600	0	0	ACFT ROLLED OFF PORT SIDE OF SHIP AFTER SUCCESSFUL ARRESTED LANDING.	Unknown
64939	2003	C GROUND	F018F	35,696	0	0	WHILE BEING TAXIED, ACFT STRUCK A PARKED DISSIMILAR ACFT ON FLT DECK.	Taxi
65047	2003	C GROUND	F018C	57,952	0	0	ACFT ROLLED ON FLIGHT DECK AND STRUCK A PARKED DISSIMILAR TYPE ACFT.	Spotting
65193	2003	C GROUND	F018A	0	0	0	AIRCRAFT ON DECK PUSHED BACKWARDS INTO OTHER AIRCRAFT.	Towing
65614	2003	C GROUND	S003B	21,755	0	0	TAXIING ACFT SLID INTO UNMANNED PARKED ACFT ON WET FLIGHT DECK.	Taxi
65620	2003	C GROUND	F014A	39,667	0	0	ACFT PORT WING STRUCK FLIGHT DECK WHILE BEING LOWERED ON ELEVATOR.	Spotting
65717	2004	C GROUND	F014A	113,682	0	0	TOWED ACFT STBD WINGTIP STRUCK AILERON & FLAP OF CHOCKED & CHAIN ACFT.	Towing
65866	2004	C GROUND	S003B	56,259	0	0	DUR TAXI EVOLUTION, ACFT TURNED BEHIND RAISED JET BLAST DEFLECTOR.	Taxi
66061	2004	C GROUND	F014B	73,350	0	0	AIRCRAFT #1 TAXIED INTO ACFT #2 DISSIMILAR ACFT PARKED ON FLIGHT DECK.	Taxi
66328	2004	C GROUND	F018F	263,551	0	0	WHILE BEING TAXIED, AIRCRAFT STRUCK PARKED AIRCRAFT EMBARKED ON SHIP.	Taxi
66409	2004	C GROUND	F018C	50,222	0	0	LEF OF ACFT BEING TOWED ON DECK STRUK CHOCKED/CHAINED ACFT P HORIZ STB	Towing
66568	2004	C GROUND	F018C	49,537	0	0	CHOCKED AND CHAINED AIRCRAFT STRUCK BY MOVING FORKLIFT.	Misc
66975	2004	C GROUND	F018E	138,056	0	0	ACFT PORT WING STRUCK FLT DECK WHILE BEING LOWERED ON ELEVATOR #2.	Spotting
67061	2004	C GROUND	F018C	1,875	0	0	MAINTAINER BLOWN INTO TOW TRACTOR BY ACFT TAXIING TO CATAPULT ONE.	Exhaust
67103	2004	C GROUND	F014B	27,673	0	0	TAXIING ACFT WINGTIP STRUCK RADOME OF PARKED ACFT ON CVN FLIGHT DECK.	Taxi
67149	2004	C GROUND	F014B	48,156	0	0	ACFT WAS TOWED INTO SPN-46 CALIBRATION ANTENNA DURING FLT DECK RESPOT.	Towing
67178	2004	C FLIGHT	S003B	96,012	0	0	TAXIING ACFT STRUCK PARKED ACFT ON FLT DECK DUR START-UP PHASE.	Taxi

Event Serial	Fiscal Year	Event Class	Type Model Series	Total Event Cost ($)	Fatalities	Major Injuries	Narrative	Category
67255	2004	C GROUND	F014B	27,673	0	0	ACFT RADOME DMG WHEN A PALLET JACK CARRYING ISOPODS PULLED INTO RADOME	Misc
67423	2004	C GROUND	F014B	47,673	0	0	TOWED AIRCRAFT WING STRUCK RADOME OF PARKED ACFT ON SHIP FLIGHT DECK.	Towing
67595	2004	C GROUND	E002C+	25,944	0	0	PARKED HELO TAIL RTR STRUCK BY TAXIING FIXED WING ACFT W/WING FOLDED.	Taxi
67604	2004	C GROUND	F018F	63,632	0	0	ACFT BACKED INTO VERTICAL LIGHT FIXTURE DURING ACFT FLT DECK MOVE.	Towing
67605	2004	C GROUND	T045C	351,008	0	0	JET BLAST DEFLECTOR STRUCK ACFT WHILE BEING DIRECTED FOR CVN LAUNCH.	Taxi
68030	2004	C GROUND	F018F	43,695	0	0	ACFT #1 WING PANEL IMPACTED ACFT #2 STABILIZER DURING TAXI ONBOARD CVN	Taxi
68057	2004	C GROUND	EA006B	23,464	0	0	ALQ-99 TACT JAMMING POD STRUCK BY TOW TRACTOR ON CVN FLIGHT DECK.	Towing
68091	2004	C GROUND	F018E	83,031	0	0	DUR TOW, ACFT'S PORT WING STRUCK STBD HORIZ STABILATOR OF PARKED ACFT.	Towing
68160	2004	C GROUND	E002C+	182,189	0	0	AFT'S RUDDER TRIM TAB STRUCK STATIC P PROP OF PARKED ACFT ON FLT DECK	Unknown
68161	2004	C GROUND	F018E	0	0	0	DURING FLT DECK VERTREP, FORCKLIFT STRUCK PORT HORIZ STAB OF PARKED AC	Misc
68369	2005	C FLTREL	F018F	2,796	0	0	AS ACFT CAT LAUNCHED, IT'S CATM-9 FINS STRUCK CATAPULT CREWMAN'S HEAD.	Contact
68370	2005	B GROUND	F018C	115,000	0	1	SQN ACFT UNDER TOW DIRECTION OF YELLOW SHIRT RAN OVR SHIP'S BLUE SHIRT	Contact
68480	2005	C FLIGHT	MH053E	176,372	0	0	LDG ACFT'S DWNWASH BLEW PARKED ACFT'S RTR BLADES INTO FLT DECK.	Exhaust
68506	2005	C GROUND	F018E	51,760	0	0	ACFT AND TOW TRACTOR DAMAGED DUR ACFT MOVE ON FLIGHT DECK. NO INJURIES	Towing
68707	2005	C FLTREL	EA006B	25,630	0	0	ACFT'S TJS POD RADOME DAMAGED IN CVN HANGAR BAY.	Unknown
69023	2005	C GROUND	F018F	169,752	0	0	ACFT UNDER FLT DECK TAXI DIR CTRL STRUCK A LIKE ACFT ON ELEVATOR FOUR.	Taxi
69123	2005	C GROUND	HH060H	35,208	0	0	TOW TRACTOR STRUCK HELO TAIL PYLON PARKED CHOCKED/CHAINED IN HELO HOLE	Towing
69133	2005	C GROUND	F018C	35,699	0	0	AIRCRAFT UNDER TOW PUSHED BACK IN TO NAVPOLE.	Towing

Event Serial	Fiscal Year	Event Class	Type Model Series	Total Event Cost ($)	Fatalities	Major Injuries	Narrative	Category
69140	2005	C GROUND	F018F	65,394	0	0	ACFT #1 STAB STRUCK PARKED ACFT #2 STBD AILERON DUR TAXI FOR CV LAUNCH	Taxi
69153	2005	C GROUND	F018F	63,500	0	0	STBD HORIZ STAB DAMAGED FM CONTACT WITH HYD GEN DUR TOW TRACTOR MOVE.	Towing
69200	2006	C GROUND	F018E	25,000	0	0	ACFT'S WING SPREAD INTO OTHER ACFT DAMAGING RIGHT AILERON.	Wingfold
69202	2006	A GROUND	T045C	1,050,699	0	0	AIRCRAFT ENGINE FOD BY INGESTION OF FLIGHT DECK CREWMAN'S CRANIAL.	Engine
69213	2006	B GROUND	F018C	115,000	0	1	ACFT RAN OVER AIRMAN'S RIGHT LEG DURING TAXI ON FLIGHT DECK.	Contact
69270	2006	C GROUND	F018F	38,767	0	0	EXT FUEL TANK DAMAGED FROM COLLISION WITH TOW TRACTOR DURING ACFT TOW.	Towing
69279	2006	C GROUND	F018E	46,400	0	0	ACFT TAXIED LEFT STABILATOR INTO STATIONARY ACFT'S LEADING EDGE FLAP.	Taxi
69291	2006	C GROUND	EA006B	95,058	0	0	ACFT UNDER FLT DECK TAXI DIR CONTROL TAXIED INTO PARKED ACFT ON DECK.	Taxi
69310	2006	B GROUND	F018F	368,328	0	0	RT WING OF ACFT #1 STRUCK THE L WING OF A PARKED ACFT #2 DURING TAXI.	Taxi
69332	2006	C GROUND	F018E	175,042	0	0	ACFT PARKED ON CV DECK DAMAGED BY ANOTHER SQN'S LIKE ACFT JET EXHAUST.	Exhaust
69348	2006	C GROUND	F018C	76,418	0	0	AIRCRAFT CANOPY DAMAGED BY ANOTHER AIRCRAFT'S EXHAUST.	Exhaust
69377	2006	C GROUND	F018F	35,883	0	0	ACFT PARKED ON FLT DECK STRUCK BY FORK LIFT TRACTOR DUR REPLENISHMENT.	Supply
69378	2006	C GROUND	F018E	47,498	0	0	ACFT#1 TAXIED INTO ACFT#2 WHILE ACFT #2 WAS STOPPED ON THE FLT DECK.	Taxi
69382	2006	C GROUND	F018F	49,887	0	0	PARKED ACFT'S STBD HORIZ STAB DAMADED BY TAXIING ACFT ON FLIGHT DECK.	Taxi
69385	2006	C GROUND	F018F	122,406	0	0	TWO LIKE ACFT STRUCK EACH OTHER'S HORIZ STABILIZER DUR FLT DECK TOWING	Towing
69415	2006	A GROUND	S003	1,544,320	0	0	PORT STAB OF ACFT TAXIING STRUCK STBD TURNING PROP OF PARKED ACFT.	Taxi, engine
69481	2007	C GROUND	F018C	46,437	0	0	ACFT # 1 RIGHT STABILATOR WAS STRUCK BY ACFT #2 LEFT STABILATOR.	Unknown
69504	2007	C GROUND	F018E	61,203	0	0	GROUND SUPPORT EQUIPMENT STRUCK PORT HORIZONTAL STABILATOR.	Unknown

149

Interest Mishaps.

Event Serial	Fiscal Year	Event Class	Type Model Series	Total Event Cost ($)	Fatalities	Major Injuries	Narrative	Category
69517	2007	C GROUND	F018E	23,996	0	0	A/C UNDER TOW DUR NIGHT RESPOT STBD STABILATOR IMPACTED TOW TRACTOR.	Towing
69553	2007	C GROUND	F018F	90,983	0	0	PORT AILERON OF ACFT UNDER TOW STRUCK PORT HORZL STAB OF STA ACFT.	Towing
69566	2007	C GROUND	EA006B	20,000	0	0	ALQ-99 POD RADOME DAMAGED ON FLT DECK. ACFT RETURNED TO FLIGHT STATUS	Unknown
69590	2007	C GROUND	F018F	74,096	0	0	PORT HORZL STABILATOR DAMGED ON ELEVATOR 4 STANCHION WHILE BEING TOWED	Towing
69602	2007	C GROUND	F018F	23,936	0	0	ACFT SUSTAINED DAMAGE TO THE LEFT HRZL STAB AFTER BEING TOWED.	Towing
69604	2007	C GROUND	F018C	46,437	0	0	ACFT UNDER TOW ONBOARD SHIP STRUCK THE LDG SIGNAL OFCR PLATFORM.	Towing
69607	2007	C GROUND	F018F	151,220	0	0	JBD 3 WAS RAISED AND IMPACTED NG-111 WHILE UNDER TOW.	Towing

150

Appendix B. Source Code Listings

This appendix contains MATLAB® and C source code used throughout this research. It is provided as an example for future work.

B.1 MATLAB®

Listing B.1: Determining time to calculate two-norms for different dimensions.

```
1 %% LT Jeff Johnston
  %
  % 30 OCT 2008
  % Determining time to calculate two-norms for different dimensions

6 clear all; close all; clc;

  %% Generate times

  max_dimension = 500;
11 max_runs = 1000;
  times = zeros(max_dimension, max_runs);
  for run_ctr = 1:1:max_runs
      for ctr = 1:1:max_dimension
          x = 1:1:ctr;
16        tic;
          d = norm(x, 2);
          times(ctr, run_ctr) = toc;
      end
  end
21
  %% Get mean time of each operation

  mean_times = zeros(size(times,1),1);
  for ctr = 1:1:size(times,1)
26    mean_times(ctr) = mean(times(ctr,:))*1E6;
  end

  %% Find a best-fit polynomial

31 p = polyfit(x', mean_times, 3);
```

```matlab
%% Example Script File for DIDO Path Planning Demonstration
% LT Jeff Johnston
% AFIT ENY
% 13JAN09

clear all; close all; clc;

%% Define OBSTACLES Variable (Structure)
global OBSTACLES;

% Each element of OBSTACLES structure is a nx1 column vector where...
    n is the
% number of obstacles.
OBSTACLES.xo = [50]; % center location on x-axis
OBSTACLES.yo = [50]; % center location on y-axis
OBSTACLES.a  = [10]; % width
OBSTACLES.b  = [10]; % height
OBSTACLES.p  = [2];  % norm: 1-diamond, 2-circle, 100-square, etc...
    ...
OBSTACLES.c  = [1];

%% Define state and control parameter boundaries
xL   = 0;    xU   = 100;
yL   = 0;    yU   = 100;
psiL = -3*pi; psiU = 3*pi;

vL   = 0;   vU = 0.8;
phiL = -pi/2;    phiU = pi/2;

bounds.lower.states = [xL; yL; psiL];
bounds.upper.states = [xU; yU; psiU];

bounds.lower.controls = [vL; phiL];
bounds.upper.controls = [vU; phiU];

t0          = 0;
tfMax    = 500;

bounds.lower.time       = [t0; t0];
bounds.upper.time       = [t0; tfMax];

%% Define desired initial and final states
x0 = 0;
y0 = 0;
psi0 = -45*pi/180;

xf = 100;
yf = 100;
psif = -45*pi/180;

bounds.lower.events = [x0; y0; psi0; xf; yf; psif];
```

```matlab
   bounds.upper.events = [x0; y0; psi0; xf; yf; psif];

   bounds.lower.path = zeros(size(OBSTACLES.xo))+0;
   bounds.upper.path = zeros(size(OBSTACLES.xo))+1000;
54
   %% Assign necessary variables to structure
   Project.cost    = 'SampleCost';
   Project.dynamics = 'SampleDynamics';
   Project.events  = 'SampleEvents';
59 Project.path = 'SamplePath';

   Project.bounds = bounds;

   %% Set DIDO Options
64
   algorithm.mode = 'spectral';
   algorithm.nodes = [40];

   %% Call DIDO
69 tStart= cputime;
   [cost, primal, dual] = dido(Project, algorithm);
   runTime = cputime-tStart

   %% Create output variables from DIDO solution structures
74
   x = primal.states(1,:);
   y = primal.states(2,:);
   psi = primal.states(3,:);

79 t = primal.nodes;

   %% Plot the resultant path
   figure;
   hold;
84 plot(x, y, ':o');
   for ctr = 1:1:length(OBSTACLES.xo)
       ezplot(strcat('((x-',num2str(OBSTACLES.xo(ctr)),...
           ')/',num2str(OBSTACLES.a(ctr)),...
           ')^',num2str(OBSTACLES.p(ctr)),...
89         '+ ((y-', num2str(OBSTACLES.yo(ctr)),...
           ')/',num2str(OBSTACLES.b(ctr)),...
           ')^',num2str(OBSTACLES.p(ctr)),...
           '-', num2str(OBSTACLES.c(ctr))),...
           [xL, xU, yL, yU]);
94 end
   axis([xL, xU, yL, yU]);
   grid on;
   xlabel('x');
   ylabel('y');
99 title('');
```

```
1 function endpointFunction = ProjectEvents(primal)
  % Event function for DIDO Path Planning Demonstration
  % LT Jeff Johnston
  % AFIT ENY
  % 13JAN09
6
  x0 = primal.states(1,1);          xf = primal.states(1,end);
  y0 = primal.states(2,1);          yf = primal.states(2,end);
  psi0 = primal.states(3,1);        psif = primal.states(3,end);

11
  endpointFunction = zeros(6,1);
  endpointFunction(1) = x0;
  endpointFunction(2) = y0;
  endpointFunction(3) = psi0;
16 endpointFunction(4) = xf;
  endpointFunction(5) = yf;
  endpointFunction(6) = psif;
```

Listing B.4:   DIDO Sample: Path.

```matlab
function pathFunction = ProjectPath(primal)
% Path constraint function for DIDO Path Planning Demonstration
% LT Jeff Johnston
% AFIT ENY
% 13JAN09

global OBSTACLES;

x = primal.states(1,:);
y = primal.states(2,:);

% Allow a border around the obstacle
border = 0.5; % m

xo = OBSTACLES.xo;
yo = OBSTACLES.yo;
a  = OBSTACLES.a + border;
b  = OBSTACLES.b + border;
p  = OBSTACLES.p;

for ctr = 1:1:length(xo)
    pathFunction(ctr,:) = log(((x-xo(ctr))./(a(ctr))).^p(ctr) +...
        ((y-yo(ctr))./(b(ctr))).^p(ctr));
end
```

Listing B.5:   DIDO Sample: Dynamics.

```matlab
function XDOT = ProjectDynamics(primal)
% Dynamics function for DIDO Path Planning Demonstration
% LT Jeff Johnston
% AFIT ENY
% 13JAN09

% States
x = primal.states(1,:);
y = primal.states(2,:);
psi = primal.states(3,:);

% Controls
v = primal.controls(1,:);
phi = primal.controls(2,:);

% Tricycle wheelbase
L = 0.5; % m

% Kinematic Equations
xdot = -v.*sin(psi).*cos(phi);
ydot = v.*cos(psi).*cos(phi);
psidot = (v./L).*sin(phi);

XDOT = [xdot; ydot; psidot];
```

Listing B.6:   DIDO Sample: Cost.

```matlab
function [EndpointCost, RunningCost] = ProjectCost(primal)
% Cost function for DIDO Path Planning Demonstration
% LT Jeff Johnston
% AFIT ENY
% 13JAN09

tf = primal.nodes(end);

EndpointCost = tf;
RunningCost = 0;
```

Listing B.7: Determine vehicle position and orientation from measured antenna locations.

```matlab
function [ rc, heading ] = det_pos_heading( r1, r2 )
%DET_POS_HEADING Returns center position and heading from wingtip
%coordinates
%
% LT Jeff Johnston
% AFIT/ENY
% 21OCT2008
%
%Usage: [rc, heading] = det_pos_heading( r1, r2 )
%
%   r1: 1x2 vector containing coordinates of port receiver [x_1, ...
    y_1]
%   r2: 1x2 vector containing coordinates of stbd receiver [x_2, ...
    y_2]
%
%   rc: Returns 1x2 vector containing coordinates of center [x_c, ...
    y_c]
%   heading: Returns angle from north in degrees

r3 = r2 - r1;
L = norm(r3);

heading = atan2(r3(2), r3(1));
rc = r1+(L/2)*[cos(heading), sin(heading)];
heading = heading*180/pi;
```

Listing B.8: Calculate nearest neighbor distance.

```matlab
function [ dist ] = dist_from_object( loc, rc, heading, threshold,...
    wingspan, object )
%[ dist ] = DIST_FROM_OBJECT ( loc, rc, heading)
%Calculates the distance of a point from an object described by a ...
    patch
%
% LT Jeff Johnston
% AFIT/ENY
% 29OCT2008
%
%   loc: 1x2 vector containing coordinates of point [x, y]
%   rc: 1x2 vector containing coordinates of object center point [...
    x_c, y_c]
%   heading: object angle from heading north (in degrees)
%   threshold: minimum safe distance from center of object
%   wingspan: length of wingspan tip-to-tip
%   object: string containing file name of object outline

% First let's just try calculating the distance to the center ...
    point
dist = norm(rc-loc);

% If the distance to the center is less than the threshold given, ...
    use the
% nearest neighbor method
if dist < threshold
    % Load object outline and apply coordinate transformations
    load(object);
    heading_rad = -heading*pi/180;
    scaling = wingspan / ( 2 * max(outline(:,1)));
    object_outline = outline*[cos(heading_rad),...
        -sin(heading_rad); sin(heading_rad) cos(heading_rad)];
    shifting_points = zeros(size(object_outline));

    for ctr = 1:1:size(shifting_points,1)
        shifting_points(ctr,:) = rc;
    end
    object_outline = object_outline*scaling + shifting_points;

    % BRUTE FORCE NEAREST NEIGHBOR
    temp_dist = zeros(size(object_outline, 1),1);
    for ctr = 1:1:size(object_outline, 1)
        temp_dist(ctr) = norm(loc-object_outline(ctr,:));
    end
    dist = min(temp_dist);

end
```

```matlab
%% Problem file for the Aircraft Towing Problem
% LT Jeff Johnston, USN
% Lt. Col. Eric Swenson, USAF
% AFIT ENY
% 15JAN09
%
% Adapted from files provided by CDR Michael Hurni, USN, NPS

clear all; close all; clc;
path(path,'../scripts');

%% Define Global Variables

global LC LB LA OBSTACLES X;

% Global Scaling Factor
% Location states need scaling to be closer to order of magnitude ...
    of other
% states
X = 50;

% Articulated Vehicle Dimensions
% Dimensions in meters, scaled by X
LC = 3/X; % Tow Tractor Wheel Base Length
LB = 5/X; % Tow Bar Length
LA = 8/X; % Aircraft Wheel Base Length

% Measured Data Plotting Switch
% When plot_meas_data==1 the measured data recorded at NAS Oceana ...
    will be
% plotted with the planned path.
plot_meas_data = 1;

% Measured Data Guess Switch
% When guess_meas_data==1 the measured data recorded at NAS Oceana...
     will be
% used to provide an initial guess for the DIDO solution.
guess_meas_data = 1;

guess_start_end = 0;

% Measured Data Guess Plotting Switch
% When plot_guess_meas_data==1 the guess generated from the ...
    measured data
% recorded at NAS Oceana will be plotted to all for verification
plot_guess_meas_data = 1;

% Animate Optimal Solution
% When animate_soln==1 the resultant path will be animated
animate_soln = 0;
```

```matlab
48 % Rotate Axes
   T = [ cosd(48) -sind(48) ;sind(48) cosd(48)];

   % Obstacle Locations and Configurations
   OBSTACLES.xo = [ 81.0362;  140.2932; 103.8932; 116.8932; 90.8932; ...
       77.8932; 64.8932; 51.8932;  50;  20]/X;
53 OBSTACLES.yo = [109.2882;  100.8977;  64.4977;  77.4977; 51.4977; ...
       38.4977; 25.4977; 12.4977; 100; 100]/X;
   rotated_OBSTACLES = [OBSTACLES.xo OBSTACLES.yo]*T;
   OBSTACLES.xo = rotated_OBSTACLES(:,1);
   OBSTACLES.yo = rotated_OBSTACLES(:,2);
   OBSTACLES.a  = [       14;        14;        14;        14;       14; ...
             14;        10;        10;  15;  10]/X; % width
58 OBSTACLES.b  = [       22;        22;        22;        22;       22; ...
             22;        10;        10;  15;  10]/X; % height
   OBSTACLES.p  = [        4;         4;         4;         4;        4; ...
              4;         2;         2;   2;   2]);
   OBSTACLES.c  = [        1;         1;         1;         1;        1; ...
              1;         1;         1;   1;   1]);
   OBSTACLES.border = 0.5/X;
   OBSTACLES.d_des  = 20/X;
63 OBSTACLES.idx    = [1 2 3 4 5];

   % Obstacle On/Off Switch
   % When OBSTACLES.switch==1 the obstacles will be present in the ...
       path
   % planning scenario
68 OBSTACLES.switch = 1;

   %% Bound State and Control Variables
   %
   % The states for this problem are as follows (14):
73 % xc:         Tow Tractor Horizontal Location (c stands for cart)
   % yc:         Tow Tractor Vertical Location
   % beta_s
   % beta_c:     SIN and COS of Tow Tractor Heading Relative to ...
       Horizontal
   % xw:         Nose Wheel Horizontal Location (w stands for wheel)
78 % yw:         Nose Wheel Vertical Location
   % theta_s
   % theta_c:    SIN and COS of Tow Bar Heading Relative to ...
       Horizontal
   % zeta:       Tow Bar Turn Angle, beta-theta
   % xa:         Aircraft Horizontal Location (a stands for aircraft)
83 % ya:         Aircraft Vertical Location
   % psi_s
   % psi_c:      SIN and COS of Aircraft Heading Relative to ...
       Horizontal
   % phi:        Aircraft Turn Angle, theta-psi
   %
88 % The controls for this problem are as follow (2):
   % vc:         Tow Tractor Velocity
```

```matlab
    % alpha:       Tow Tractor Turn Angle
    %
    % All angles in radians
 93 % All distances in meters scaled by X
    % All velocities in meters/second scaled by X

    % Lower and Upper Bounds for Locations
    xmin = 50/X; xmax = 200/X; ymin = -200/X; ymax = 59/X;
 98 xcL = xmin; xcU = xmax; xwL = xmin; xwU = xmax; xaL = xmin; xaU = ...
       xmax;
    ycL = ymin; ycU = ymax; ywL = ymin; ywU = ymax; yaL = ymin; yaU = ...
       ymax;

    % Lower and Upper Bounds for Headings
    % -1 <= SIN(*), COS(*) <= 1, for all *
103 beta_sL  = -1; beta_sU  = 1;
    beta_cL  = -1; beta_cU  = 1;
    theta_sL = -1; theta_sU = 1;
    theta_cL = -1; theta_cU = 1;
    psi_sL   = -1; psi_sU   = 1;
108 psi_cL   = -1; psi_cU   = 1;

    % Lower and Upper Bounds for Turn Angles
    turn_angle_max = 4*pi/8;
    zetaL = -turn_angle_max; zetaU = turn_angle_max;
113 phiL  = -turn_angle_max; phiU  = turn_angle_max;

    % Lower and Upper Bounds for Inputs
    vcL    = 0/X;    vcU    = 0.5/X;
    alphaL = -pi/2; alphaU = pi/2;
118
    bounds.lower.states = [xcL; ycL; beta_sL; beta_cL; xwL; ywL; ...
       theta_sL; theta_cL; zetaL; xaL; yaL; psi_sL; psi_cL; phiL];
    bounds.upper.states = [xcU; ycU; beta_sU; beta_cU; xwU; ywU; ...
       theta_sU; theta_cU; zetaU; xaU; yaU; psi_sU; psi_cU; phiU];

    bounds.lower.controls = [vcL; alphaL];
123 bounds.upper.controls = [vcU; alphaU];

    %% Bound the Initial and Final Times

    t0          = 0;
128 tfMax    = 600;

    bounds.lower.time       = [t0; t0];
    bounds.upper.time       = [t0; tfMax];

133 %% Set the Initial and Final Conditions

    % Measured Start Location of Aircraft
    xa0    = 129.2289/X;
    ya0    = 89.8569/X;
```

```matlab
138 rotated_xy0 = [xa0 ya0]*T;
    xa0 = rotated_xy0(1);
    ya0 = rotated_xy0(2);
    psi0    = (-130.6658+90-48)*pi/180;
    % xa0 = 0;
143 % ya0 = 50/X;
    % psi0 = 0;
    psi_s0 = sin(psi0);
    psi_c0 = cos(psi0);

148
    % Calculated Start Location of Nose Wheel (and Tow Bar)
    xw0      = xa0+LA*cos(psi0);
    yw0      = ya0+LA*sin(psi0);
    theta0   = psi0;
153 theta_s0 = sin(theta0);
    theta_c0 = cos(theta0);
    phi0 = theta0-psi0;

    % Calculated Start Location of Tow Tractor
158 xc0      = xw0+LB*cos(theta0);
    yc0      = yw0+LB*sin(theta0);
    beta0    = psi0;
    beta_s0 = sin(beta0);
    beta_c0 = cos(beta0);
163 zeta0     = beta0-theta0;

    % Measured Final Location of Aircraft
    xaf    = 29.0362/X;
    yaf    = 57.2882/X;
168 rotated_xyf = [xaf yaf]*T;
    xaf = rotated_xyf(1);
    yaf = rotated_xyf(2);
    psif    = (49.2842+90-48)*pi/180;
    % xaf = 100/X;
173 % yaf = 150/X;
    % psif = 0;
    psi_sf = sin(psif);
    psi_cf = cos(psif);

178
    % Calculated Final Location of Nose Wheel (and Tow Bar)
    xwf      = xaf+LA*cos(psif);
    ywf      = yaf+LA*sin(psif);
    thetaf   = psif;
183 theta_sf = sin(thetaf);
    theta_cf = cos(thetaf);
    phif   = thetaf-psif;

    % Calculated Final Location of Tow Tractor
188 xcf      = xwf+LB*cos(thetaf);
    ycf      = ywf+LB*sin(thetaf);
```

```matlab
    betaf   = psif;
    beta_sf = sin(betaf);
    beta_cf = cos(betaf);
193 zetaf     = betaf-thetaf;

    % Upper and Lower Boundaries for Initial and Final States
    %
    % Force aircraft to attain its exact final state but allows cart ...
       and tow bar
198 % to be at an offset.  DIDO requires [2*n x 1] column vector where...
       n is the
    % number of states.
    %
    % Define maximum allowable offsets
    x_off  = 5/X;
203 y_off  = 5/X;
    a_off  = pi/8;
    sc_off = 0.4;
    %
    % Create bounds vector
208 bounds.lower.events = [xc0; yc0; beta_s0; beta_c0; xw0; yw0; ...
       theta_s0; theta_c0; zeta0; xa0; ya0; psi_s0; psi_c0; phi0; xcf-...
       x_off; ycf-x_off; beta_sf-sc_off; beta_cf-sc_off; xwf; ywf; ...
       theta_sf-sc_off; theta_cf-sc_off; zetaf-a_off; xaf; yaf; psi_sf...
       ; psi_cf; phif-a_off];
    bounds.upper.events = [xc0; yc0; beta_s0; beta_c0; xw0; yw0; ...
       theta_s0; theta_c0; zeta0; xa0; ya0; psi_s0; psi_c0; phi0; xcf+...
       y_off; ycf+y_off; beta_sf+sc_off; beta_cf+sc_off; xwf; ywf; ...
       theta_sf+sc_off; theta_cf+sc_off; zetaf+a_off; xaf; yaf; psi_sf...
       ; psi_cf; phif+a_off];

    % bounds.lower.events = [xc0; yc0; beta_s0; beta_c0; xw0; yw0; ...
       theta_s0; theta_c0; zeta0; xa0; ya0; psi_s0; psi_c0; phi0; xcf;...
        ycf; beta_sf; beta_cf; xwf; ywf; theta_sf; theta_cf; zetaf; ...
       xaf; yaf; psi_sf; psi_cf; phif];
    % bounds.upper.events = [xc0; yc0; beta_s0; beta_c0; xw0; yw0; ...
       theta_s0; theta_c0; zeta0; xa0; ya0; psi_s0; psi_c0; phi0; xcf;...
        ycf; beta_sf; beta_cf; xwf; ywf; theta_sf; theta_cf; zetaf; ...
       xaf; yaf; psi_sf; psi_cf; phif];
213
    bounds.lower.path = zeros(length(OBSTACLES.idx), 1)+0;
    bounds.upper.path = zeros(length(OBSTACLES.idx), 1)+100;

    %% Plot the Initial/Final Conditions
218 draw_switch = 1;

    if draw_switch == 1;
        figure;
        hold on;
223     draw_aircraft([xa0*X, ya0*X], (psi0-pi/2)*180/pi, 11.43, '...
            fa18c', 'g');
```

164

```matlab
        draw_aircraft([xc0*X, yc0*X], (beta0-pi/2)*180/pi, 4, 'cart', ...
            'w');
        plot([xw0*X xc0*X],[yw0*X yc0*X],'r');

        draw_aircraft([xaf*X, yaf*X], (psif-pi/2)*180/pi, 11.43, '...
            fa18c', 'g');
        draw_aircraft([xcf*X, ycf*X], (betaf-pi/2)*180/pi, 4, 'cart', ...
            'w');
        plot([xwf*X xcf*X],[ywf*X ycf*X],'r');

        meas_xy_rot = meas_xy*T;

        if plot_meas_data == 1
            plot(meas_xy_rot(1:3000,1), meas_xy_rot(1:3000,2), 'm-.');
        end

        if OBSTACLES.switch == 1
            for ctr = 1:1:length(OBSTACLES.idx)
                ezplot(strcat('((x-',num2str(OBSTACLES.xo(OBSTACLES....
                    idx(ctr))*X),...
                        ')/',num2str(OBSTACLES.a(OBSTACLES.idx(ctr))*X)...
                            ,...
                        ')^',num2str(OBSTACLES.p(OBSTACLES.idx(ctr))),...
                        '+ ((y-', num2str(OBSTACLES.yo(OBSTACLES.idx(ctr))...
                            *X),...
                        ')/',num2str(OBSTACLES.b(OBSTACLES.idx(ctr))*X)...
                            ,...
                        ')^',num2str(OBSTACLES.p(OBSTACLES.idx(ctr))),...
                        '-', num2str(OBSTACLES.c(OBSTACLES.idx(ctr)))),...
                        [-200,200,-200,200]);
            end
        end

        title('');
        xlabel('x');
        ylabel('y');
        axis([55 205 -95 55]);
        grid on;
    end

    %% Define DIDO Constraints

    Project.cost     = 'ProjectCost';
    Project.dynamics = 'ProjectDynamics';
    Project.events   = 'ProjectEvents';
    Project.path     = 'ProjectPath';

    Project.bounds = bounds;

    %% Provide a Trajectory Guess

if guess_meas_data==1
```

```matlab
     load meas_data.mat;
     meas_xy = meas_xy*T;
     meas_hdg = meas_hdg+90-48;

     % Indices of measured data to use for guess generation
     idx_use = [1; 1320; 1520; 1620; 1920; 2120; 2220; 3000];
     idx_start = 800;
     guess.controls = zeros(2,length(idx_use));
     guess.states   = zeros(14, length(idx_use));
     guess.time     = zeros(1,length(idx_use));
     for ctr = 1:1:length(idx_use)
         guess.controls(:,ctr) = [vcU; 0];
         guess.states(10,ctr)  = meas_xy(idx_use(ctr), 1)/X;
         guess.states(11,ctr)  = meas_xy(idx_use(ctr), 2)/X;
         guess.states(12,ctr)  = sin((meas_hdg(idx_use(ctr)))*pi...
             /180);
         guess.states(13,ctr)  = cos((meas_hdg(idx_use(ctr)))*pi...
             /180);
         guess.states(14,ctr)  = 0;
         guess.states(5, ctr)  = guess.states(10,ctr)+LA*guess....
             states(13,ctr);
         guess.states(6, ctr)  = guess.states(11,ctr)+LA*guess....
             states(12,ctr);
         guess.states(7, ctr)  = guess.states(12,ctr);
         guess.states(8, ctr)  = guess.states(13,ctr);
         guess.states(9, ctr)  = guess.states(14,ctr);
         guess.states(1, ctr)  = guess.states(5, ctr)+LB*guess....
             states(8, ctr);
         guess.states(2, ctr)  = guess.states(6, ctr)+LB*guess....
             states(7, ctr);
         guess.states(3, ctr)  = guess.states(7, ctr);
         guess.states(4, ctr)  = guess.states(8, ctr);
         guess.time(ctr)       = (ctr-1)*500/length(idx_use);
     end
     algorithm.guess = guess;

     if plot_guess_meas_data==1
         hold on;
         for ctr = 1:1:length(idx_use)
             draw_aircraft([guess.states(10,ctr)*X, guess.states...
                 (11,ctr)*X], (meas_hdg(idx_use(ctr))-90), 11.43, '...
                 fa18c', 'g');
             draw_aircraft([guess.states(1, ctr)*X, guess.states(2,...
                  ctr)*X], (meas_hdg(idx_use(ctr))-90), 4, 'cart', '...
                 w');
             plot([guess.states(5, ctr)*X guess.states(1, ctr)*X],[...
                 guess.states(6, ctr)*X guess.states(2, ctr)*X],'r')...
                 ;
             plot(meas_xy(1:3000,1), meas_xy(1:3000,2), 'm-.');
```

166

```matlab
                    text(guess.states(1, ctr)*X,guess.states(2, ctr)*X,...
                        strcat('t=',num2str(guess.time(ctr))),'FontSize'...
                        ,10,'FontName','Arial');
                    text(guess.states(1, ctr)*X,guess.states(2, ctr)*X-5,...
                        strcat('hdg=',num2str(meas_hdg(idx_use(ctr)))),'...
                        FontSize',10,'FontName','Arial');
                end
                title('Measured Data and Generated Guesses');
                xlabel('x');
                ylabel('y');
        end
    end

    if guess_start_end == 1
        guess.controls = [vcU vcU; 0 0];
        guess.states(:,1) = [xc0; yc0; beta_s0; beta_c0; xw0; yw0; ...
            theta_s0; theta_c0; zeta0; xa0; ya0; psi_s0; psi_c0; phi0];
        guess.states(:,2) = [xcf; ycf; beta_sf; beta_cf; xwf; ywf; ...
            theta_sf; theta_cf; zetaf; xaf; yaf; psi_sf; psi_cf; phif];
        guess.time = [0 tfMax];
        algorithm.guess = guess;
    end

    %% Set DIDO Run Options

    algorithm.mode = 'spectral';

    % Number of Nodes
    algorithm.nodes = 50;

    %% Execute DIDO

    tStart= cputime;      % start CPU clock
    [cost, primal, dual] = dido(Project, algorithm);
    runTime = cputime-tStart;
    disp(strcat('Run Time is: ', num2str(runTime)));

    %% Store Trajectory Results

    % Define the States for Readability
    xc      = primal.states(1,:)*X;
    yc      = primal.states(2,:)*X;
    beta_s  = primal.states(3,:);
    beta_c  = primal.states(4,:);
    xw      = primal.states(5,:)*X;
    yw      = primal.states(6,:)*X;
    theta_s = primal.states(7,:);
    theta_c = primal.states(8,:);
    zeta    = primal.states(9,:);
    xa      = primal.states(10,:)*X;
    ya      = primal.states(11,:)*X;
    psi_s   = primal.states(12,:);
```

```matlab
353 psi_c   = primal.states(13,:);
    phi     = primal.states(14,:);

    % Define the Controls for Readability
    vc = primal.controls(1,:)*X;
358 alpha = primal.controls(2,:);

    % Resolve Angles Stored as SIN and COS
    beta  = atan2(beta_s, beta_c);
    theta = atan2(theta_s, theta_c);
363 psi   = atan2(psi_s, psi_c);

    % Define the Time Vector
    t = primal.nodes;

368 save kinematics.mat;

    %% Plot Resultant Path

    figure;
373 hold on;

    draw_aircraft([xa0*X, ya0*X], (psi0-pi/2)*180/pi, 11.43, 'fa18c', ...
        'g');

    draw_aircraft([xaf*X, yaf*X], (psif-pi/2)*180/pi, 11.43, 'fa18c', ...
        'g');
378
    if OBSTACLES.switch == 1
        for ctr = 1:1:length(OBSTACLES.idx)
            ezplot(strcat('((x-',num2str(OBSTACLES.xo(OBSTACLES.idx(...
                ctr))*X),...
                ')/',num2str(OBSTACLES.a(OBSTACLES.idx(ctr))*X),...
383             ')^',num2str(OBSTACLES.p(OBSTACLES.idx(ctr))),...
                '+ ((y-', num2str(OBSTACLES.yo(OBSTACLES.idx(ctr))*X)...
                    ,...
                ')/',num2str(OBSTACLES.b(OBSTACLES.idx(ctr))*X),...
                ')^',num2str(OBSTACLES.p(OBSTACLES.idx(ctr))),...
                '-', num2str(OBSTACLES.c(OBSTACLES.idx(ctr)))),...
388             [-200,200,-200,200]);
            if OBSTACLES.idx(ctr) == 1
                draw_aircraft([OBSTACLES.xo(OBSTACLES.idx(ctr))*X, ...
                    OBSTACLES.yo(OBSTACLES.idx(ctr))*X], (psif-pi/2)...
                    *180/pi, 11.43, 'fa18c', 'w');
            else
                draw_aircraft([OBSTACLES.xo(OBSTACLES.idx(ctr))*X, ...
                    OBSTACLES.yo(OBSTACLES.idx(ctr))*X], (psi0-pi/2)...
                    *180/pi, 11.43, 'fa18c', 'w');
393         end
        end
    end
```

```matlab
    if plot_meas_data == 1
        plot(meas_xy_rot(1:3000,1), meas_xy_rot(1:3000,2), 'm-.');
    end

    axis([55 205 -95 55]);
    xlabel('x');
    ylabel('y');
    title('');
    grid on;
    print -depsc -r300 '~/Documents/workspace/AFIT Thesis/src/Chapter4...
        /img/mlplot_naso_path_planning_1.eps';

    for ctr = 1:1:length(xa)
        draw_aircraft([xa(ctr), ya(ctr)], (psi(ctr)-pi/2)*180/pi, ...
            11.43, 'fa18c', 'g');
        draw_aircraft([xc(ctr), yc(ctr)], (beta(ctr)-pi/2)*180/pi, 4, ...
            'cart', 'w');
        plot([xw(ctr) xc(ctr)],[yw(ctr) yc(ctr)],'r');
    end

    plot(xa, ya,'-o');
    plot(xw, yw,'b*');
    plot(xc, yc,'rx');
    print -depsc -r300 '~/Documents/workspace/AFIT Thesis/src/Chapter4...
        /img/mlplot_naso_path_planning_3.eps';

    xlabel('X-axis (m)');
    ylabel('Y-axis (m)');
    title('Vehicle Trajectory');

%% Plot the states vs. time

    %Plot the states and controls vs time
    figure;
    subplot(2,1,1); plot(t, xa, '-o', t, ya, '-x');
    title('Aircraft Postion');
    xlabel('time (s)');
    ylabel('x-y position');
    legend('x (m)', 'y (m)');
    grid;
    subplot(2,1,2); plot(t, psi*180/pi, '-ro');
    title('Aircraft Angle From Global Y-Axis');
    xlabel('time (s)');
    ylabel('states');
    legend('\psi (deg)');
    grid;
    %
    %Plot the hamiltonian vs time
    figure;
    plot(t, dual.Hamiltonian, '-o');
    title('Hamiltonian Evolution');
    xlabel('time (s)');
```

```matlab
    ylabel('Hamiltonian Value');
    grid;

448 %Plot the costates
    figure;
    plot(t, dual.dynamics(1,:), '-o',...
         t, dual.dynamics(2,:), '-x',...
         t, dual.dynamics(3,:), '-.',...
453      t, dual.dynamics(4,:), '-+',...
         t, dual.dynamics(5,:), '-x',...
         t, dual.dynamics(6,:), '-.',...
         t, dual.dynamics(7,:), '-+',...
         t, dual.dynamics(8,:), '-x',...
458      t, dual.dynamics(9,:), '-.',...
         t, dual.dynamics(10,:), '-+',...
         t, dual.dynamics(11,:), '-x',...
         t, dual.dynamics(12,:), '-.',...
         t, dual.dynamics(13,:), '-+',...
463      t, dual.dynamics(14,:), '-*');
    title('Costates');
    xlabel('time (s)');
    ylabel('costates');
    legend('\lambda_x', '\lambda_y', '\lambda_\theta', '\lambda_v_r', ...
        '\lambda_v_l');
468 grid;

    %Plot the state covectors
    figure;
    plot(t, dual.states(1,:), '-o',...
473      t, dual.states(2,:), '-x',...
         t, dual.states(3,:), '-.',...
         t, dual.states(4,:), '-+',...
         t, dual.states(5,:), '-x',...
         t, dual.states(6,:), '-.',...
478      t, dual.states(7,:), '-+',...
         t, dual.states(8,:), '-x',...
         t, dual.states(9,:), '-.',...
         t, dual.states(10,:), '-+',...
         t, dual.states(11,:), '-x',...
483      t, dual.states(12,:), '-.',...
         t, dual.states(13,:), '-+',...
         t, dual.states(14,:), '-*');
    title('State covectors');
    xlabel('time (s)');
488 ylabel('state covectors');
    legend('\mu_x', '\mu_y', '\mu_\theta', '\mu_v_r', '\mu_v_l');
    grid;

    %Plot the control covectors
493 figure;
    plot(t, dual.controls(1,:)./4, '-o', t, dual.controls(2,:)./4, '-x...
        ');
```

```matlab
    title('Control Covectors');
    xlabel('time (s)');
    ylabel('control covectors');
498 legend('\mu_a_r', '\mu_a_l');
    grid;

    %Plot the Path covectors
    figure;
503 plot(t, dual.path(1,:), '-o');
    title('Path Covectors');
    xlabel('time (s)');
    ylabel('path covectors');
    legend('\mu_h_1');
508
    %Plot the Controls vs time
    figure;
    subplot(2,1,1); plot(t, vc, '-o');
    %legend('v (m/s)');
513 title('Controls - Velocity of Cart');
    xlabel('time (s)');
    ylabel('v (m/s)');
    subplot(2,1,2); plot(t, alpha*180/pi, '-x');
    title('Controls - Steering angle \alpha');
518 xlabel('time (s)');
    ylabel('alpha (deg)');
    grid;

    %% Animate the Solution
523
    if animate_soln==1
        draw_DIDO_soln;
    end
```

Listing B.10:   DIDO Aircraft Towing Problem: Events.

```matlab
function endpointFunction = ProjectEvents(primal)
% Event file for the Aircraft Towing Problem
% LT Jeff Johnston, USN
% Lt. Col. Eric Swenson, USAF
% AFIT ENY
% 15JAN09
%
% Adapted from files provided by CDR Michael Hurni, USN, NPS

% Designate the Initial and Final States
xc0      = primal.states(1,1);   xcf      = primal.states(1,end);
yc0      = primal.states(2,1);   ycf      = primal.states(2,end);
beta_s0  = primal.states(3,1);   beta_sf  = primal.states(3,end);
beta_c0  = primal.states(4,1);   beta_cf  = primal.states(4,end);
xw0      = primal.states(5,1);   xwf      = primal.states(5,end);
yw0      = primal.states(6,1);   ywf      = primal.states(6,end);
theta_s0 = primal.states(7,1);   theta_sf = primal.states(7,end);
theta_c0 = primal.states(8,1);   theta_cf = primal.states(8,end);
zeta0    = primal.states(9,1);   zetaf    = primal.states(9,end);
xa0      = primal.states(10,1);  xaf      = primal.states(10,end);
ya0      = primal.states(11,1);  yaf      = primal.states(11,end);
psi_s0   = primal.states(12,1);  psi_sf   = primal.states(12,end);
psi_c0   = primal.states(13,1);  psi_cf   = primal.states(13,end);
phi0     = primal.states(14,1);  phif     = primal.states(14,end);

% Put the Initial and Final States in endpointFunction

% Pre-allocate endpointFunction
endpointFunction = zeros(28,1);

% Initial Conditions
endpointFunction(1)  = xc0;
endpointFunction(2)  = yc0;
endpointFunction(3)  = beta_s0;
endpointFunction(4)  = beta_c0;
endpointFunction(5)  = xw0;
endpointFunction(6)  = yw0;
endpointFunction(7)  = theta_s0;
endpointFunction(8)  = theta_c0;
endpointFunction(9)  = zeta0;
endpointFunction(10) = xa0;
endpointFunction(11) = ya0;
endpointFunction(12) = psi_s0;
endpointFunction(13) = psi_c0;
endpointFunction(14) = phi0;

% Final Conditions
endpointFunction(15) = xcf;
endpointFunction(16) = ycf;
endpointFunction(17) = beta_sf;
endpointFunction(18) = beta_cf;
```

```
   endpointFunction(19) = xwf;
   endpointFunction(20) = ywf;
54 endpointFunction(21) = theta_sf;
   endpointFunction(22) = theta_cf;
   endpointFunction(23) = zetaf;
   endpointFunction(24) = xaf;
   endpointFunction(25) = yaf;
59 endpointFunction(26) = psi_sf;
   endpointFunction(27) = psi_cf;
   endpointFunction(28) = phif;
```

```matlab
function pathFunction = ProjectPath(primal)
% Path file for the Aircraft Towing Problem
% LT Jeff Johnston, USN
% Lt. Col. Eric Swenson, USAF
% AFIT ENY
% 15JAN09
%
% Adapted from files provided by CDR Michael Hurni, USN, NPS

% Load Global Variables
global OBSTACLES;

if OBSTACLES.switch == 1;

    % Define State Variables For Use in Constraint
    xc = primal.states( 1,:);
    yc = primal.states( 2,:);
    xw = primal.states( 5,:);
    yw = primal.states( 6,:);
    xa = primal.states(10,:);
    ya = primal.states(11,:);

    % Define a Border Around Each Obstacle
    border = OBSTACLES.border;

    % Define Obstacle Parameters
    xo = OBSTACLES.xo;
    yo = OBSTACLES.yo;
    a  = OBSTACLES.a + border;
    b  = OBSTACLES.b + border;
    p  = OBSTACLES.p;
    c  = OBSTACLES.c;

    % Pre-allocate pathFunction
    pathFunction=zeros(length(OBSTACLES.idx),length(xa));

    for ctr = 1:length(OBSTACLES.idx)
        pathFunction(ctr,:) = log(((xa-xo(OBSTACLES.idx(ctr))))./(a...
            (OBSTACLES.idx(ctr)))).^p(OBSTACLES.idx(ctr)) +...
            ((ya-yo(OBSTACLES.idx(ctr)))./(b(OBSTACLES.idx(ctr))))...
                .^p(OBSTACLES.idx(ctr)));
    end
else
    pathFunction = 0;
end
```

```matlab
function xdot = ProjectDynamics(primal)
% Dynamics file for the Aircraft Towing Problem
% LT Jeff Johnston, USN
% Lt. Col. Eric Swenson, USAF
% AFIT ENY
% 15JAN09
%
% Adapted from files provided by CDR Michael Hurni, USN, NPS

% Load Global Variables
global LC LB LA;

% Define the States for Readability
%xc      = primal.states(1,:);
%yc      = primal.states(2,:);
beta_s  = primal.states(3,:);
beta_c  = primal.states(4,:);
%xw       = primal.states(5,:);
%yw       = primal.states(6,:);
theta_s = primal.states(7,:);
theta_c = primal.states(8,:);
zeta    = primal.states(9,:);
%xa       = primal.statse(10,:);
%ya       = primal.states(11,:);
psi_s   = primal.states(12,:);
psi_c   = primal.states(13,:);
phi     = primal.states(14,:);

% Define the Controls for Readability
vc    = primal.controls(1,:);
alpha = primal.controls(2,:);

% Resolve Angles Stored as SIN and COS
beta  = atan2(beta_s, beta_c);
theta = atan2(theta_s, theta_c);
psi   = atan2(psi_s, psi_c);

% Tow Tractor Kinematics
xc_dot = vc.*cos(beta);
yc_dot = vc.*sin(beta);
beta_dot = vc.*tan(alpha)./LC;
beta_s_dot = cos(beta).*beta_dot;
beta_c_dot = -sin(beta).*beta_dot;

% Nose Wheel (and Tow Bar) Kinematics
vw = vc.*cos(zeta);
xw_dot = vw.*cos(theta);
yw_dot = vw.*sin(theta);
theta_dot = vc.*sin(zeta)./LB;
theta_s_dot = cos(theta).*theta_dot;
theta_c_dot = -sin(theta).*theta_dot;
```

```matlab
52 zeta_dot = beta_dot - theta_dot;

   % Aircraft Kinematics
   va = vw.*cos(phi);
   xa_dot = va.*cos(psi);
57 ya_dot = va.*sin(psi);
   psi_dot = vw.*sin(phi)./LA;
   psi_s_dot = cos(psi).*psi_dot;
   psi_c_dot = -sin(psi).*psi_dot;
   phi_dot = theta_dot - psi_dot;
62
   %=======================================================
   xdot = [xc_dot; yc_dot; beta_s_dot; beta_c_dot; xw_dot; yw_dot; ...
       theta_s_dot; theta_c_dot; zeta_dot; xa_dot; ya_dot; psi_s_dot; ...
       psi_c_dot; phi_dot];
```

Listing B.13:   DIDO Aircraft Towing Problem: Cost.

```matlab
function [EndpointCost, RunningCost] = ProjectCost(primal)
% Cost file for the Aircraft Towing Problem
% LT Jeff Johnston, USN
% Lt. Col. Eric Swenson, USAF
% AFIT ENY
% 15JAN09
%
% Adapted from files provided by CDR Michael Hurni, USN, NPS

% Define Cost Parameters
%tf = primal.nodes(end);
alpha = primal.controls(2,:);

% Calculate Cost
%min_steer = 1./(4*(alpha-pi/4)).^2;
min_steer = abs(alpha);

%EndpointCost = tf;
EndpointCost = 0;
RunningCost = min_steer;
```

Listing B.14:   Source code of GPS logging software used for custom GPS recorders.

```c
//Modified 08OCT08 by LT Jeff Johnston
//Originally written by Don Smith, AFIT Ctr, ANT Center
//
//Modified to write filenames in sequential order of creation

#include <stdio.h>
#include <stdlib.h>
//#include <conio.h>
#include <time.h>

int main(int argc, char** argv)
{
        FILE* SerialDevice = NULL;
        FILE* LogFile = NULL;
        FILE* run_file;
        char Buffer[2000];
        char logfilename[256];
        char date[20];
        char command_exec[1024];
        short int run = 0;

        // Mark run file to continuously count # of times run
        //NEED to add "run_file.txt" file to same directory as ...
            main program
        //WILL SEGFAULT IF YOU DON'T!!!
        run_file = fopen("run_file.txt","r");
        fscanf(run_file,"%d",&run);
        run=run+1;
        fclose(run_file);
        run_file = fopen("run_file.txt","w");
        fprintf(run_file,"%d",run);
        fclose(run_file);

        /* Open the serial device on COM2 readonly*/
        SerialDevice = fopen("/dev/ttyS2", "r");
        if (!SerialDevice) {
                fprintf(stderr, "Unable to open /dev/ttyS2 for ...
                    reading\n");
                return -1;
        }

        /* Create and open the log file */
        //sprintf(logfilename,"/mnt/mmc/test21/data%d",date); //...
            Old command uses random number
        sprintf(logfilename,"/mnt/mmc/gps_data/data%d",run); //...
            Write file name with run number appended to end
        LogFile = fopen(logfilename, "w");  //Opens file for ...
            writing in ascii mode, use wb for binary
        if (!LogFile) {
```

```c
45                     fprintf(stderr, "Unable to create and open /mnt/...
                          mmc/gps_data/data%d for writing\n");
                   return -2;
           }

           /* In an infinite loop: read from serial device, write to ...
              log file */
50         while (1) {

                   //Use fread/fwrite if data is binary
                   //fread(Buffer, 1, 100, SerialDevice); //Read 100 ...
                      bin elements of size 1
                   //fwrite(Buffer, 1, 100, LogFile); //Write 100 bin...
                       elements of size 1
55
                   //Use fets/fputs if data is ASCII
                   if (fgets(Buffer, 2000, SerialDevice) == NULL) {
                           fprintf(stderr, "Error or end of file ...
                              detected\n");
                           return -3;
60                 }

                   if (fputs(Buffer, LogFile) == EOF) {
                           fprintf(stderr, "Error writing data to /...
                              mnt/mmc/gps_data/data\n");
                           return -4;
65                 }
           }
           /* Execution never reaches here but it makes the compiler ...
              happy */
           fclose(LogFile);
           return 0;
70 }
```

Appendix C. Data Disc

A disc containing the data collected in the tests described in Chapter III was created for distribution with this thesis document. The files and folders it contains are described here.

The folder *gps_data* contains a dated folder for each section of the test with results presented in Chapter IV. The folders *21OCT08*, *22OCT08*, and *23OCT08* contain data collected at AFIT, while *20NOV08* contains data collected at NAS Oceana. Each folder contains a subfolder *exports* which holds the carrier-phase differential solutions generated by NovAtel Waypoint GrafNav™. Each solution file is named with the measurement device used and contains a description of the contents. They are ASCII encoded with DOS end of line characters. Each dated folder also contains a compressed binary file with the raw measurement data from each device stored as *raw_data.tar.gz*. These gzipped tarballs can be extracted using the GNU *tar*[1] and *gzip*[2] utilities, available for virtually any operating system. The *20NOV08* folder also contains MATLAB® script files used to generate the results of the data collection.

The *path_planning* folder provides the DIDO Aircraft Towing Problem files used to compute the path presented in Figure 4.24 on page 117 as well as the script *draw_DIDO_soln.m* to create an animation of the resulting motion.

The final folder, *scripts*, contains MATLAB® functions and data objects used to generate both the results of data collection and the path planning plots.

---

[1]http://www.gnu.org/software/tar/
[2]http://www.gzip.org/

Bibliography

1. Arya, Sunil, David M. Mount, Nathan S. Netanyahu, Ruth Silverman, and Angela Y. Wu. "An Optimal Algorithm for Approximate Nearest Neighbor Searching in Fixed Dimensions". *J.ACM*, 45(6):891–923, 1998. URL `http://doi.acm.org/10.1145/293347.293348`.

2. Bolzern, P., R. M. DeSantis, and A. Locatelli. "An Input-Output Linearization Approach to the Control of an n-Body Articulated Vehicle". *Journal of Dynamic Systems, Measurement, and Control*, 123(3):309–316, 2001. URL `http://link.aip.org/link/?JDS/123/309/1;10.1115/1.1387010`.

3. Bolzern, P., R. M. DeSantis, A. Locatelli, and D. Masciocchi. "Path-tracking for Articulated Vehicles with Off-axle Hitching". *Control Systems Technology, IEEE Transactions on*, 6(4):515–523, 1998.

4. Cobb, H. Stewart. *GPS Pseudolites: Theory, Design, and Applications.* Ph.D. thesis, Stanford University, 1997. URL `http://waas.stanford.edu/~wwu/papers/gps/PDF/Thesis/StewartCobbThesis97.pdf`.

5. Commander, Naval Air Forces (CNAF). "The Naval Aviation Maintenance Program (NAMP)", 30 Jun 2008. COMNAVAIRFORINST 4790.2A.

6. Commander, Naval Air Systems Command. "CV Flight/Hangar Deck NATOPS Manual", 2005. NAVAIR 00-80T-120.

7. Department of Defense (DoD). "Unmanned Systems Roadmap 2007-2032", 2007.

8. Department of Defense (DoD). "Accident Investigation, Reporting, and Record Keeping", 2008. DODI 6055.07.

9. Department of the Navy (DON). "Naval Aviation Safety Program", 2007. OPNAVINST 3750.6R.

10. Dogan, A. "Probabilistic Approach in Path Planning for UAVs". *Intelligent Control. 2003 IEEE International Symposium on*, 608–613, 2003.

11. Fox, Richard and Michael L. Nelson. "A Generic Path Planning Strategy for Autonomous Vehicles". URL `http://citeseerx.ist.psu.edu/viewdoc/summary?doi=10.1.1.38.250`. Unpublished.

12. Friedman, J. H., F. Baskett, and L. J. Shustek. "An Algorithm for Finding Nearest Neighbors". *Computers, IEEE Transactions on*, C-24(10):1000–1006, Oct. 1975.

13. Giardina, Thomas J. *An Interactive Graphics Approach to the Flight Deck Handling Problem.* Master's thesis, Naval Postgraduate School, 1974.

14. Gong, Qi, Wei Kang, and I. M. Ross. "A Pseudospectral Method for the Optimal Control of Constrained Feedback Linearizable Systems". *Automatic Control, IEEE Transactions on*, 51(7):1115–1129, 2006.

15. GPS NAVSTAR JPO. *NAVSTAR GPS Space Segment / Navigation User Interfaces*. Technical report, 1999.

16. Grisso, Robert, Richard Oderwald, Mark Alley, and Conrad Heatwole. "Precision Farming Tools: Global Positioning System (GPS)". *Virginia Cooperative Extension*, 442(503), 2003. URL `http://www.ext.vt.edu/pubs/bse/442-503/442-503.pdf`.

17. gumstix. "gumstix.com - way small computing", 2008.

18. Ho, C. M., A. T. Mannucci, U. J. Lindqwister, and X. Q. Pi. "Global Ionospheric Perturbations Monitored by the Worldwide GPS Network", 1996. URL `http://trs-new.jpl.nasa.gov/dspace/handle/2014/25455`.

19. Hsu, David, Robert Kindel, Jean-Claude Latombe, and Stephen Rock. "Randomized Kinodynamic Motion Planning with Moving Obstacles". *The International Journal of Robotics Research*, 21(3):233–255, 2002.

20. Hurni, Michael A., Pooya Sekhavat, and I. Michael Ross. "Autonomous Trajectory Planning Using Real-Time Information Updates". *AIAA Guidance, Navigation and Control Conference and Exhibit*. Honolulu, HI, 18-21 August 2008. AIAA 2008-6305.

21. Hurni, Michael A., Pooya Sekhavat, and I. Michael Ross. "An Algorithm for Autonomous Optimal Control Trajectory Planning in Real-Time". *Proceedings of the 19th AAS/AIAA Space Flight Mechanics Meeting*. Savannah, GA, 9-12 February 2009.

22. Hurni, Michael A., Pooya Sekhavat, and I. Michael Ross. "An Info-Centric Trajectory Planner for Unmanned Ground Vehicles". *International Conference on the Dynamics of Information Systems*. Gainesville, FL, 28-30 January 2009.

23. Jackson, Paul. *Jane's All the World's Aircraft*, volume 2001-2002. Sampson Low Marston and Co. London, 2001. ISBN 0 7106 2307 0. URL `http://online.janes.com/`.

24. Johnson, Alan K. and Kriston P. Woolley. *A Simulation of a Computer Graphics-Aided Aircraft Handling System*. Master's thesis, Naval Postgraduate School, 1975.

25. King, R. S. *Systems Definition Study of Carrier Aircraft Deck Operations Control System (CADOCS)*. Technical Report NAEL-ENG-7453, Naval Air Engineering Center, 21 Apr 1967. AD877803.

26. Krozel, J. and D. Andrisani II. "Intelligent Epsilon-Optimal Path Prediction for Vehicular Travel". *Systems, Man and Cybernetics, IEEE Transactions on*, 25(2):345–353, Feb 1995.

27. Larsson, U., C. Zell, K. Hyyppa, and A. Wernersson. "Navigating an Articulated Vehicle and Reversing with a Trailer". *Robotics and Automation, 1994. Proceed-*

ings., 1994 IEEE International Conference on, (on robust state estimation):2398–2404 vol.3, 1994.

28. Lee, T. H., H. K. Lam, F. H. F. Leung, and P. K. S. Tam. "A Fast Path Planning-and-Tracking Control for Wheeled Mobile Robots". *Robotics and Automation, 2001.Proceedings 2001 ICRA.IEEE International Conference on*, 2:1736–1741, 2001.

29. Lewis, L. R., I. M. Ross, and Qi Gong. "Pseudospectral Motion Planning Techniques for Autonomous Obstacle Avoidance". *Decision and Control, 2007 46th IEEE Conference on*, 5997–6002, 2007.

30. Lewis, Laird-Philip Ryan. *Rapid Motion Planning and Autonomous Obstacle Avoidance for Unmanned Vehicles*. Master's thesis, Naval Postgraduate School, 2006.

31. Mahr, Randolph, Bruce Chiodi, and Mike Jones. "Aviation Data Management and Control Systems (ADMACS)", 2008. Presentation, Naval Air Systems Command.

32. Microsoft. "Tampa Authorities deploy latest technology for Super Bowl Security", 2009. URL `http://www.microsoft.com/industry/government/news/e_sponder_super_bowl.mspx`.

33. Misra, Pratap and Per Enge. *Global Position System: Signals, Measurements, and Performance*. Ganga-Jamuna Press, Lincoln, MA, 2006. ISBN 0-9709544-1-7.

34. Naval Air Systems Command (NAVAIR). *Unmanned Combat Air System CV Demonstration (UCAS-D) Performance Specification*. Technical Report NA-4150-UCAS-1003, 2007.

35. Naval Safety Center. "Flight Deck Awareness Guide", 2003. URL `http://www.safetycenter.navy.mil/aviation/downloads/index.asp`.

36. Ng, Teck Chew, J. I. Guzman, and M. D. Adams. "Autonomous Vehicle-following Systems : A Virtual Trailer Link Model". *Intelligent Robots and Systems, 2005. (IROS 2005). 2005 IEEE/RSJ International Conference on*, 3057–3062, 2005.

37. Northrop Grumman Corporation, Newport News. "ACOMS Spot Sheet Lite", 2003.

38. Novatel Inc. "OEMV Family Firmware Reference Manual", 2008.

39. Novatel Inc. "OEMV Family Installation and Operation User Manual", 2008.

40. NovAtel Waypoint Products Group. "Waypoint GrafNav/GrafNet", 2007. URL `http://www.novatel.com/products/waypoint_grafnav.htm`.

41. Park, Myoungkuk, Woojin Chung, Munsang Kim, and Jaebok Song. "Control of a Mobile Robot with Passive Multiple Trailers". *Robotics and Automation, 2004. Proceedings. ICRA '04. 2004 IEEE International Conference on*, 5:4369–4374 Vol.5, 2004.

42. Rainwater, C. W. *CADOCS Subsystems; Parameter Definition.* Technical Report NAEC-ENG-7536, Naval Air Engineering Center, 24 Mar 1967. AD852865.

43. Rainwater, C. W. *Exploratory Study of an Automated Carrier Aircraft Deck Operations Control System.* Technical Report NAEL-ENG-7375, Naval Air Engineering Center, 21 Oct 1966. AD819612.

44. Rainwater, C. W. and G. R. Ruddick. *CADOCS Subsystem Requirements Studies.* Technical Report NAEC-ENG-7466, Naval Air Engineering Center, 26 Jan 1968. AD905456.

45. Rider, Timothy L. "Blue Force Tracking to Expand Across Force". *Army Acquisition, Logistics, and Technology*, (September-October):2, 2004.

46. Ross, I. M. *User's Manual for DIDO: A MATLAB Application Package for Solving Optimal Control Problems.* Elissar, Monterey, CA, 2007. Document TR 705.

47. Segall, Paul and James Davis. "GPS APPLICATIONS FOR GEODYNAMICS AND EARTHQUAKE STUDIES". *Annual Review of Earth and Planetary Sciences*, 25:301, 1997.

48. Stentz, A. "Optimal and Efficient Path Planning for Partially-known Environments". *Robotics and Automation, 1994. Proceedings., 1994 IEEE International Conference on*, 3310–3317 vol.4, 1994.

49. Tiboni, Frank and Matthew French. "Blue Force Tracking Gains Ground". *Federal Computer Week*, 2008(12/15), 2004. URL `http://www.fcw.com/print/10_7/news/82385-1.html`.

50. Tiron, Roxana. "Army's Blue-Force Tracking Technology Was a Tough Sell". *National Defense*, (December), 2003.

51. Tolman, Brian, R. Benjamin Harris, Tom Gaussiran, David Munton, Jon Little, Richard Mach, Scot Nelsen, and Brent Renfro. "The GPS Toolkit: Open Source GPS Software". *Proceedings of the 16th International Technical Meeting of the Satellite Division of the Institute of Navigation.* Long Beach, California, September 2004.

52. United States Coast Guard. "CONUS GPS PDOP Chart - USCG Navigation Center", 2009. URL `http://www.navcen.uscg.gov/gps/pdop.htm`.

53. Vallado, David A. *Fundamentals of Astrodynamics and Applications.* Kluwer Academic Publishers, Dordrecht, Boston, London, 2001. ISBN 1-881883-12-4.

54. Venetsky, Larry, Mark Husni, and Mark Yager. *Gesture Recognition for UCAV-N Flight Deck Operations.* Technical Report ADA422629, Naval Air Systems Command, 23 Jan 2003.

55. Wilt, Jim and Valerie Bjorn. "Noise and Advanced Hearing Protection", 2006. URL `http://www-nehc.med.navy.mil/downloads/occmed/hctoolbox/Toolbox_files/NAVAIR%20Advanced%20Hearing%20Protection.ppt`.

56. Yang, Guang and V. Kapila. "Optimal Path Planning for Unmanned Air Vehicles with Kinematic and Tactical Constraints". *Decision and Control, 2002, Proceedings of the 41st IEEE Conference on*, 2:1301–1306 vol.2, 2002.

Vita

Lieutenant Jeffrey S. Johnston graduated from Boonsboro High School in Boonsboro, Maryland. He entered undergraduate studies at the University of Maryland in College Park, Maryland where he graduated with a Bachelor of Science degree in Aerospace Engineering in May 2003. In October 2001 he enlisted in the United States Navy through the Baccalaureate Degree Completion Program and received his commission through Officer Candidate School, NAS Pensacola, Florida in 2004.

Following Aviation Maintenance Duty Officer training he was assigned to Strike Fighter Squadron THREE FOUR, the Blue Blasters, an FA-18C Hornet squadron stationed at NAS Oceana, Virginia Beach, VA where he served as Material Control Officer, Aircraft Division Officer, and Assistant Maintenance Officer. From June to December 2004 he was deployed with his squadron onboard USS John F. Kennedy (CV 67) and participated in Operation Iraqi Freedom. He deployed with his squadron again from March to August 2006 onboard USS Abraham Lincoln (CVN 72) to the Western Pacific.

In August 2007 he entered the Graduate School of Engineering and Management at the Air Force Institute of Technology. Upon graduation he will be assigned to Space and Naval Warfare Systems Command (SPAWAR), Space Field Activity, Chantilly, VA.

Permanent address: 2950 Hobson Way
Air Force Institute of Technology
Wright-Patterson AFB, OH 45433

NONPRINT FORM

1. Type of Product: CD-ROM	2. Operating System/Version: MAC/PC/*NIX	3. New Product or Replacement: New	4. Type of File: GPS Data MATLAB

5. Language/Utility Program:

MATLAB, GNU tar/gzip

6. # of Files/# of Products: 60	7. Character Set: ASCII/Binary	8. Disk Capacity: 700 MB
	9. Compatibility: MAC/PC/*NIX	10. Disk Size: 4 3/4''

11. Title:

A Feasibility Study of a Persistent Monitoring System for the Flight Deck
of U.S. Navy Aircraft Carriers - GPS/MATLAB Data Disc

12. Performing Organization: AFIT/ENY WPAFB, OH 45433	13. Performing Report #: AFIT/GAE/ENY/09-M12	14. Contract #: N/A
		15. Program Element #: N/A

16. Sponsor/Monitor: N/A	17. Sponsor/Monitor # Acronym: N/A	19. Project #: N/A
	18. Sponsor/Monitor #: N/A	20. Task #: N/A
		21. Work Unit #: N/A

22. Date: 26-03-2009	23. Classification of Product: U
24. Security Classification Authority: N/A	**25. Declassification/Downgrade Schedule:** N/A

26. Distribution/Availability:

A: APPROVED FOR PUBLIC RELEASE; DISTRIBUTION UNLIMITED

27. Abstract:

This research conducted a study of the movements of USN personnel and an FA-18C aircraft being towed at NAS Oceana, VA. Using two precision GPS recorders mounted on the aircraft wingtips, the position and orientation of the aircraft, in two-dimensions, are calculated and the errors in the solution are explored. The distance between personnel and the aircraft is calculated in the nearest neighbor sense.

28. Classification of Abstract:

Unclassified

29. Limitation of Abstract:

Unlimited

30. Subject Terms:
AIRCRAFT CARRIERS, GLOBAL POSITIONING SYSTEM, MOTION, FLIGHT DECKS, KINEMATICS, PATH PLANNING, AVIATION SAFETY

30a. Classification of Subject Terms:
Unclassified

31. Required Peripherals:

N/A

32. # of Physical Records:

33. # of Logical Records:

34. # of Tracks:

35. Record Type:

36. Color:

37. Recording System:

38. Recording Density:

39. Parity:

40. Playtime:

41. Playback Speed:

42. Video:

43. Text:

44. Still Photos:

45. Audio:

46. Other:

47. Documentation/Supplemental Information:

Includes 1 page README file

48. Point of Contact and Telephone Number:

LT Jeffrey S. Johnston, USN

AFIT Telephone: 937-225-6565

REPORT DOCUMENTATION PAGE

The public reporting burden for this collection of information is estimated to average 1 hour per response, including the time for reviewing instructions, searching existing data sources, gathering and maintaining the data needed, and completing and reviewing the collection of information. Send comments regarding this burden estimate or any other aspect of this collection of information, including suggestions for reducing this burden to Department of Defense, Washington Headquarters Services, Directorate for Information Operations and Reports (0704–0188), 1215 Jefferson Davis Highway, Suite 1204, Arlington, VA 22202–4302. Respondents should be aware that notwithstanding any other provision of law, no person shall be subject to any penalty for failing to comply with a collection of information if it does not display a currently valid OMB control number. PLEASE DO NOT RETURN YOUR FORM TO THE ABOVE ADDRESS.

1. REPORT DATE (DD–MM–YYYY)	2. REPORT TYPE	3. DATES COVERED (From — To)
26-03-2009	Master's Thesis	September 2007 – March 2009

4. TITLE AND SUBTITLE	5a. CONTRACT NUMBER
A Feasibility Study of A Persistent Monitoring System For The Flight Deck of U.S. Navy Aircraft Carriers.	5b. GRANT NUMBER
	5c. PROGRAM ELEMENT NUMBER

6. AUTHOR(S)	5d. PROJECT NUMBER
LT Jeffrey S. Johnston, USN	5e. TASK NUMBER
	5f. WORK UNIT NUMBER

7. PERFORMING ORGANIZATION NAME(S) AND ADDRESS(ES)	8. PERFORMING ORGANIZATION REPORT NUMBER
Air Force Institute of Technology Graduate School of Engineering and Management (AFIT/ENY) 2950 Hobson Way WPAFB OH 45433-7765	AFIT/GAE/ENY/09-M12

9. SPONSORING / MONITORING AGENCY NAME(S) AND ADDRESS(ES)	10. SPONSOR/MONITOR'S ACRONYM(S)
Intentionally left blank	
	11. SPONSOR/MONITOR'S REPORT NUMBER(S)

12. DISTRIBUTION / AVAILABILITY STATEMENT

APPROVED FOR PUBLIC RELEASE; DISTRIBUTION UNLIMITED

13. SUPPLEMENTARY NOTES

14. ABSTRACT

This research analyzes the use of modern Real Time Locating Systems (RTLS), such as the Global Positioning System (GPS), to improve the safety of aircraft, equipment, and personnel onboard a United States Navy (USN) aircraft carrier. The results of a detailed analysis of USN safety records since 1980 show that mishaps which could potentially be prevented by a persistent monitoring system result in the death of a sailor nearly every other year and account for at least $92,486,469, or 5.55% of the total cost of all flight deck and hangar bay related mishaps. A system to continually monitor flight deck operations is proposed with four successive levels of increasing capability. A study of past and present work in the area of aircraft carrier flight deck operations is performed.

This research conducted a study of the movements of USN personnel and an FA-18C aircraft being towed at NAS Oceana, VA. Using two precision GPS recorders mounted on the aircraft wingtips, the position and orientation of the aircraft, in two-dimensions, are calculated and the errors in this solution are explored. The distance between personnel and the aircraft is calculated in the nearest neighbor sense. Pseudospectral motion planning techniques are presented to provide route prediction for aircraft, support equipment, and personnel.

Concepts for system components, such as aircraft and personnel receivers, are described. Methods to recognize and communicate the presence of hazardous situations are discussed. The end result of this research is the identification of performance requirements, limitations, and definition of areas of further research for the development of a flight deck persistent monitoring system with the capability to warn of hazardous situations, ease the incorporation of UAVs, and reduce the risk of death or injury faced by sailors on the flight deck.

15. SUBJECT TERMS

AIRCRAFT CARRIERS, GLOBAL POSITIONING SYSTEM, MOTION, FLIGHT DECKS, KINEMATICS, PATH PLANNING, AVIATION SAFETY

16. SECURITY CLASSIFICATION OF:			17. LIMITATION OF ABSTRACT	18. NUMBER OF PAGES	19a. NAME OF RESPONSIBLE PERSON
a. REPORT	b. ABSTRACT	c. THIS PAGE	UU	205	Lt Col Eric D. Swenson
U	U	U			19b. TELEPHONE NUMBER (Include Area Code) (937) 785-3636 x7479 eric.swenson@afit.edu